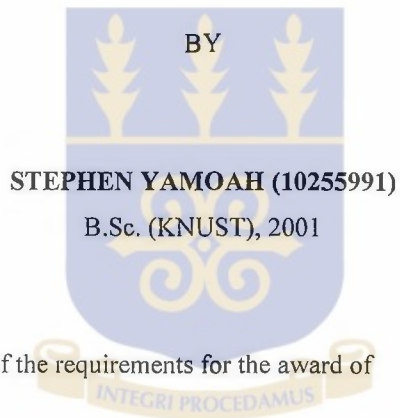


**THERMAL ANALYSIS OF A PEBBLE BED HIGH TEMPERATURE GAS  
COOLED REACTOR**

A Thesis submitted to the:

DEPARTMENT OF NUCLEAR ENGINEERING  
GRADUATE SCHOOL OF NUCLEAR AND ALLIED SCIENCES  
UNIVERSITY OF GHANA, LEGON



In partial fulfillment of the requirements for the award of

**MASTER OF PHILOSOPHY**

**in**

**NUCLEAR ENGINEERING DEGREE**

**June, 2009**



## DECLARATION

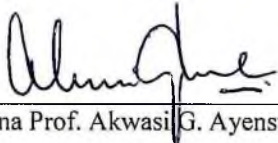
I hereby declare that with the exception of references to other people's work which have duly been acknowledged, the compilation of the Thesis submitted to the University of Ghana, Legon for the degree leading to an award of Master of Philosophy (M.Phil) in Nuclear Engineering is the result of my own research work under the supervision of Prof. E. H. K. Akaho and Nana Prof. Akwasi G. Ayensu and that no part of this work has been presented for another degree in this University or elsewhere



Sign   
Stephen Yamoah

INTEGRI PROCEDAMUS

Sign   
Prof. E. H. K. Akaho

Sign   
Nana Prof. Akwasi G. Ayensu

## DEDICATION

This work is dedicated to my wife Mrs. Cecilia Frimpong-Yamoah and my mother Ms. Elizabeth D. Asare.



## ACKNOWLEDGEMENT

My greatest gratitude to God Almighty for his grace and blessing that has sustained me through out this work. I wish to express my sincerest gratitude to my respected supervisors Professor E. H. K. Akaho and Nana Professor Akwasi G. Ayensu all of the Graduate School of Nuclear and Allied Sciences, University of Ghana, Legon for accepting to supervise my work and providing the necessary guidance and motivation.

My gratitude also goes to my wife, my mother, brothers and sisters and all my friends who in diverse ways contributed to the successful completion of this work.

Finally I would like to acknowledge my colleague students of the Graduate School of Nuclear and Allied Sciences, University of Ghana, Legon for their contributions towards this work.

<b>TABLE OF CONTENT</b>	<b>PAGE</b>
DECLARATION	i
DEDICATION	ii
ACKNOWLEDGEMENT	iii
LIST OF TABLES	ix
LIST OF FIGURES	x
LIST OF SYMBOLS	xii
LIST OF ABBREVIATIONS	xvii
ABSTRACT	xix
CHAPTER ONE: INTRODUCTION	1
1.1 High temperature gas cooled nuclear reactor	1
1.2 Research problem statement	5
1.3 Relevance of the research work	6
1.4 Objectives of the research	7
1.5 Outline of the Thesis	8

CHAPTER TWO: LITERATURE REVIEW	10
2.1 Pebble bed reactor (PBR)	10
2.1.1 Configuration description	10
2.1.2 Reactor unit and components	12
2.1.3 Reactor control systems	16
2.2 Reactor fuel	17
2.2.1 Fuel management	20
2.3 The helium coolant	21
2.4 Safety considerations	22
2.5 Safety systems	26
2.5.1 Core conditioning system	26
2.5.2 Reactor cavity cooling system	27
2.5.3 Active cooling system	28
2.6 Development challenges	29
2.7 Heat transfer mechanisms in the pebble bed reactor	35
2.7.1 Heat removal during normal operation	36
2.7.2 Decay heat removal	39

2.8	Effects of porosity on heat and mass transfer of the PBR	41
2.9	Summary	43
CHAPTER THREE: METHODOLOGY		45
3.1	Introduction	45
3.2	Mathematical model of the pebble bed reactor heat transfer and pressure drop	47
3.2.1	Pressure drop	47
3.2.2	Convective heat transfer	54
3.2.3	Temperature profile in the fuel pebble	61
3.2.4	Heat conductivity in packed beds	68
3.3	Material properties of helium	73
3.3.1	Mass density of helium	73
3.3.2	Dynamic viscosity	73
3.3.3	Thermal conductivity	73
3.4	Development of the code for thermal analysis	73
3.4.1	Input data	82
3.4.2	Program solution and implementation algorithm	82

3.4.2.1	Simulation of pressure drop across the pebble bed	82
3.4.2.2	Simulation of convective heat transfer	83
3.4.2.3	Simulation of temperature profile in the fuel pebble	84
3.4.2.4	Simulation of effective thermal conductivity across the pebble bed core	84
3.5	Summary	85
CHAPTER FOUR: RESULTS AND DISCUSSION		86
4.1	Pressure drop	86
4.2	Convective heat transfer	89
4.3	Temperature profile in the fuel pebble	91
4.4	Effective radial thermal conductivity	92
4.5	Effects of porosity on heat transfer and pressure drop	94
CHAPTER FIVE: CONCLUSIONS AND RECOMMENDATIONS		97
5.1	Conclusions	97
5.2	Recommendations	99

REFERENCES	101
------------	-----

APPENDIX A	107
------------	-----

**LIST OF TABLES**

<b>TABLE</b>		<b>PAGE</b>
3.1	Parameters used in the analysis	82

**LIST OF FIGURES**

<b>FIGURE</b>	<b>PAGE</b>
2.1 Schematic horizontal section through the reactor unit	13
2.2 Schematic vertical section through the reactor unit	14
2.3 Layers of the pebble bed reactor fuel	18
2.4 Spherical fuel element (diameter 6 cm)	19
2.5 Schematic diagram of the three-shaft recuperated Brayton cycle.	37
3.1 Heat transfer model of pebble cooling	55
3.2 Main Computational Flow Chart	75
3.3 Computational Flow Chart for CONVECTION_SUB	77
3.4 Computational Flow Chart for FUELTEMPT_SUB	78
3.5 Computational Flow Chart for CONRAD_SUB	79
3.6 Computational Flow Chart for COMBINEDEFFECTS_SUB	80
3.7 Computational flow chart for COREFUELRTATIO_SUB	80
3.8 Computational Flow Chart for PRESSUREDROP_SUB	81
4.1 Plot of Pressure drop coefficient against modified Reynolds number	86

4.2	Plot of Pressure drop profile for different core height	87
4.3	Limiting curve of the diameter ratio as a function of modified Reynolds number	88
4.4	Convective heat transfer for pebble bed	89
4.5	Mass flow rate dependence of heat transfer coefficient	90
4.6	Temperature dependence of heat transfer coefficient	91
4.7	Temperature profile in a fuel pebble	92
4.8	Effective radial conductivity distribution across the pebble bed	93
4.9	Effective thermal conductivity of the pebble bed in helium	93
4.10	Effect of porosity on heat transfer	95
4.11	Effect of porosity on pressure drop	95

**LIST OF SYMBOLS**

$P$	Pressure (Pa)
$\Delta P$	Pressure drop (Pa)
$H$	Height (m)
$\psi$	Pressure drop coefficient
$Re$	Reynolds number
$d_h$	The length scale (the hydraulic diameter of the pebble forming the bed) (m)
$\rho$	Density of the fluid ( $\text{kg/m}^3$ )
$\eta$	Dynamic viscosity of the fluid ( $\text{kg/s.m}$ )
$u_p$	Mean velocity of the gas between the particles (m/s)
$A$	Vessel cross sectional area ( $\text{m}^2$ )
$A_s$	Sphere surface area ( $\text{m}^2$ )
$A_x$	Heat exchange surface area ( $\text{m}^2$ )
$d$	Sphere/Pebble diameter (m)
$\varepsilon$	Porosity of the bed

$V_s$	Volume of all spheres ( $m^3$ )
$V$	Total volume of the packed bed ( $m^3$ )
$Re_h$	Reynolds number corresponding to the hydraulic diameter
$m$	Mass flow rate (kg/s)
$u$	Mean velocity of flow (m/s)
$D$	Core diameter (m)
$R_c$	Core radius (m)
$\varepsilon_t$	Average porosity
$Q$	Heat transferred (W)
$A_p$	Surface area for heat transfer ( $m^2$ )
$T_g$	Gas temperature (K)
$T_{surf}$	Surface temperature of pebble (K)
$q$	Heat flux ( $W/m^2$ )
$\Delta T$	Average temperature difference between the surface and bulk of the gas (K)
$Nu$	Nusselt number
$Nus$	Nusselt number of the single sphere

Nul	Nusselt number of the single sphere for laminar flow
Nut	Nusselt number of the single sphere for turbulent flow
Nu <sub>h</sub>	Nusselt number corresponding to the hydraulic diameter
$\lambda$	Thermal conductivity of the coolant (W/m.K)
Pr	Prandtl number
Pe	Peclet number
$f\varepsilon$	Arrangement factor
S	Circumference of aspect contour (m)
L	Characteristics streaming length (m)
R <sub>fz</sub>	Radius of pebble fuel region (m)
R <sub>peb</sub>	Radius of pebble graphite region (m)
r	Radius of fuel pebble (m)
$\lambda_I$	Thermal conductivity of the material in the fuel region (W/m.K)
$\lambda_{II}$	Thermal conductivity of the material in the graphite region (W/m.K)
T <sub>I</sub>	Temperature in the fuel region (K)
T <sub>II</sub>	Temperature in the graphite region (K)
q <sub>v</sub>	Volumetric power density in the fuel region (W/m <sup>3</sup> )

$q_p$	Power produced in the pebble (W)
$Q_c$	Volumetric core power density ( $W/m^3$ )
$P_W$	Reactor power (W)
$T_{pc}, T_m$	Pebble centre point temperature/maximum pebble temperature (K)
$q_{ra}$	Radial heat flux ( $W/m^2$ )
$q_{ax}$	Axial heat flux ( $W/m^2$ )
$h_{cd} (rad)$	Radial conductive heat transfer coefficient ( $W/m.K$ )
$h_{cd} (ax)$	Axial conductive heat transfer coefficient ( $W/m.K$ )
$\lambda_{ra}, \lambda_{ax}$	Effective thermal conductivity in the radial and axial directions respectively ( $W/m.K$ )
$\lambda_g$	Thermal conductivity of the gas ( $W/m.K$ )
$\lambda_o$	Overall thermal conductivity ( $W/m.K$ )
$\lambda_{gap}$	Effective thermal conductivity across the gap ( $W/m.K$ )
$\lambda_{fs}$	Effective thermal conductivity through the fluid and solid phase ( $W/m.K$ )
$\lambda_s$	Thermal conductivity of the solid particles ( $W/m.K$ )

$\Delta T_{rad}, \frac{dT}{dr}$  Temperature difference in the radial direction (K/m)

$\Delta T_{ax}, \frac{dT}{dz}$  Temperature difference in the axial direction (K/m)

T Absolute temperature (K)

$\sigma$  Stefan – Boltzmann constant ( $W/m^2 \cdot T^4$ )

$\varepsilon_r$  Emissivity

B Form factor

$\alpha$  Heat transfer coefficient ( $W/m^2 \cdot K$ )

$\Lambda_{ra} = \lambda_{ra} / \lambda_g$  Conductivity ratio in the radial direction

$\Lambda_{ax} = \lambda_{ax} / \lambda_g$  Conductivity ratio in the axial direction

**LIST OF ABBREVIATIONS**

PEBTAN	Pebble Bed Thermal Analysis
HTGR	High Temperature Gas-cooled Reactor
HTR	High Temperature Reactor
LWR	Light Water Reactor
PBR	Pebble Bed Reactor
RCS	Reactivity Control System
RSS	Reserved Shutdown System
RPV	Reactor Pressure Vessel
LEU	Low Enriched Uranium
TRISO	Triple-coated Isotopic
OTTO	Once-Through-Then-Out
PBMR	Pebble Bed Modular Reactor
D-LOFC	Depressurised Loss of Forced Cooling
CCS	Core Conditioning System
PCU	Power Conversion Unit

RCCS	Reactor Cavity Cooling System
ACS	Active Cooling System
DCC	Depressurised Conduction Cooldown
PCC	Pressurised Conduction Cooldown
PWR	Pressurised Water Reactor
LPC	Low Pressure Compressor
HPC	High Pressure Compressor
HPT	High Pressure Turbine
LPT	Low Pressure Turbine
PT	Power Turbine
ICS	Inventory Control System
CFD	Computational Fluid Dynamics
VSOP	Very Superior Old Program
TINTE	Time-dependent Neutronics and Temperature
MCNP	Monte Carlo N-Particle

## ABSTRACT

The pebble bed type of high temperature gas cooled nuclear reactor is a promising option for next generation reactor technology and has the potential to provide high efficiency and cost effective electricity generation. The reactor unit heat transfer poses a challenge due to the complexity associated with it. In the pebble bed, heat is generated in kernels inside the fuel sphere. The generated heat is conducted to the sphere surface where it is transferred to the coolant (helium gas) by means of convection. In the bed itself when a temperature gradient exists across the bed, heat is transferred between pebbles by means of conduction and interstitial radiation in the radial and axial directions. This necessitates a heat transfer model that deals with radiation as well as thermal convection and conduction. Modeling such a complex thermal hydraulic system requires the use of variety of techniques and simulation tools ranging from a one-dimensional model to large scale three-dimensional model using computer codes based on analytical or computational fluid dynamics. In this research, a simplified analytical model of the pebble bed type high temperature nuclear reactor heat transfer was developed to analyze the convection, conduction and radiation heat transfer phenomena, as well as the loss of pressure through friction in the pebble bed. Correlations derived from experimental data or directly from experimental testing were used to approximate the thermo-physical properties of the pebble bed. The developed model was implemented on a personal computer using a simulation code PEBTAN (**PEbble Bed Thermal ANalysis** code) which was written in FORTRAN 95 programming

language. Simulation and numerical experiments were conducted, and the results showed very good agreement with published data. The model can adequately account for the heat transfer phenomenon, and the loss of pressure through friction in the pebble bed type high temperature nuclear reactor. The model can serve as the bases for a more detailed three dimensional computational fluid dynamic analysis.

## CHAPTER ONE

### INTRODUCTION

#### 1.1 HIGH TEMPERATURE GAS COOLED NUCLEAR REACTOR

High temperature gas cooled nuclear reactor is one of the renewed reactor designs to play a role in the nuclear power industry and is considered as a promising option for next generation reactor technology for energy production [1, 2]. The interest in the high temperature nuclear reactor concept was given a substantial boost due to the growing demand for an enhancement of the safety standards of nuclear power plants.

The advancement and basic concept of the high temperature gas cooled reactor (HTGR) were proposed for the first time in 1940 by Keller [3]. For the HTGR, Keller stated that “the closed cycle gas turbine power plant using helium or helium mixtures appears to be one of the best systems for generating power by the use of uranium pile” The HTGRs have been built and operated in the USA and Great Britain (with prismatic fuel elements) and Germany (pebble bed reactors) since the late fifties.

The high temperature nuclear reactor (HTR) is a helium gas cooled, graphite moderated nuclear reactor and the fuels are in small particles as fuel geometry. The fuel particles are coated with graphite and loaded into graphite fuel elements.

The high temperature properties of helium permit the reactor to achieve high thermal efficiency of 50% upwards [4].

The reactor is considered as inherently safe because of the choices of materials used, the confinement of fuel in multiple layers, the thermal inertial of the graphite moderator, the high thermal efficiency features as well as flexible fuel cycle with capability to achieve high burn up levels [5].

The inherently safe features of the high temperature gas cooled nuclear reactor include;

1. Negative temperature coefficient which result in natural shutdown of the reactor during power excursion
2. Graphite moderated, thus providing longer neutronic transient time scale
3. Large thermal inertia of the graphite moderator resulting in slow core temperature rise
4. Helium coolant which is chemically and neutronically inert as well as being single phase
5. The ability of the fuel particles to retain fission products to higher temperatures of approximately 1600 °C
6. Passive removal of decay heat through natural processes of convection, conduction and radiation during depressurised loss of forced cooling. This is effective due to low power density.
7. Simplicity in design compared to current light water reactors (LWRs)

The inherently safe concept of the reactor requires that decay heat must be removed passively from the core under any designed accident conditions and keep the maximum fuel temperature below 1600°C so as to contain the fission products inside the fuel. This eliminates the possibility of core melt down and large release of radioactive fission products into the environment.

Passive removal of decay heat requires passive safety measures, that is, measures that rely on natural processes to limit the core temperature in situations where all other active control fails and that do not require human action [3, 6].

Other desired features of the high temperature gas cooled nuclear reactor are the modularity concept, relatively low cost and short construction period. The modularity concept allows for a 2 to 3 year construction period with expansion capabilities to meet large utility demand projections [4].

The reactor design is such that it is power-limited or inherently self controlling due to Doppler broadening. This effect reduces the reactivity of the reactor as the reactor temperature rises.

The potential of the high temperature nuclear reactor to fulfill the inherent safety requirements lies primarily in the combination of low power density and a very high temperature up to which the coated particles can retain the fission products. The lower power density of the reactor means that the fuel is less likely to attain

high enough temperature to induce failure. The relatively high thermal conductivity of graphite (30-50 W/mk) compared to that of pure water (3 W/mk) ensures that heat is transferred quickly away from the fuel and out of the core even in the event of a loss of forced cooling or depressurisation [7].

The development of the high temperature nuclear reactor from the beginning has evolved along two main tracks, differing in the manner in which the reactor is fuelled, namely;

1. The prismatic or block type design of high temperature reactor. In this type of HTR, the coated particles are loaded in cylindrical fuel compacts that are inserted in prismatic graphite fuel elements. The elements contain other holes for control rods, flow of coolant gas, and rods with burnable poison.
2. The pebble bed type design of high temperature reactor. In this type of HTR, the coated particles are loaded in spherical graphite elements, the size of a tennis ball. Such a pebble typically contain 10-20 thousand coated particles bedded in a graphite matrix of 5 cm diameter protected by a layer of graphite giving the pebble a total diameter of 6 cm [6]. A randomly packed bed of these spheres in the core cavity of the reactor forms the core. The coolant flow through the bed from top to bottom. Depending on the size of the core, control rods are inserted directly into the bed, or into the reflector encircling the bed.

## 1.2 RESEARCH PROBLEM STATEMENT

The pebble bed type high temperature nuclear reactor is considered to be inherently safe, because of the negative temperature reactivity feedback, low power density and large thermal inertia of the core. The reactor unit heat transfer poses a challenge in that it includes a complex three dimensional geometry and various materials and fluid types.

In the pebble bed, heat is generated in kernels inside the fuel sphere. The generated heat is conducted to the sphere surface where the heat is transferred to the coolant which is helium gas, by means of forced convection. In the bed itself when a temperature gradient exists across it, heat is transferred between pebbles by means of conduction and interstitial radiation in the radial and axial directions.

In addition, the nuclear reaction that produces the heat is temperature dependent thus making the mechanisms above very interrelated. Modeling such a complex thermal hydraulics system requires the use of variety of techniques and simulation tools ranging from the one-dimensional model to large scale three-dimensional model using computer codes based on analytical or computational fluid dynamics.

In this research, analysis of the fluid flow and heat transfer phenomena in the reactor core as well as the pressure drop through friction in the pebble bed was carried out using a computer code based on an analytical model. The code was used to solve the combined convective, conductive and radiative heat transfer

equations and to predict the pressure drop in the pebble bed core. By so doing, it was possible to predict the thermal response of the high temperature nuclear reactor of the pebble bed type. The model was implemented on a personal computer using FORTRAN 95 to simulate various conditions and scenarios to predict the thermal response of the high temperature nuclear reactor of the pebble bed type.

### **1.3 RELEVANCE OF THE RESEARCH WORK**

Thermal analysis of the pebble bed type high temperature nuclear reactor is important for safe operation and utilisation of the reactor for electricity generation. The complexity associated with the pebble bed reactor unit heat transfer requires models that can correctly evaluate and simulate the thermal response of the reactor. Again the reliable simulation of the fluid flow and heat transfer phenomena in the reactor core as well as the pressure drop in the pebble bed is very essential for the safety analysis of the reactor.

The present research work is based on the use of analytical expressions describing the convective, conductive and radiative heat transfer processes as well as the pressure drop through friction in the pebble bed core. The model provides knowledge and understanding of the heat transfer and fluid flow mechanisms associated with the pebble bed type high temperature nuclear reactor.

#### 1.4 OBJECTIVES OF THE RESEARCH

The main objectives of the research were;

1. To develop analytical model of the pebble bed type high temperature nuclear reactor which can reliably predict the thermal response of the reactor.
2. To develop a computer simulation code in FORTRAN 95 which can be used for the thermal analysis of the pebble bed type high temperature nuclear reactor during normal operation.

The specific objectives involved the analysis of the;

1. influence of porosity of the bed on convective heat transfer,
2. temperature dependence on the convective heat transfer coefficient,
3. temperature distribution in the fuel pebble,
4. heat flux in the pebble bed in order to account for hot spots in the reactor core taking into consideration:
  - (a) The heat flux through the gap between neighbouring spheres due to heat conduction and radiation and
  - (b) Heat conducted and radiated through the fluid and solid phase from layer to layer.
5. dependence of pressure drop coefficient and the effects of pressure drop on Reynolds number,
6. effects of porosity of the bed on pressure drop,
7. effects of core to fuel element diameter ratio on pressure drop.

## 1.5 OUTLINE OF THE THESIS

The thermal analysis of a pebble bed high temperature gas cooled reactor involves developing an analytical model to analyse the fluid flow and heat transfer mechanisms within the reactor core as well as predicting the pressure drop due to friction in the pebble bed.

As stated earlier, heat transfer equations for convection, conduction and radiation processes as well as loss of pressure in a heaped bed of identical diameter were solved for the pebble bed type high temperature nuclear reactor. A computer code called PEBTAN written in FORTRAN 95 was developed to simulate the heat transfer and fluid flow phenomena.

The Thesis contains the following chapters:

Chapter one (1) presents the introduction and the objectives of the research.

Chapter Two (2) presents the literature review of the research, covering detailed studies on pebble bed reactor (PBR) and including safety, the reactor fuel, the helium coolant and development challenges. The thermal characteristic of the pebble bed reactor with respect to the heat transfer mechanism was also reviewed.

Chapter Three (3) presents the methodology used in the research. The research methodologies involved the use of correlations derived from experimental data or directly from experimental testing to approximate the thermo-physical properties

of the pebble bed reactor in order to model the heat transfer phenomena of the reactor. This included;

1. Formulation of mathematical equations to establish relationships for convection, conduction and radiation heat transfer of the pebble bed type high temperature nuclear reactor as well as the pressure drop through friction in the bed,
2. Develop algorithms/flow charts using FORTRAN 95,
3. Run and debug FORTRAN 95 programme for solving the heat transfer equations and the pressure drop in the bed of the pebble bed type high temperature nuclear reactor ,
4. Simulation and validation of the code

Chapter Four (4) presents analysis and discussion of the simulation results.

Chapter Five (5) presents conclusions and recommendations of the Thesis.

## CHAPTER TWO

### LITERATURE REVIEW

In this chapter, detailed literature review of the pebble bed reactor, including safety, coolant properties, fuel type and the development challenges of the pebble bed reactor are presented. The heat transfer processes during normal operation and decay heat removal of the pebble bed reactor are also reviewed. The chapter ends with a discussion of the effects of porosity on heat transfer of the pebble bed reactor.

#### **2.1 PEBBLE BED REACTOR (PBR)**

##### **2.1.1 CONFIGURATION DESCRIPTION**

The design of the pebble bed reactor is based on the high temperature gas cooled nuclear reactor technology which was originally developed in Germany [8]. The pebble bed reactor has been receiving significant attention due to many desired characteristics such as its inherent safety, simplicity in operation, modularity concept, relatively low cost and short construction period.

The German AVR pebble bed research reactor ( $40 \text{ MW}_{\text{th}}$  and  $15 \text{ MW}_e$ ) operated for 22 years demonstrating the effectiveness of the technology. The  $300 \text{ MW}_e$  version of the pebble bed reactor also built in Germany was shut down due to both mechanical and political problems [4]. The use of spherical fuel elements, referred to as fuel pebbles is a characteristic of the reactor.

As a result of advances made in nuclear reactor and helium gas turbine technologies, new version of the pebble bed reactor has been produced. The new designs now use direct or indirect cycle helium gas turbines to produce electricity instead of steam cycles with a target thermal efficiency in the range of 45% compared to 32% for steam cycles [4].

To allow for rapid and modular construction, as well as maintaining the inherent safety features, the optimum size for a pebble bed reactor was concluded to be about 250 MW<sub>th</sub> (120 MW<sub>e</sub>) [4]. Should the need arise for a 1,100 MW<sub>e</sub> plant, 10 modules of the 250 MW<sub>th</sub> plant could be built at the same site and a single control room could operate all the 10 units using advanced control system employing many of the multi-plant features of modern gas fired power plants in terms of modularity and automatic operation.

The pebble bed reactor core contains approximately 360,000 uranium fuel pebbles, each about the size of a tennis ball. Each pebble contains about 7 to 9 g of low enriched uranium in 10,000 to 20,000 (depending on the design) tiny grains of sand-like microsphere coated particles each with its own hard silicon carbide shell embedded in a graphite matrix material [7, 9]. On-line refueling is possible with pebble bed reactors which allow new fuels to be inserted during operation and used fuels to be discharged and stored on site for the life of the plant. The pebbles are located in the reactor core structure whose cross section is shown in Figs. 2.1 and 2.2.

The working cooling fluid is helium. The helium enters the reactor vessel through a pipe of circular cross section near the bottom of the vessel. The helium is then passed through an inlet plenum which then feeds the helium to the risers. The helium flows upwards through the risers and is distributed to the riser channels that lead upward to an upper plenum above the core. At this point the helium coolant is directed downward from the upper plenum into the core and moves downward through the paths defined by the voids between the pebbles, which vary in size with radial poisoning. The helium at this point moves from the core into a lower plenum having being heated to a higher temperature of approximately 400° C to 500° C [10]. The hot helium is directed to a pipe of circular cross section (the hot duct) before it enters the power conversion unit.

### 2.1.2 REACTOR UNIT AND COMPONENTS

The reactor unit consists of the fuel, the metallic core barrel, the reactivity control system (RCS) and the reserve shutdown system (RSS) all contained inside the reactor pressure vessel. Figures 2.1 and 2.2 show the horizontal and vertical sections through the reactor unit respectively. The core of the reactor unit consists of an annulus filled with 60 mm fuel spheres.

The annular fuel section surrounds the fixed central reflector. The reactivity control system and shut down system are placed in both the central and side reflectors.

The main function of the reactor unit is to generate heat. The coolant which flows from top to the bottom of the core transfers the heat to the Brayton cycle (a thermodynamic cycle using gas as the working fluid) for electricity generation. The central safety function of the reactor is to keep the release of fission products from the fuel as low as possible during normal and accident operating conditions. To achieve this safety function, the fuel is protected by ensuring safe shutdown of the reactor and the ability to remove decay heat during normal operating and accident conditions.

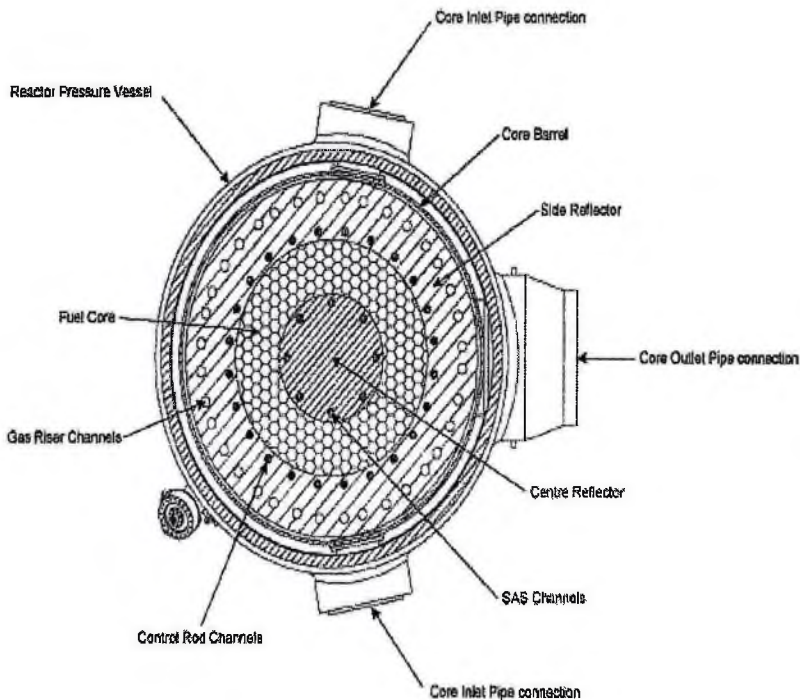


Figure 2.1: Schematic horizontal section through the reactor unit [8]

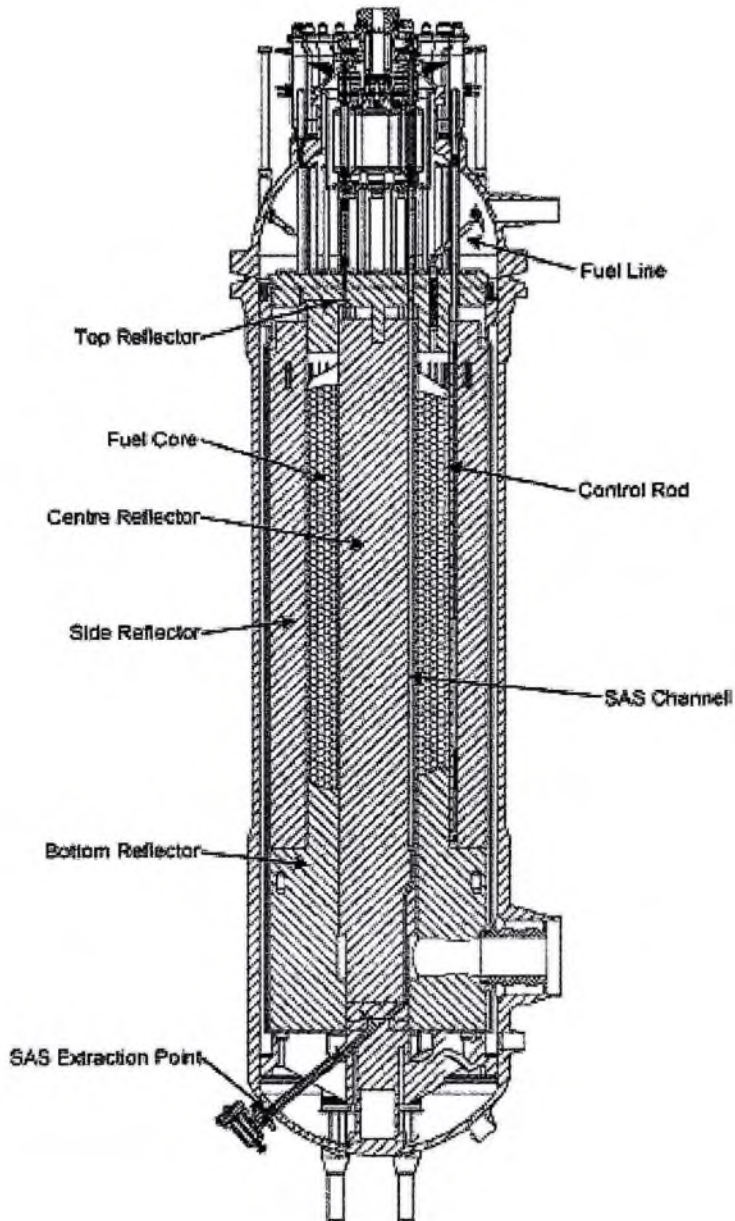


Figure 2.2: Schematic vertical section through the reactor unit [8]

The design of the PBR is characterized by the inherent safety features with respect to passive decay heat removal through conduction, radiation and natural convection. The passive safety concept was first introduced in the German HTR-module (pebble fuel) design [11] and subsequently extended to other modular HTR designs in recent years.

The passive heat transfer path ensures that heat is transferred from the fuel to the environment beyond the reactor pressure vessel (RPV). The effectiveness of the heat transfer path ensures that the reactor unit survives a depressurised loss of forced cooling without exceeding any of the component temperature limits, and the PBR does not require coolant to remove decay heat from the fuel [8].

The fuel spheres contained in the annular core of the reactor unit are recycled continuously through the core and are discharged when they have reached their burnup grade after five (5) to ten (10) years depending on the design [6]. The recycling of the fuel is carried out while the reactor is at full power. This results in constant power and temperature profile in the core once an equilibrium core has been established.

Due to the initial lack of poisonous products in the initial core, graphite balls and fuel balls are uniformly mixed together in order to reduce the reactivity. In response to fission products buildup during the fuel cycle, the graphite balls are gradually discharged out. The reactor is then transferred gradually from the initial

core to the equilibrium core when there are no any graphite balls in the core [12]. The equilibrium core represents the conditions that the reactor will experience for the majority of the design life.

The metallic core barrel supports the annular pebble fuel core and the graphite neutron reflector in the centre and on the outside of the fuel annulus. Vertical channels in the centre and outer reflectors are provided for the reactivity control elements.

### 2.1.3 REACTOR CONTROL SYSTEMS

Two diverse systems, the reactivity control system (RCS) and the reserve shutdown system (RSS) are provided for shutting the reactor down, one being control rods inserted into the channels in the side reflector and the other being small neutron absorbing spheres which are dropped into channels in the central reflector.

The reactivity control systems (RCS) consist of control rod containing  $B_4C$  as neutron absorber that can be raised or lowered in channels in the side reflector. The RCS controls the reactivity and shutdown of the reactor whilst the reserve shutdown system (RSS) provides a backup system for long term shutdown of the core.

The RSS can insert small graphite spheres containing  $B_4C$  into channels in the centre reflector to add enough neutron absorption to keep the reactor subcritical at long term shutdown conditions. Both the RCS and RSS can insert their respective neutron absorbers into the core under gravity alone, even if all the power fails.

Shutdown of the reactor is done by inserting the control rods. Start-up is effected by making the reactor critical, and by using nuclear heat up of the core and removing this heat in the power conversion unit by motoring the turbo-generator. At a specified temperature, the Brayton cycle is initiated and the system becomes self sustaining.

## **2.2. REACTOR FUEL**

The pebble bed reactor fuel is based on a proven, high-quality German fuel design consisting of low enriched uranium triple-coated isotropic (LEU-TRISO) particles contained in a molded graphite sphere. The coated particles comprise a kernel of uranium dioxide surrounded by four coating layers as shown in Fig. 2.3 to form the fuel sphere or pebbles with a total diameter of 6 cm. It can be seen from Fig. 2.4 that the outer of the fuel pebble is made of graphite shells of 1 cm thickness surrounding an inner fuel zone of 5 cm thickness to give the fuel the total thickness of 6 cm.

The fuel zone has a graphite matrix containing approximately 10,000 to 20,000 TRISO fuel micro spheres. In the centre of the pellet, the  $UO_2$  fuel is surrounded

by a porous carbon layer which allows fission products to collect without over-pressurising the coated fuel particles. The porous carbon layer acts as a pressure vessel. Following this layer, is a thin coating of pyrolytic carbon made of a very dense form of heat-treated carbon. A third layer of silicon carbide (SiC) which is a strong refractory material follows the pyrolytic carbon layer. This layer assures that no fission products are released even at temperatures reaching 1600 °C that may be associated with any anticipated accident and provides the first level of containment for the fission products within the fuel kernel itself [6]. A fourth layer of pyrolytic carbon forms the last barrier of the fuel particle.

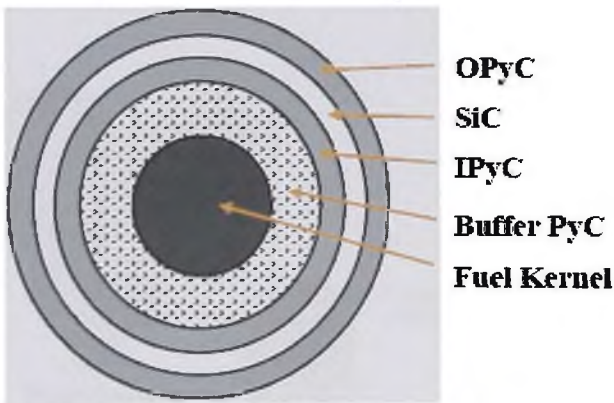


Fig. 2.3: Layers of the pebble bed reactor fuel

The porous carbon forming the first layer surrounding the  $\text{UO}_2$  kernel accommodates any mechanical deformation that the  $\text{UO}_2$  kernel may undergo during the lifetime of the fuel as well as gaseous fission products diffusing out of the kernel. The pyrolytic carbon and silicon carbide layers on the other hand

provide an impenetrable barrier designed to contain the fuel and radioactive fission products resulting from nuclear reactions in the kernel.

The TRISO particle in which the fuel is dispersed forms containment for the fuel inside and this may be considered as a miniature pressure vessel. Approximately, about 10,000 to 20,000 of the coated particles about a millimeter in diameter are mixed with graphite powder and a phenolic resin which is then pressed into shapes of about 50 mm diameter balls.

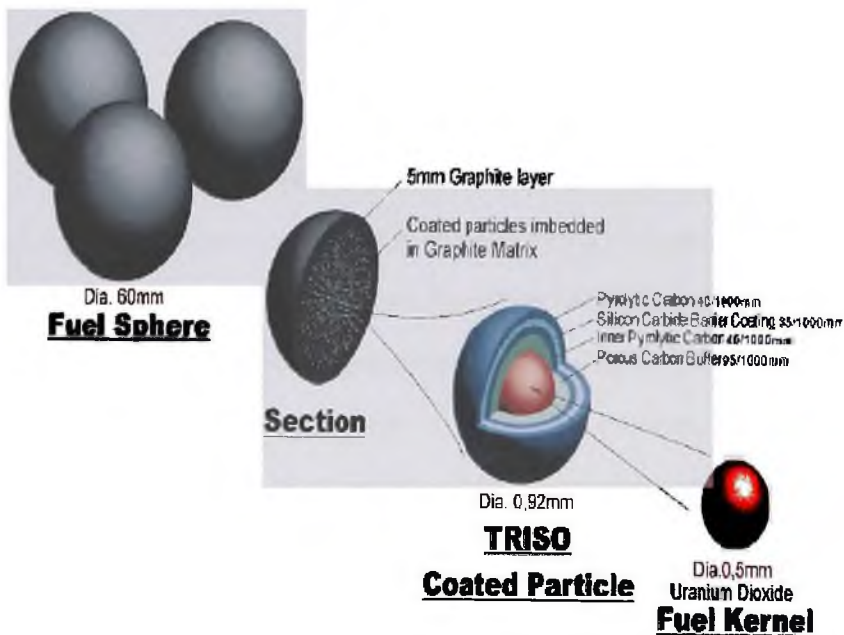


Figure 2.4: spherical fuel element (diameter 6 cm) [5, 13]

A “non-fuel” zone is formed by adding a 5 mm thick layer of pure carbon, and the resulting sphere sintered and annealed to make them hard and durable. Finally the spherical fuel pebbles are machined to a uniform diameter of 60 mm, about the size of a tennis ball with each fuel pebble containing about 7 to 9 g of uranium enriched to about 8% [7].

### 2.2.1. FUEL MANAGEMENT

The fuel management of the pebble bed type high temperature nuclear reactor involves three different strategies listed in order of decreasing complexity and power density [6]. These are the multipass scheme, the once-through-then-out (OTTO) scheme and the peu-à-peu scheme. The strategies are presented as follows;

1. The multipass scheme: Under this scheme, pebbles are added to the top of the bed and extracted at the bottom. The burnup grade of the extracted pebble is then measured and if found to be below a certain value, it is added back to the top of the bed. The pebble bed height under this scheme is more or less constant and presents a flat power profile. This scheme provides an efficient method of using fuel, however, refueling and measuring equipment is required and this increases the complexity of the reactor. Again the extraction of pebbles can present problems, as has been experienced in the past [6].
2. The once-through-then-out (OTTO) scheme: Under this scheme, pebbles are added to the top of the bed and extracted at the bottom. The pebbles

are discarded without measuring the burnup grade, and new pebbles are added to the top of the bed. Recycling and measuring equipment is not required in this scheme making the reactor simpler than in the multipass scheme. The pebble bed height remains more or less constant.

3. The peu-à-peu scheme: Under this scheme, the pebble bed starts with a large cavity above it. Pebbles are then added to the top but are not extracted. This results in a steadily increase in the pebble bed height in the core. The core after a certain period of time becomes full and all the pebbles are discharged requiring a complete shutdown of the reactor once every five to ten years depending on the design. This scheme avoids possible problems associated with extraction of pebbles during operation.

### **2.3. THE HELIUM COOLANT**

Helium gas is used as the coolant and energy transfer medium in a closed thermodynamic cycle gas turbine. The helium coolant used to transfer heat from the core to the power generating systems is chemically inert due to the fact that air with oxygen cannot ingress into the primary circuit, and get into the high temperature core to oxidize the graphite used in the reactor. Thus, chemical reactions and oxidation are sidelined in the construction of the pebble bed type high temperature reactor which means that the helium does not react with the graphite. The coolant is also nuclear inert because helium does not easily absorb neutrons or impurities. Also the helium coolant does not interfere in the neutron moderation process and does not experience phase change. It has a fairly high

heat capacity and thermal conductivity. Therefore, compared to water, it is both efficient and less likely to become radioactive.

#### **2.4. SAFETY CONSIDERATIONS**

The pebble bed modular reactor (PBMR) is considered as inherently safe. It is impossible for the reactor to reach a state where radioactive fission products are released above pre-defined levels [6]. The basis of the safety of the pebble bed reactor is founded on two principles [4].

The first is the very low power density of the reactor, some 10 to 20 times lower than in a light water reactor (LWR) [6] and the high heat capacity of graphite or high thermal conductivity as a result of large mass of graphite in the core. This means that the amount of energy generated and heat produced is volumetrically low and that there are natural mechanisms such as conductive and radiative heat transfer that will remove the heat even if no convection core cooling is provided.

In the situation where the chain reaction has stopped and all heat is produced by radioactive decay of fission products, the low power density and high heat capacity (high thermal conductivity) become very important. Should a loss of power occur or a loss of active cooling is supposed, the decay heat has to be transported by passive means (free convection, conduction and radiation) out of the core zone towards the reactor vessel wall where it can be dissipated.

A low power density means that the fuel is less likely to attain a higher enough temperature to induce failure and this helps to limit the amount of heat to be transported to the reactor vessel wall. The high heat capacity due to the high thermal conductivity of graphite (30-50 W/mk) as compared to pure  $\text{UO}_2$  (3 W/mk) ensures that heat is transferred quickly away from the fuel and out of the core and thereby limit the value of the temperature during the transfer process.

Based on the above, it can be deduced that in the event of a total loss of primary coolant without operator intervention, the reactor core heatup rate would be so slow and the maximum fuel temperature would not exceed 1600 °C. The pebble bed modular reactor core has a high surface area-to-volume ratio which means that the amount of heat that it losses through its surface is greater that the amount of heat generated by the decay of fission products in the core. Therefore, the reactor is not expected to reach a temperature at which significant fuel damage can occur.

The conclusion is that fuel damage due to core melt-down is not expected. This is supported by tests and analysis performed in Germany, Japan, China, South Africa and the USA [4].

The second reason is that the high temperature resistance of the fuel due to the high quality of the silicon carbide used forms the tiny containment for each of the 10,000 to 20,000 coated fuel particles in a pebble.

The design of the fuel particle ensures that no radiologically significant quantities of gaseous or metallic fission products are released from the fuel element at temperatures of up to 1600 °C. Tests performed to date on fuel reliability shows that microspheres can be routinely manufactured with initial defects of less than 1 in 10,000 [4]. This is corroborated by extensive studies conducted on the behavior of coated particles under various temperature conditions. The results from the studies show that on the average less than one particle per pebble will fail as long as the temperature remain below 1600 °C [7,14,15].

In terms of safety analysis, this means that 1 in 10,000 of these microspheres has a defect that would release the fission products into the coolant. However, since the amount of fuel in each particle is very small that, even with this assumption and under accident conditions, the release from the core would be so low that no offsite emergency measures would be required. Though it is recognised that the fuel cannot be made perfectly, the reactor is still safe because of the natural safety features (i.e. passive heat removal) that prevent fuel damage. One can therefore say that the quality of the fuel is a key factor in the safety of the pebble bed modular reactor.

Another safety issue that needs to be addressed with all graphite reactors is the ingress of air and water. The large mass of graphite in the pebble bed reactor core must be kept isolated from ingress of air or water to avert the potential for and the consequences of a graphite fire. In the event of ingress of air and water, the hot

graphite in the core would react with air and water in exothermic reactions. These reactions could lead to generation of carbon monoxide and hydrogen, both highly combustible gases which could result in core damage. Again, the ingress may inject positive reactivity at a rate that could result in fuel failure, before the said failure could be pre-empted by the negative reactivity feedback from the subsequent temperature increase.

Fortunately, the pebble bed reactor core does not contain water, nor zirconium that burn in air at high temperatures that could make the reactor reach the temperatures for melting the fuel. During a depressurised loss of forced cooling (D-LOFC), the negative temperature reactivity shuts down the chain reaction thus cutting off heat buildup in the core. Passive safety requires that the decay heat be removed from the core by conduction and radiation before the fuel reaches its failure temperatures [3, 5].

The key issues for the pebble bed reactor are the amount of air available to the core from the reactor cavity, the resistance of the pebble bed to natural circulation flow, and whether a chimney can form to allow a flow of air into the core. Tests and analysis shows that though at high temperatures, graphite is oxidised and consumed, the conditions that will require “burning” are not obtainable in pebble bed reactors, for example temperatures of the orders of 3,000 C [4].

Another safety issue is that the pebble bed reactor use a solid moderator (graphite) in the core which can at the same time be utilised as a structural material. The advantage of solid moderator is that the moderating behaviour is fairly constant, unlike water moderator in water cooled reactors that can change phase.

## **2.5. SAFETY SYSTEMS**

This section summarises only the designed safety features that are most important for the purpose of this study.

### **2.5.1. CORE CONDITIONING SYSTEM (CCS)**

The core conditioning system (CCS) removes core heat when the Brayton cycle is not operational, in order to facilitate start-up or cool-down operations. The CCS consists of two separate but identical systems each with 50% capability and is connected to the RPV and the power conversion unit (PCU) by feed and return pipes [16]. The CCS is manually activated and is designed to perform the following functions:

1. Cool the reactor down to a temperature that will allow a restart in the event of plant trip
2. Remove decay heat when the reactor is shut down and the Brayton cycle is not operational.
3. Before the Brayton cycle is initiated, the reactor is made critical with only the CCS in operation during start-up. Under this condition the CCS provides the required core mass flow and to remove core fission heat.

### 2.5.2. REACTOR CAVITY COOLING SYSTEM (RCCS)

The reactor cavity cooling system (RCCS) has the primary function of removing and dissipating to the sea or the environment the waste heat from the reactor cavity during all design base events ( i.e. all normal and upset events such as pressurised or depressurised loss of forced cooling). This is achieved through the circulation of water through the RCCS.

During normal operating modes, heat is removed from the core by the helium forced through the core by the power conversion unit (PCU) or by the core conditioning system (CCS). In the event that none of the above systems are available the negative temperature reactivity of the core would shut down the reactor and heat is removed from the fuel to the core structures and then to the reactor pressure vessel (RPV) through conduction and thermal radiation. The heat from the RPV is then transported to the cooling chambers of the cavity cooling system by convection and thermal radiation. This ensures that the maximum allowable RPV and fuel temperatures are not exceeded.

The RCCS consists of three identical cooling trains, where each train is an independent, low-pressure, closed-loop, pump-driven, water-based cooling system sized to dissipate 50% of the maximum heat rejected by the reactor under a depressurised loss of forced cooling event [16]. The system is made up of a series of low carbon steel water chambers that are arranged vertically around and concentric to the RPV with three inlet and outlet headers arranged around the top

of the chambers. To allow for free expansion and contraction, the structure is suspended from a support ring that rests on the concrete wall of the reactor cavity. Anti-siphoning device fitted to the system prevents the chambers from being emptied in the event of a low-level break in the pipe work outside of the reactor cavity.

The three cavity cooling systems are connected to a back-up cooling tower which comes on line automatically if a fault is detected in any of the cavity cooling system pumps. In the event of failure of the pumps and/or heat exchangers and the loss of the cooling towers, the water contained in the chambers heats up to the boiling point over a period of about twenty four (24) hours. Should the failure continue the hot water in the chambers is converted, over a period of about seven to nine days [16], to a low pressure steam which is released into the atmosphere. The ability of the RCCS to remove heat from the reactor cavity without external power source is one of the features that make the PBR an inherently safe nuclear reactor.

### 2.5.3. ACTIVE COOLING SYSTEM (ACS)

The active cooling system (ACS) is a water-based system with specific design and control components to cool the required high level systems and components. The ACS removes heat from the power conversion unit (PCU) (the pre-cooler, inter-cooler and generator) and from other auxiliary systems such as the RCCS and CCS and transfer the heat to the heat sink. The ACS is made up of four

subsections namely; the open circuit, the main closed circuit, the auxiliary closed circuit and the back-up cooling towers.

## **2.6. DEVELOPMENT CHALLENGES**

The development of the pebble bed reactor started in the late 1950's by the late Prof. Robert Schulten who is recognized as the "father" of the pebble bed technology. Critical pebble bed reactors have been built in Germany, Switzerland, Russia, Japan, The Netherlands, USA and China.

The construction of 110 MW<sub>th</sub> pebble bed modular reactor in South Africa (started after receiving a favourable record of decision in August 2003) has been uprated to 400 MW<sub>th</sub> (165 MW<sub>e</sub>) [4]. China has also developed a 10 MW<sub>th</sub> (4 MW<sub>e</sub>) prototype pebble bed reactor called HTR-10 after licensing the technology from Germany [17]. The reactor which is currently in operation is being used as a research demonstration plant facility to lay the grounds for full scale demonstration plant. The HTR-10 nuclear reactor in China achieved criticality in December 2000. In the Netherlands, Petten Research Institute is developing pebble bed reactors for industrial applications in the range of 15 MW<sub>th</sub> [4]. The inherently safe nature of the reactor and the on-line refueling are among the key considerations for the conceptual design of the modular pebble bed reactor being developed by the Massachusetts Institute of Technology (MIT) [18].

The development challenge of the pebble bed type high temperature nuclear reactor is that currently there is no operating reactor that can supply measurements on which the loads can be based or data for operational control. Thus, the reactor design currently rely on analysis and simulations to guide the development effort of new reactor concept, giving the designers “experience” of the behavior of this “virtual reactor”.

Another challenge is the coupling of the neutronic and thermo-hydraulic behavior of the reactor in a closed loop direct thermodynamic cycle. The result of this is that any change to a component in the cycle causes a change to the flow conditions, which affects all the components in the cycle.

The complex thermal flow design of the cycle requires the use of variety of analysis techniques and simulation tools ranging from the one-dimensional model that do not capture all the significant physical phenomena to large scale three-dimensional computational fluid dynamics codes that, for practical reasons cannot simulate the entire plant as a single integrated unit [19].

Using thermal-fluid network approach, reactor models for systems simulation have previously been developed in which a network of elements was assembled. Here, elements are one dimensional entities that represent either flow or heat transfer paths for convection, conduction and radiation. Du. Toit et al [20] used such approach, the element based approach in FLOWNEX, the code used for the

pebble bed modular reactor plant simulation. FLOWNEX allows detailed steady state and transient thermal-flow simulations of the complete power plant. A simplified model for the pebble bed nuclear reactor contained in FLOWNEX consists of three main parts namely: (a) heat transfer and fluid flow of the gas within the core, (b) heat conduction within pebbles, and (c) nuclear power and decay heat model.

The design and layout of the pebble bed modular reactor requires the need for the simulation of a wider range of reactor phenomena. Thus a theoretical basis and formulation of the thermal hydraulics of a more comprehensive reactor model capable of capturing the significant physical phenomena has been developed [19]. The pressure drop through the reactor core; the convective heat transport by the gas; the convective heat transfer between the gas and the solids; the radiative, contact and convective heat transfer between the pebbles and the heat conduction in the pebbles were accounted for in the model. Good comparison was obtained between the simulated and measured results from the SANA test rig (SANA was designed to provide a data basis for automatic heat removal from a pebble bed) indicating that the model sufficiently accounts for all the phenomena [19].

G. P. Greyvenstein and H.J Van Antwerpen [20] used a finite volume-based network method to predict heat, mass and momentum transfer in a pebble bed reactor. The model was much in greater detail that it can be used to validate other models and agreed excellently with the element-based reactor model.

Dudley T. et al [21] as a first step, developed a two dimensional thermal-hydraulic model configuration in the radial and axial directions which was subsequently extended to a three dimensional configuration. The developed three dimensional configuration represents the most comprehensive model to simulate the PBMR core thermal-hydraulics. Verification of thermo-dynamic and heat transfer properties of two steady state (100% and 40%) conditions between the three dimensional reactor core thermal-hydraulic model and FLOWNEX and TINTE design codes shows that the 100% steady state were accurate compared with the TINTE model while the 40% were reasonable but less accurate.

A three dimensional thermal-hydraulic code called TH3D is being developed at the Institute of Nuclear Technology and Energy Systems (IKE), University of Stuttgart with the objective of providing a tool which can be used to analyse , design, and safety related issues in high temperature reactors and modular HTR's [22]. The code covers operational conditions with forced cooling as well as accident situations with heat removal by conduction and natural circulation. The results of the new code TH3D compared to those of well known well established thermal-hydraulic code (such as THERMIX/KONVEK) generally show a good agreement.

Due to the complex geometry as well as the complex feeding and shutdown mechanisms of the pebble bed nuclear reactor, three dimensional nuclear heat production, gas flow and heat transport mechanisms was investigated by

employing the existing computational fluid dynamics code CFX-4 for the three dimensional analysis [23]. The results for both steady state and transient was validated by comparison with several steady state and transient experiments conducted at the SANA test rig and show good agreement with the experimental measurement of pebble temperature.

Simoneau et al [24] used the STAR-CD general computational fluid dynamics code to develop a three dimensional model that simulates the passive heat removal in a modular prismatic block high temperature reactor during a loss of active cooling accident. The model solves the combined convective, conductive and radiative heat transfer within a 30° section of the core and reactor vessel. Two commonly loss of active cooling scenarios was considered in the steady; depressurised conduction cooldown (DCC) and pressurised conduction cooldown (PCC). The results show that the effects of heat transfer through internal natural circulation is negligible during the depressurised event on the thermal behavior of the system.

Comparison of the PCC and DCC events shows that during PCC, extra convective heat transfer reduces the peak temperature of both the fuel and the pressure vessel. However, PCC events lead to thermal stratification and hence much higher temperatures in the upper reactor structures.

In the German AVR reactor, the inherently safe concept of the reactor was even tested by simply switching off the blower so that the cooling flow was completely stagnated. It was observed that the pebble temperature stayed well below those at which the particles release radioactive elements [4].

Van der Merwe et al [25] performed a numerical evaluation of the heat transfer correlation at the pebble bed-reflector interface for the South African pebble bed modular reactor and the results of two numerical codes, FLOWNEX and other codes (THERMIX, TINTE) were compared to experimental results from the SANA experimental test facility and the HTR-10 pebble bed reactor in China. The comparison with the SANA experimental facility confirmed the findings by other researchers that another correlation should be obtained for the effective conductivity at the interface boundary to remove any uncertainty by using a correction factor at the interface boundary. Comparison with the HTR-10 experimental results also indicated that the convection correlation displayed similar uncertainties under forced flow conditions.

The study also revealed that the porosity at the pebble bed reflector interface was outside the applicable range of the general heat transfer correlations and the smaller ratio of the core diameter to fuel element diameter ( $D/d$ ) has a more pronounced influence on heat transfer in the region. These uncertainties and limitations need to be investigated through derivation of new localized correction or modifications to existing correlations from experiments.

## **2.7. HEAT TRANSFER MECHANISM IN THE PEBBLE BED REACTOR**

The pebble bed type high temperature nuclear reactor unit heat transfer poses a challenge in that it includes a complex three dimensional geometry and various materials and fluid types. In the pebble bed zone, heat is generated inside spheres by nuclear reaction, conducted to the sphere surface and transferred to the fluid by convection.

When a temperature gradient exists across the bed, heat is transferred between pebbles by means of conduction through contact resistances as well as surface radiation [20, 26]. The challenge is to balance the thermal heat flux by minimising the heat loss from the reactor during normal operation and allowing sufficient heat to be removed from the core during a loss of forced cooling event [27].

In the pebble bed type high temperature nuclear reactor, heat transfer occurs among fuel pebbles, graphite blocks (moderator) or the reactor vessel (wall) and the coolant. These include convection heat transfer between the fluid and the fuel particles and between the fluid and the walls, conduction heat transfer between adjacent fuel particles and between fuel particles and the wall as well as radiation heat transfer between surfaces of particles and the walls.

The complexity of the heat transfer mechanism necessitates a heat transfer model that deals with radiation as well as thermal conduction and convection. In

pressurised water reactors (PWR), hundred percent (100%) of heat generated from the fuel rods is transferred to the coolant by convection [1]. However, in the case of gas cooled nuclear reactors, only part of the heat from the fuel pebbles is transferred to the coolant by convection. The remaining part is then transferred through conduction and surface radiation.

### 2.7.1. HEAT REMOVAL DURING NORMAL OPERATION

In the pebble bed, heat is generated by nuclear fission reaction in the fuel spheres. To remove the heat generated, the coolant (helium gas) enters the reactor pressure vessel at a specified inlet low temperature and pressure at the top. The coolant then flows down the core between the voids in the hot fuel spheres, extract the heat from the fuel spheres and exit the vessel at the bottom having being heated to a higher temperature. The hot helium is carried to a direct cycle helium gas turbine system or to an indirect helium to helium intermediate heat exchanger gas turbine system [8]. In most pebble bed modular reactors, the direct Brayton cycle as shown in Fig. 2.5 is chosen as the thermodynamic cycle for the high cycle efficiency that can be achieved [28].

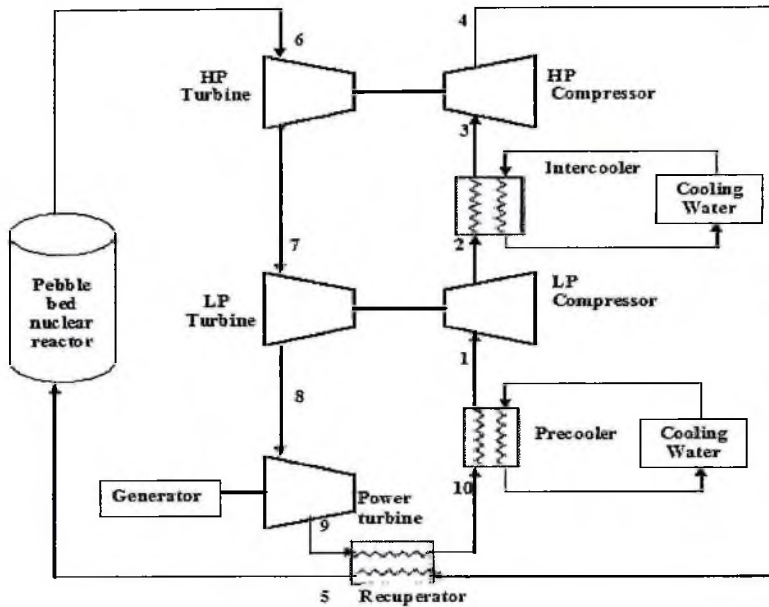


Figure 2.5: Schematic diagram of the three-shaft recuperated Brayton cycle[28].

Starting at point 1, helium at a low pressure and temperature, state 1, is compressed by a low pressure compressor (LPC) to an intermediate pressure, state 2. The helium then passes through inter-cooler which cools it to state 3. The helium at this point passes through a high pressure compressor (HPC) compressing it to state 4. Between states 4 and 5, the helium is preheated in a recuperator to give the initial pressure (P) and temperature (T) of the helium coolant before it enters the reactor core.

After flowing downward through the paths defined by the voids between pebbles in the reactor core, the helium extracts the heat from the fuel pebbles in the core to state 6 after which the hot high pressure helium is expanded in a high pressure

turbine (HPT) to state 7 and a further expansion takes place in a low pressure turbine (LPT) to state 8. The high pressure turbine drives the high pressure compressor while the low pressure turbine drives the low pressure compressor.

The heated helium at state 8 is further expanded in the power turbine (PT) which converts the energy in the gas to shaft power that is split between the work required to drive the compressor and the work required to drive the generator to state 9 which is approximately the same pressure at 10 and 1. From state 9 to 10, the still hot helium is cooled in the recuperator and further cooled in the pre-cooler to state 1 to complete the cycle. The heat rejected from state 9 to 10 is equal to the heat transferred to the helium from state 4 to 5.

Various valves are used for control of the cycle and the pressure in the circuit can be adjusted by the inventory control system (ICS) through injecting or extracting gas in the circuit. This is used to control the mass flow rate of the helium in the circuit. At normal operation, the design options which allow an increase in the average coolant outlet temperature while maintaining fuel temperature at acceptable levels, include reducing bypass flows and controlling flow distribution.

The bypass helium flows through the gaps between the blocks. The bypass flow cools the reflector but does not contribute to the nuclear heat removal.

The most limiting core design requirement which controls the core outlet temperature is the maximum acceptable fuel compact temperature. Two factors determine the ultimate fuel temperature during normal operation and following an event. These are;

1. Production of heat in the core which is dependent on the surface temperature of the pebble and the power generated by a pebble;
2. Removal of heat from the core;

### 2.7.2 DECAY HEAT REMOVAL

In the pebble bed type high temperature nuclear reactor, decay heat for example can be removed through conduction and radiation from the fuel to the reactor vessel and by radiation and natural convection from the reactor vessel to a water circuit which is located on the vault walls. Natural convection can also occur within the core during passive cooling in addition to conduction and thermal radiation.

However, if the circuit is depressurised, the convective heat transfer remains negligible [24]. This is known as depressurised conduction cooldown (DCC) or depressurised loss of coolant event which is the worst case accident event for modular pebble bed reactor when the forced cooling of the pebbles ceases and the vessel depressurises. The pebble bed modular reactor (PBMR) is able to withstand such events without significant core damage for two reasons [14, 29, 30]:

1. The PBMR has a strong negative fuel temperature feedback which inhibits the fission chain reaction with a modest increase in temperature;
2. Decay heat is transferred from the core to the surrounding reflector and containment through conduction and radiation at a sufficiently high rate to prevent the fuel from ever reaching failure temperature.

On the other hand, for pressurised conduction cooldown (PCC), that is when the circuit remains pressurised, the convective heat transfer becomes effective and as a result a different thermal response is observed in the core structures. Thus, PCC implies combined convective, conductive and radiative heat transfer and a combination of these heat transfer modes each with very dynamical characteristics pose a computational challenge.

An important phenomenon of the decay heat removal is that the heat transfer mechanism of the pebble bed modular reactor is passive and does not require helium coolant pressure. The annular core geometry also provides for short heat transfer path to the outside of the RPV resulting in acceptable fuel temperatures.

In a packed bed, the overall heat transfer is considered to consist of [31];

1. The conduction heat transfer in both the radial and axial directions between the particles in the bed
2. The convective heat transfer between the bed particles and the flowing gas

3. The heat transfer due to the effect of the convective mode on the conduction
4. The heat transfer due to radiation. This can take place between (a) the bed particles (b) the flowing gas and the wall and (c) the bed particles and the flowing gas
5. The wall to bed heat transfer consisting of the heat transfer between (a) the bed wall and the bed particles and (b) the bed wall and the flowing medium.

The most obvious heat transfer mode from the fuel is the convective heat transfer to the interstitial fluid, as this has the largest contact surface with the fuel. Heat conduction in the radial and axial direction is also important due to temperature gradient in the radial and axial directions.

## **2.8. EFFECTS OF POROSITY ON HEAT AND MASS TRANSFER OF THE PBR**

The pebble bed reactor can be considered as a fixed or a packed bed reactor [32]. Packed bed reactor design is based upon the mechanisms of heat and mass transfer, and the flow and pressure drop of the fluid through the bed of solids [32-35]. These mechanisms are all influenced by the porosity of the packed bed. The porosity of a packed bed reactor vary sharply near the wall resulting in a severely distorted velocity profile near the wall which reaches a maximum in the near-wall region. This phenomenon is known as flow or wall channeling.

For the pebble bed reactor, wall channeling may lead to a reduction in the wall temperature and an increase in the graphite reflector life-time. Wall channeling may also lead to a non-uniform temperature distribution at the outlet of the bed. Therefore, knowledge of the porosity distribution within a packed bed is important to any rigorous analysis of the transport phenomena of the pebble bed reactor.

Vortmeyer and Shuster [36] confirmed the wall channeling phenomena when they evaluated the steady state flow profiles in rectangular and circular packed beds. Bedenig [32] determined the variation of the porosity of the bed as a function of the height from the bottom of the reactor. The results show that the porosity near the bottom is large and diminishes rapidly away from the bottom.

The experimental study of Goodling et al [37] demonstrated the periodic variation in the porosity away from a containing wall. Furthermore it was observed from the study that the radial porosity distribution exhibited an exponential variation combined with a damped oscillation.

The periodic variation in the porosity away from a containing wall was also confirmed by the investigation of Sederman et al [38] using magnetic resonance imaging technique to study the radial porosity distribution in cylindrical packed beds filled with water.

Therefore in the design and analysis of pebble bed reactor, it is important that the occurrence of flow distortions should be investigated to determine the effect it has on all the associated phenomena in the reactor. This requires knowledge of the variation of the porosity in packed beds.

C. G. Du Toit [32] analysed the variation of the porosity in the axial and radial directions numerically. The typical damped oscillatory variation in the porosity near the wall and bottom was observed and was found to be in good agreement with what had been found by Goodling et al [37] and Sederman et al [38]. The results also show that the oscillations are damped out after which the porosity hovers around 0.39, which was specified as the bulk porosity.

## 2.9 SUMMARY

In conclusion, a major safety basis of the pebble bed type high temperature nuclear reactor is the low power density and large thermal capacity, together with the high temperature resistance of the fuel. The provision of safety systems such as the reactor cavity cooling system, the core conditioning system and the active cooling system are among the design characteristics that makes the pebble bed modular reactor inherently safe. The passive removal of decay heat through natural processes of convection, conduction and radiation during depressurised loss of forced cooling and the ability of the fuel particle to retain fission products to high temperatures up to 1600 °C are all features that make the pebble bed modular reactor inherently safe.

In order to maintain the safety features which the pebble bed modular reactor is known for, more and more interest have to be focused on the thermal response of the reactor with respect to heat removal during normal operation and decay heat following a depressurised loss of forced cooling. Computerised simulations have been developed to analyse various aspects of the thermal characteristics of the pebble bed type high temperature nuclear reactor.

In this research, an analytical model of the fluid flow and heat transfer phenomena in the reactor core as well as the pressure drop in the pebble bed was developed to solve the heat transfer and fluid flow equations in the pebble bed core. A simulation code (PEBTAN) written in FORTRAN 95 was also developed to enable the simulation of various scenarios and conditions. By so doing, it was possible to predict the thermal response of the pebble bed type high temperature nuclear reactor.

In the next chapter, the mathematical model of the pebble bed reactor heat transfer and pressure drop and the PEBTAN code for thermal analysis are presented.

## CHAPTER THREE

### METHODOLOGY

#### 3.1. INTRODUCTION

The chapter discusses the mathematical model of the pebble bed reactor heat transfer and the loss of pressure through friction in the pebble bed. A simulation code called PEBTAN developed to solve the model is also presented.

The most obvious heat transfer mode from the fuel pebble during normal operation is the convection heat transfer to the interstitial fluid (helium gas), as the fluid has the largest contact surface with the fuel. Heat conduction in the radial and axial direction is also important due to temperature gradient in the radial and axial directions. During extreme loss of pressurised flow, heat is transferred from the core by conduction and radiation.

The following are accounted for in the analysis;

1. The pressure drop through friction over the core
2. The heat transfer coefficient between the pebbles and the gas
3. The effective thermal conductivity of the packed bed.

The pressure drop across the bed was calculated using the Ergun equation. The correlation by Kugeler and Schulten was used to tabulate the convective heat transfer to the interstitial fluid. The Zehner Schluender correlation was used to

tabulate a complex relation that combines the conduction through the pebbles, the conduction through the gas between the pebbles and the conductance by radiation in both the radial and axial directions. In all these, the pebble bed was considered as having a uniform porosity or void fraction.

The large scatter in the results of pressure drop through packed beds was mostly due to the essential effects the porosity has on the pressure drop. The strong influence the porosity has on pressure drop causes a non-uniform velocity distribution across the pebble bed. Again the radial variation of porosity generates a near-wall bypass flow resulting in higher velocity near the wall which is not only important for the local flow and heat transfer in the region, but also influences the total pressure drop. Therefore a model of the influence of porosity on heat transfer and pressure drop has been developed to analyse the sensitivity of heat transfer and pressure drop to changes in the porosity.

In the following subsection, the mathematical formulation of the model comprising the pressure drop, the convection heat transfer, the temperature profile in the fuel pebble and heat conductivity in packed beds have been discussed in more detail.

The last section explains how the code solved the heat transfer equations and the pressure drop in the bed.

## 3.2. MATHEMATICAL MODEL OF THE PEBBLE BED REACTOR HEAT TRANSFER AND PRESSURE DROP

### 3.2.1. PRESSURE DROP

The pressure drop through friction across the pebble bed is an important phenomenon that ultimately affects the heat transfer effectiveness. The importance of the pressure drop is such that it enables proper sizing of the turbo-machines and also determine the flow distribution through the core structures consisting mainly of graphite blocks. Although the leakage or bypass flow through the core structures is minimised by design, large pressure drop over the pebble bed will cause leakage or bypass flow to occur.

The leakage or bypass flow cools the reflector encircling the core and does not contribute to the core heat transfer process. The leakage (bypass flow) should therefore be minimised to ensure that the helium coolant passes through the pebble bed and therefore minimised the temperature of the pebbles during normal operation. This is necessary since lower temperatures during normal operation will lead to lower temperatures during loss of forced cooling events.

The pressure drop ( $\Delta P$ ) of the flow through a pebble bed of height H can be expressed as [39]

$$\Delta P = \psi \frac{H}{d_h} \frac{\rho}{2} u_p^2 \quad (3.1)$$

where  $\psi$  is the pressure drop coefficient, which is dependent on Reynolds number (Re) defined as

$$\text{Re}_h = \frac{d_h u_p \rho}{\eta} = \left( \frac{(m/A) d_h}{\eta} \right) \quad (3.2)$$

$d_h$  is hydraulic diameter of pebbles forming the bed (i.e. the equivalent diameter of a circular cross section which yields the same force balance as that for a non-circular cross section),

$\rho$  is density of the fluid (helium gas),

$\eta$  is dynamic viscosity of the fluid (helium gas),

$u_p$  is mean velocity of the gas between the particles,

$A$  is vessel cross sectional area,

$\dot{m}$  is mass flow rate of gas in the bed

$\text{Re}_h$  is Reynolds number corresponding to the hydraulic diameter.

The pebble bed reactor can be considered as a fixed or packed bed reactor [32]. The design of packed bed reactor is based upon the mechanisms of heat and mass transfer and the flow and pressure drop of the fluid through the bed of solids. Therefore knowledge of the porosity distribution within a packed bed is important to any rigorous analysis of the transport phenomena in the bed since the mechanisms such as heat and mass transfer and the flow and pressure drop of the fluid through the bed of solids are all sensitive to the porosity of the packed bed.

Consider the packed bed to consist of spheres of equal diameter (uniform spheres),  $d_h$  and  $u_p$  can be expressed in terms of quantities that can directly be measured. By taking  $d$  as the sphere diameter, (diameter of pebbles forming the bed), and  $\varepsilon$  as the porosity, the porosity can be expressed as,

$$\varepsilon = 1 - \frac{V_s}{V} \quad (3.3)$$

where  $V_s$  is the volume of all spheres and  $V$  is the total volume of the packed bed.

and

$$d_h = \frac{4(V - V_s)}{\frac{2}{3}A_s} \quad (3.4)$$

For a sphere, the area ( $A_s$ ) and volume ( $V_s$ ) can respectively be expressed as

$$A_s = 4\pi r^2 \text{ and } V_s = \frac{4}{3}\pi r^3 \quad (3.5)$$

Expressing  $A_s$  in terms of  $V_s$ , gives

$$A_s = \frac{4}{3}\pi r^3 \frac{3}{r} = \frac{3V_s}{r} \quad (3.6)$$

But  $r = \frac{d}{2}$ . Substituting this into equation (3.6) simplifies to

$$A_s = \frac{6V_s}{d} \quad (3.7)$$

Substituting equation (3.7) into equation (3.4), and after simplification, equation (3.8) is obtained.

$$d_h = \frac{4(V - V_s)}{\frac{2}{3} \frac{6V_s}{d}} = \frac{d(V - V_s)}{V_s} = d \left( \frac{V}{V_s} - 1 \right) \quad (3.8)$$

But from equation (3.3),  $\frac{V}{V_s} = \frac{1}{1 - \varepsilon}$  (3.9)

Substituting equation (3.9) into (3.8), gives

$$d_h = d \left( \frac{1}{1-\varepsilon} - 1 \right) = d \left( \frac{1-1+\varepsilon}{1-\varepsilon} \right) = d \left( \frac{\varepsilon}{1-\varepsilon} \right) \quad (3.10)$$

The mean velocity  $u_p$  of the gas between the particles relate to the mean velocity of flow as  $u = \varepsilon u_p$ . Thus,

$$u_p = \frac{u}{\varepsilon} \quad (3.11)$$

Substituting equations (3.10) and (3.11) into equations (3.1) and (3.2) gives,

$$\Delta P = \psi \frac{H}{d \left( \frac{\varepsilon}{1-\varepsilon} \right)} \frac{\rho u^2}{2 \varepsilon^2} = \psi \frac{H 1-\varepsilon}{d \varepsilon^3} \frac{\rho}{2} u^2 = \psi \frac{H 1-\varepsilon}{d \varepsilon^3} \frac{1}{2\rho} \left( \frac{m}{A} \right)^2 \quad (3.12)$$

where  $\rho u = \frac{m}{A}$

$$\text{And } \text{Re}_h = \frac{d \left( \frac{\varepsilon}{1-\varepsilon} \right) \frac{u}{\varepsilon} \rho}{\eta} = \frac{\rho u d}{\eta(1-\varepsilon)} = \frac{\left( \frac{m}{A} \right) d}{\eta(1-\varepsilon)} \quad (3.13)$$

$$\text{But } \text{Re} = \frac{\rho u d}{\eta} = \frac{\left( \frac{m}{A} \right) d}{\eta} \quad (3.14)$$

$$\text{Hence } \text{Re}_h = \frac{\text{Re}}{1-\varepsilon} \quad (3.15)$$

Re-arranging equation (3.12) and making  $\psi$  the subject of the equation, equation (3.16) is obtained

$$\psi = \frac{d}{H} \frac{\varepsilon^3}{1-\varepsilon} \frac{\Delta P}{\frac{\rho}{2} u^2} = \frac{d}{H} \frac{\varepsilon^3}{1-\varepsilon} \frac{\Delta P}{\frac{1}{2\rho} \left(\frac{m}{A}\right)^2} \quad (3.16)$$

The dependence of the pressure drop coefficient on Reynolds number has been investigated by numerous experimenters for unique size spherical packing, multi-size spherical packing and multi-shape packing [39].

For application to the pebble bed type high temperature nuclear reactor of fixed randomly packed bed with spherical particles, the dependence of  $\psi$  on Re is given by the correlation [39, 40, 41];

$$\psi = \frac{320}{\frac{\text{Re}}{1-\varepsilon}} + \frac{6}{\left(\frac{\text{Re}}{1-\varepsilon}\right)^{0.1}} \quad (3.17)$$

with  $10^0 < \frac{\text{Re}}{1-\varepsilon} < 10^5$  and  $0.36 < \varepsilon < 0.42$

The first term of equation (3.17) represents the asymptotic solution for laminar flow while the second term represents the turbulent flow. That is,

$$\psi_l = 320 \left(\frac{\text{Re}}{1-\varepsilon}\right)^{-1} \text{ and } \psi_t = 6 \left(\frac{\text{Re}}{1-\varepsilon}\right)^{-0.1} \quad (3.18)$$

where  $\psi_l$  and  $\psi_t$  represents the pressure drop coefficient for laminar and turbulent flow respectively.

The effect of porosity on pressure drop was investigated from equation (3.17) by assuming that

$$\psi = A \left( \frac{\text{Re}}{1-\varepsilon} \right)^{-n} = A(1-\varepsilon)^n \text{Re}^{-n} \quad (3.19)$$

where  $n = 1.0$  for laminar flow and  $n = 0.1$  for turbulent flow.

From equation (3.19), equation (3.12) can be written as

$$\Delta P = A(1-\varepsilon)^n \text{Re}^{-n} \frac{H}{d} \frac{\rho}{2} u^2 \frac{1-\varepsilon}{\varepsilon^3} \quad (3.20)$$

From the relation

$$\frac{d\Delta P}{\Delta P} = \frac{\partial(\Delta P)}{\partial \varepsilon} \frac{d\varepsilon}{\Delta P} \quad (3.21)$$

Differentiating equation (3.20) with respect to  $\varepsilon$  gives

$$d\Delta P = A \text{Re}^{-n} \frac{H}{d} \frac{\rho}{2} u^2 \left[ -n(1-\varepsilon)^{n-1} + \left( \frac{-\varepsilon^3 - (1-\varepsilon)3\varepsilon^2}{\varepsilon^6} \right) \right] d\varepsilon \quad (3.22)$$

$$d\Delta P = A \text{Re}^{-n} \frac{H}{d} \frac{\rho}{2} u^2 \left[ -n(1-\varepsilon)^{n-1} + \left( \frac{3\varepsilon^3 - 3\varepsilon^2 - \varepsilon^3}{\varepsilon^6} \right) \right] d\varepsilon$$

$$d\Delta P = A \text{Re}^{-n} \frac{H}{d} \frac{\rho}{2} u^2 \left[ -n(1-\varepsilon)^{n-1} + \left( \frac{2\varepsilon^3 - 3\varepsilon^2}{\varepsilon^6} \right) \right] d\varepsilon$$

$$d\Delta P = A \text{Re}^{-n} \frac{H}{d} \frac{\rho}{2} u^2 \left[ -n(1-\varepsilon)^{n-1} + \frac{\varepsilon^2}{\varepsilon^6} (2\varepsilon - 3) \right] d\varepsilon \quad (3.23)$$

Dividing equation (3.23) by equation (3.20) gives

$$\frac{d\Delta P}{\Delta P} = \frac{A \text{Re}^{-n} \frac{H}{d} \frac{\rho}{2} u^2 \left[ -n(1-\varepsilon)^{n-1} + \frac{\varepsilon^2}{\varepsilon^6} (2\varepsilon - 3) \right] d\varepsilon}{A(1-\varepsilon)^n \text{Re}^{-n} \frac{H}{d} \frac{\rho}{2} u^2 \frac{1-\varepsilon}{\varepsilon^3}} \quad (3.24)$$

Equation (3.24) is simplified to get

$$\frac{d\Delta P}{\Delta P} = \left[ -n(1-\varepsilon)^{n-1} + \frac{\varepsilon^2}{\varepsilon^6}(2\varepsilon-3) \right] d\varepsilon \times \left[ (1-\varepsilon)^{-n} \left( \frac{\varepsilon^3}{1-\varepsilon} \right) \right]$$

$$\frac{d\Delta P}{\Delta P} = -n(1-\varepsilon)^{n-1} (1-\varepsilon)^n \left( \frac{\varepsilon^3}{1-\varepsilon} \right) d\varepsilon + \frac{\varepsilon^2}{\varepsilon^6} (2\varepsilon-3) (1-\varepsilon)^{-n} \left( \frac{\varepsilon^3}{1-\varepsilon} \right) d\varepsilon$$

$$\frac{d\Delta P}{\Delta P} = \frac{-n(1-\varepsilon)^{-1} \varepsilon^3}{(1-\varepsilon)} d\varepsilon + \frac{2\varepsilon-3}{(1-\varepsilon)^n (1-\varepsilon)} \frac{d\varepsilon}{\varepsilon}$$

$$\frac{d\Delta P}{\Delta P} = \frac{-n(1-\varepsilon)^{-1} \varepsilon d\varepsilon}{(1-\varepsilon)\varepsilon \times \varepsilon^{-3}} + \frac{2\varepsilon-3}{(1-\varepsilon)^n (1-\varepsilon)} \frac{d\varepsilon}{\varepsilon} \quad (3.25)$$

Further simplification of equation (3.25) reduces to

$$\frac{d\Delta P}{\Delta P} = \frac{-n\varepsilon}{1-\varepsilon} \frac{d\varepsilon}{\varepsilon} + \frac{2\varepsilon-3}{1-\varepsilon} \frac{d\varepsilon}{\varepsilon} = -\frac{3-\varepsilon(2-n)}{1-\varepsilon} \frac{d\varepsilon}{\varepsilon}$$

$$\frac{d\Delta P / \Delta P}{d\varepsilon / \varepsilon} = -\frac{3-\varepsilon(2-n)}{1-\varepsilon} \quad (3.26)$$

In the pebble bed type high temperature nuclear reactor, the core diameter to fuel element diameter ratio  $\frac{D}{d}$  is very large and that the wall effects on the overall flow through the pebble bed is negligibly small. Thus, to investigate the effects of the  $\frac{D}{d}$  ratio on pressure drop, the average porosity  $\varepsilon$ , which is dependent on  $\frac{D}{d}$  should be taken into account.

From the experimental results of Carman and Barthels [39], the average porosity was estimated to be

$$\varepsilon_i = \frac{0.78}{(D/d)^2} + 0.375 \quad (3.27)$$

Substituting equation (3.27) into equations (3.12) and (3.16) gives

$$\Delta P = \psi_i \frac{H}{d} \frac{1 - \varepsilon_i}{\varepsilon_i^3} \frac{1}{2\rho} \left( \frac{m}{A} \right)^2 \quad (3.28)$$

And

$$\psi_i = \frac{320}{\text{Re}} + \frac{6}{\left( \frac{\text{Re}}{1 - \varepsilon_i} \right)^{0.1}} \quad (3.29)$$

where  $\varepsilon_i$  is defined by equation (3.27)

### 3.2.2. CONVECTIVE HEAT TRANSFER

Convective heat transfer from the fuel to the interstitial fluid is the most obvious heat transfer mode as the fluid has the largest contact surface with the fuel.

Properties such as Reynolds number, Schmidt number, Prandtl number and porosity all have effect on the effectiveness of heat transfer from spheres of fixed packed bed to the coolant. Figure 3.1 shows a model of three heat transfer regions when computing pebble temperature.

The coolant temperature surrounding the pebble is assumed to be constant and all the thermal power is assumed to be generated within the fuelled region of the pebble, conducted through the graphite shell and deposited into the coolant by

convection. Though neutron thermalisation and gamma heating result in heat being generated in the graphite shell region, the error introduced by this assumption is well within the accuracy limits of this analysis [7].

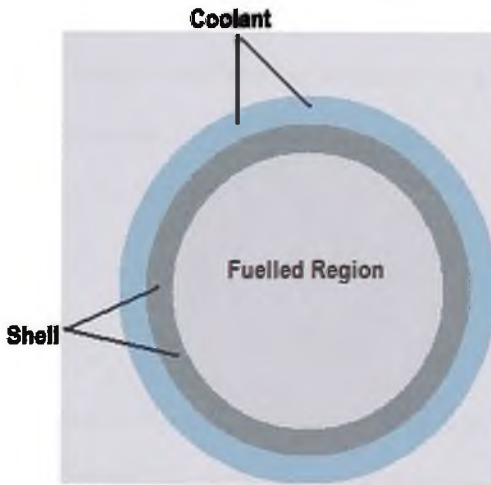


Fig. 3.1: Heat transfer model of pebble cooling

From Newton's law of cooling, the heat flow ( $Q$ ) from the pebble surface to the fluid is proportional to the surface area  $A_p$  for heat transfer and the difference between the gas temperature  $T_g$  and the surface temperature  $T_{surf}$  of the solid structure.

Mathematically

$$Q = \alpha A_p (T_{surf} - T_g) \quad (3.30)$$

where  $A_p$  is the pebble surface area and  $\alpha$  is the convective heat transfer coefficient.

From equation (3.30), the heat flux  $q$  is expressed as

$$q = \alpha \Delta T \quad (3.31)$$

where  $\Delta T$  is the average temperature difference between the surface and the bulk of the gas.

The heat transfer coefficient  $\alpha$  expresses the proportion and contains everything that is not known of the heat transfer process.

From equation (3.31)

$$\alpha = \frac{q}{\Delta T} \quad (3.32)$$

In order to describe the heat transfer in the pebble bed reactor correctly, relations must be defined for the heat transfer by forced convection in a dimensionless form as,

$$Nu_h = \frac{\alpha d_h}{\lambda} = f(\text{Re}_h; \text{Pr}) \quad (3.33)$$

where  $\lambda$  is the thermal conductivity of the coolant (helium gas),  $\text{Pr}$  is the Prandtl number and  $Nu_h$  is the Nusselt number corresponding to the hydraulic diameter.

From equation (3.10) and (3.14)

$$d_h = d \left( \frac{\varepsilon}{1-\varepsilon} \right) \text{ and } \text{Re}_h = \frac{\text{Re}}{1-\varepsilon} \text{ respectively.}$$

Substituting into equation (3.33) gives

$$Nu = \frac{\alpha d}{\lambda} \left( \frac{\varepsilon}{1-\varepsilon} \right) = f \left( \frac{\text{Re}}{1-\varepsilon}; \text{Pr} \right) \quad (3.34)$$

Rearranging equation (3.34),

$$Nu = \frac{\alpha d}{\lambda} = \frac{1-\varepsilon}{\varepsilon} f\left(\frac{Re}{1-\varepsilon}; Pr\right) \quad (3.35a)$$

and 
$$\alpha = \frac{\lambda Nu}{d} \quad (3.35b)$$

The Nusselt number (Nu) gives the ratio of convective heat transfer to conductive heat transfer using the fluid thermal conductivity, the heated equivalent diameter and the heat transfer coefficient. It measures the enhancement of heat transfer from a surface that occurs in a real situation, compared to the heat transfer if just conduction occurred. The Reynolds number gives the ratio of the inertia forces to viscous forces, using the mass flow rate, the flow area, the dynamic viscosity and the equivalent diameter. The Prandtl number gives the ratio between the hydrodynamic and thermal boundary layer thickness, using the specific heat capacity of the fluid, the dynamic viscosity and the thermal conductivity of the fluid.

Equation (3.35a) is generally written in the form [39]

$$Nu = a \frac{1-\varepsilon}{\varepsilon} \left(\frac{Re}{1-\varepsilon}\right)^{n'} Pr^m \quad (3.36)$$

where 'a' is a constant and  $n' = 0.6$  for Reynolds number range  $5 \times 10^2 < Re < 10^4$  and  $m = 1/3$ .

To investigate the influence of porosity on convective heat transfer, we can write the expression

$$\frac{d(Nu)}{Nu} = \frac{\partial(Nu)}{\partial \varepsilon} \frac{d\varepsilon}{Nu} \quad (3.37)$$

By differentiating equation (3.36), the following expression is obtained

$$d(Nu) = a \text{Pr}^m \left[ \frac{-\varepsilon - (1-\varepsilon)}{\varepsilon^2} + n' \left( \frac{\text{Re}}{1-\varepsilon} \right)^{n'-1} \left( \frac{\text{Re}}{(1-\varepsilon)^2} \right) \right] d\varepsilon \quad (3.38a)$$

$$d(Nu) = a \text{Pr}^m \left[ \frac{-\varepsilon - (1-\varepsilon)}{\varepsilon^2} + n' \left( \frac{\text{Re}}{1-\varepsilon} \right)^{n'} \left( \frac{1}{1-\varepsilon} \right) \right] d\varepsilon \quad (3.38b)$$

Equation (3.38b) is divided by equation (3.36) to obtain equation (3.39)

$$\frac{d(Nu)}{Nu} = \frac{a \text{Pr}^m \left[ \frac{-\varepsilon - (1-\varepsilon)}{\varepsilon^2} + n' \left( \frac{\text{Re}}{1-\varepsilon} \right)^{n'} \left( \frac{1}{1-\varepsilon} \right) \right] d\varepsilon}{a \text{Pr}^m \left[ \left( \frac{1-\varepsilon}{\varepsilon} \right) \left( \frac{\text{Re}}{1-\varepsilon} \right)^{n'} \right]} \quad (3.39)$$

After rearrangement, equation (3.39) becomes

$$\frac{d(Nu)}{Nu} = \left[ \left\{ -1 - \frac{(1-\varepsilon)}{\varepsilon} \right\} \left( \frac{1}{1-\varepsilon} \right) \left( \frac{\text{Re}}{1-\varepsilon} \right)^{n'} + \frac{n' \varepsilon}{(1-\varepsilon)(1-\varepsilon)} \right] d\varepsilon \quad (3.40)$$

As  $n' \ll 0$ ,  $\left( \frac{\text{Re}}{1-\varepsilon} \right)^{n'} \Rightarrow 1$ .

Equation (3.40) is simplified to the form

$$\frac{d(Nu)}{Nu} = \left[ \frac{1}{1-\varepsilon} + \frac{1-\varepsilon}{(1-\varepsilon)\varepsilon} - \frac{n' \varepsilon}{(1-\varepsilon)^2} \right] d\varepsilon$$

$$\frac{d(Nu)}{Nu} = -\frac{d\varepsilon}{1-\varepsilon} \left[ \frac{1-n' \varepsilon}{\varepsilon} \right]$$

$$\frac{d(Nu)}{Nu} = -\frac{1-n'\varepsilon}{1-\varepsilon} \frac{d\varepsilon}{\varepsilon}$$

$$\frac{d(Nu)/Nu}{d\varepsilon/\varepsilon} = -\frac{1-n'\varepsilon}{1-\varepsilon} \quad (3.41)$$

To adequately account for convective heat and mass transfer, a relationship among Nusselt number, Reynolds number, Prandtl number and porosity needs to be established. In a paper published by Gnielinski [39, 42], experimental results of about 20 authors were evaluated to establish this relationship. In establishing the relationship, it was assumed that the heat transfer of spheres in a pebble bed can be related to the heat transfer from a single sphere by introducing an arrangement factor  $f\varepsilon$ , which depends on the porosity.

From the evaluation study and assumption, the following relationship was established [39, 42].

$$\text{i.e.} \quad Nu = f\varepsilon \times Nus \quad (3.42)$$

$$\text{where} \quad f\varepsilon = 1 + 1.5(1 - \varepsilon) \quad (3.43)$$

and Nus is the Nusselt number of a single sphere expressed as [39]

$$Nus = 2 + \sqrt{Nu_l^2 + Nu_t^2} \quad (3.44)$$

with  $Nu_l$  and  $Nu_t$  being Nusselt number of the single sphere for laminar and turbulent flow respectively.

Putting equations (3.42), (3.43) and (3.44) together leads to the expression

$$Nu = [1 + 1.5(1 - \varepsilon)] \times \left[ 2 + \sqrt{Nu_i^2 + Nu_t^2} \right]$$

which is further simplified to the form

$$Nu = (2.5 - 1.5\varepsilon) \times \left( 2 + \sqrt{Nu_i^2 + Nu_t^2} \right) \quad (3.45)$$

In the evaluation of  $Nu_i$  and  $Nu_t$ , Gnielinski [39, 42] used the idea that the heat transfer from arbitrary particles can be predicted by applying the equations for a flat plate if a suitable length scale and velocity are introduced. The length scale is the distance travelled by a fluid particle on its way along the body expressed as  $L = \frac{A_x}{S}$  where  $A_x$  is the heat exchanging surface area and  $S$  is the circumference of the aspect contour.

Relating the flat plate to the sphere,

$$L = \frac{\pi d^2}{\pi d} = d \quad (3.46)$$

i.e. for spherical particles the length scale is equal to the sphere diameter. The characteristics velocity is the mean velocity of the pores as defined by equation (3.11).

Thus, according to Gnielinski [39, 42] the Nusselt number for laminar and turbulent flows are respectively expressed as

$$Nu_i = 0.664 \left( \frac{Re}{\varepsilon} \right)^{1/2} Pr^{1/3} \quad (3.47)$$

and

$$Nu_t = \frac{0.037 \left( \frac{Re}{\varepsilon} \right)^{0.8} Pr}{1 + 2.443 \left( \frac{Re}{\varepsilon} \right)^{-0.1} \left( Pr^{\frac{2}{3}} - 1 \right)} \quad (3.48)$$

The heat transfer coefficient can therefore be evaluated from the definition of Re and Nu for  $5 \times 10^2 < Re < 10^4$  and Re up to  $5 \times 10^5$  with  $0.36 < \varepsilon < 0.42$ .

### 3.2.3. TEMPERATURE PROFILE IN THE FUEL PEBBLE

The distribution of temperature in the fuel pebble is computed using a one dimensional model of heat generation and conduction through a uniform sphere. For both normal and severe accident conditions, the fuel temperature must be kept below specified limits (1600 °C). Heat is removed from the fuel pebble by the primary coolant during normal operation and by conduction and radiation during extreme loss of pressurised flow events.

There are three heat transfer regions as shown in fig 3.1 which must be determined for the pebble. The modular pebble bed reactor fuel consists of a central fuel zone (with radius  $R_{fz}$ ), surrounded by a layer of pure graphite (with radius  $R_{peb}$ ). The coolant surrounds the fuel pebble.

The temperature profile within the pebble is a function of the power produced within the pebble, and the material properties of the fuel zone, outer graphite layer and the coolant. The coolant temperature surrounding the pebble is assumed to be uniform. The temperature profile inside a fuel pebble is determined by assuming

that the TRISO particles are evenly dispersed, so that the inner fuel zone of the pebble has a uniform volumetric power density. Consequently all the thermal power is assumed to be generated within the fuelled region of the pebble, conducted through the graphite shell, and deposited into the coolant by convection. Neutron thermalization and gamma heating in the graphite shell region also generate heat in the fuel pebble. However, the error introduced as a result of this assumption is considered to be within the accuracy limits [7, 43].

Thus for the temperature in the three zones of the fuel pebble (fuel zone, graphite shell and the coolant) the following equations apply [43]:

1. Fuel region (zone I)

$$\frac{1}{r^2} \frac{d}{dr} \left( r^2 \lambda_I \frac{dT_I}{dr} \right) + q_v = 0, \quad (3.49)$$

where

$r$  is radius of the fuel,

$\lambda_I$  is thermal conductivity of the material in the fuel region,

$T_I$  is temperature in the fuel region

$q_v$  is volumetric power density in the fuel zone, assumed to be uniform.

2. Graphite shell (zone II)

$$\frac{1}{r^2} \frac{d}{dr} \left( r^2 \lambda_{II} \frac{dT_{II}}{dr} \right) = 0 \quad (3.50)$$

where

$\lambda_{II}$  is thermal conductivity of the material in the graphite zone.

$T_{II}$  are temperature in the graphite zone.

### 3. Coolant region

$$4\pi R_{peb}^2 \alpha (T_{surf} - T_g) - \frac{4}{3} q_v \pi R_{fz}^3 = 0 \quad (3.51)$$

where

$T_{surf} - T_g$  is temperature difference between the pebble surface and the bulk coolant.

The volumetric power density is related to the volumetric core power density ( $Q_c$ ) by [43]

$$q_v = \frac{Q_c}{1 - \varepsilon} \left( \frac{R_{peb}}{R_{fz}} \right)^3 \quad (3.52)$$

And

$$Q_c = \frac{P_w}{\pi R_c^2 H} [\text{W/m}^3] \quad (3.53)$$

$P_w$  is core power,  $R_c$  is core radius and  $H$  is core height

From equation (3.49), assuming  $\lambda_f$  is constant with temperature and multiplying

through by  $\frac{r^2}{\lambda_f}$ , leads to the expression

$$\frac{d}{dr} \left( r^2 \frac{dT_f}{dr} \right) = -\frac{q_v r^2}{\lambda_f} \quad (3.54)$$

Integrating equation (3.54) gives

$$r^2 \frac{dT_f}{dr} = -\frac{q_v r^3}{3\lambda_f} + C_1 \quad (3.55)$$

Dividing equation (3.55) by  $r^2$ , leads to

$$\frac{dT_I}{dr} = -\frac{q_v r}{3\lambda_l} + C_1 r^{-2} \quad (3.56)$$

Integrating equation (3.56) gives

$$T_{I(r)} = -\frac{q_v r^2}{6\lambda_l} - \frac{C_1}{r} + C_2 \quad (3.57)$$

where  $C_1$  and  $C_2$  are constants.

Boundary conditions (BC):

Applying BC 1;  $\frac{dT_I}{dr} = 0$ , for;  $r = 0$  to equation (3.56), gives

$$C_1 = 0$$

Thus, equation (3.57) reduces to

$$T_{I(r)} = -\frac{q_v r^2}{6\lambda_l} + C_2 \quad (3.58)$$

and BC2;  $T_I = T_m$ , for;  $r = 0$  to equation (3.58), gives

$$T_m = C_2$$

Hence equation (3.58) reduces to

$$T_{I(r)} = -\frac{q_v r^2}{6\lambda_l} + T_m \quad (3.59)$$

From equation (3.59)

$$T_{I(r)} - T_m = \Delta T_I = -\frac{q_v r^2}{6\lambda_l} \quad (3.60)$$

For  $r = R_{fz}$ ,

$$\Delta T_I = -\frac{q_v R_{fz}^2}{6\lambda_I} = -\frac{q_p}{8\lambda_I \pi R_{fz}} \quad (3.61)$$

where  $q_p$  is the power produced in the pebble and is expressed as

$$q_p = \frac{1}{3} q_v \pi R_{fz}^3 \quad (3.62)$$

From equation (3.50) and assuming  $\lambda_{II}$  is constant with temperature simplifies to

$$\frac{d}{dr} \left( r^2 \frac{dT_{II}}{dr} \right) = 0 \quad (3.63)$$

By integrating equation (3.63), equation (3.64) is obtained

$$r^2 \frac{dT_{II}}{dr} = K_1 \quad (3.64)$$

Dividing equation (3.64) by  $r^2$  gives

$$\frac{dT_{II}}{dr} = K_1 r^{-2} \quad (3.65)$$

Integration of equation (3.65) leads to

$$T_{II}(r) = -\frac{K_1}{r} + K_2 \quad (3.66)$$

where  $K_1$  and  $K_2$  are constants

Boundary conditions (BC):

Applying BC3;  $\frac{dT_I}{dr} = \frac{dT_{II}}{dr}$ , for;  $r = R_{fz}$  to equations (3.56) and (3.65) gives

$$\frac{dT_I}{dr} = -\frac{q_v R_{fz}}{3\lambda_I} + \frac{C_1}{R_{fz}^2} \text{ and } \frac{dT_{II}}{dr} = \frac{K_1}{R_{fz}^2} \quad (3.67)$$

Rearranging equation (3.67) leads to

$$-\frac{q_v R_{fz}}{3\lambda_l} + \frac{C_1}{R_{fz}^2} = \frac{K_1}{R_{fz}^2} \quad (3.68)$$

But  $C_1 = 0$ . Hence equation (3.68) reduces to

$$K_1 = -\frac{q_v R_{fz}^3}{3\lambda_l} \quad (3.69)$$

Substituting  $K_1$  into equation (3.66) simplifies to

$$T_{II(r)} = \frac{q_v R_{fz}^3}{3\lambda_l r} + K_2 \quad (3.70)$$

Applying BC4;  $T_I = T_{II}$ , for;  $r = R_{fz}$  to (3.70), equation (3.71) is obtained

$$-\frac{q_v R_{fz}^2}{6\lambda_l} + T_m = \frac{q_v R_{fz}^2}{3\lambda_l} + K_2 \quad (3.71)$$

which simplifies to

$$K_2 = T_m - \frac{q_v R_{fz}^2}{6\lambda_l} - \frac{q_v R_{fz}^2}{3\lambda_l} \quad (3.72)$$

Further simplification of equation (3.72) gives

$$K_2 = T_m - \frac{q_v R_{fz}^2}{2\lambda_l} \quad (3.73)$$

Substituting equation (3.73) into equation (3.70) gives

$$T_{II(r)} = \frac{q_v R_{fz}^3}{3\lambda_l r} - \frac{q_v R_{fz}^2}{2\lambda_l} + T_m \quad (3.74)$$

Applying BC5;  $T_{II} = T_{so}$ , for;  $r = R_{peb}$  to equation (3.74) leads to

$$T_{II} = \frac{q_v R_{fz}^3}{3\lambda_l R_{peb}} - \frac{q_v R_{fz}^2}{2\lambda_l} + T_m \quad (3.75)$$

which is further reduced to

$$T_{II} - T_m = -\frac{q_v R_{fz}^2}{2\lambda_l} + \frac{q_v R_{fz}^3}{3\lambda_l R_{peb}} \quad (3.76)$$

Further simplification of equation (3.76) gives

$$\Delta T_{II} = T_{si} - T_{so} = -\frac{q_v R_{fz}^2}{3\lambda_l} \left(1 - \frac{R_{fz}}{R_{peb}}\right) = -\frac{q_p}{4\pi\lambda_l} \left(\frac{1}{R_{fz}} - \frac{1}{R_{peb}}\right) \quad (3.77)$$

where  $T_{si}$  and  $T_{so}$  are the inner and outer surface temperatures of the fuel pebble.

From eqn. (3.51),

$$\Delta T_c = T_{surf} - T_g = \frac{\frac{4}{3} q_v \pi R_{fz}^3}{4\pi R_{peb}^2 \alpha} = \frac{q_p}{4\pi\alpha R_{peb}^2} \quad (3.78)$$

Applying boundary condition  $T_{(R)} = T_{(s)}$  (known temperature at sphere surface,

$R$ ), From (3.58),  $C_2 = T_s + \frac{q_v R^2}{6\lambda_l}$ . Therefore the temperature distribution in the

$$\text{sphere is given by } T_{(r)} = -\frac{q_v R_{fz}^2}{6\lambda_l} + T_s + \frac{q_v R^2}{6\lambda_l} = \frac{q_v}{6\lambda_l} (R^2 - R_{fz}^2) + T_s \quad (3.79)$$

The pebble centre point temperature ( $T_{pc}$ ) which gives the maximum temperature

is obtained by putting  $R_{fz} = 0$  in equation (3.79). This leads to

$$T_{pc} = T_m = \frac{q_v R^2}{6\lambda_l} + T_s \quad (3.80)$$

### 3.2.4. HEAT CONDUCTIVITY IN PACKED BEDS

Heat fluxes occur in the pebble bed type high temperature nuclear reactor parallel and normal to the main flow direction due to temperature gradients in the radial and axial directions. It is therefore important to know the magnitude of the flux in order to calculate the dispersion of hot spots in the reactor core.

Due to the highly complex nature of the formulations to calculate the heat transfer between the pebbles, an approximation is introduced to deal with the contact and radiation heat transfer between the surfaces of the pebbles.

If it is assumed that the pebble bed is a one-phase continuum, fluxes in the radial and axial directions can be calculated as,

$$q_{ra} = h_{cd(rad)} \Delta T_{(rad)} = -\lambda_{ra} \frac{dT}{dr} \quad (3.81)$$

and

$$q_{ax} = h_{cd(ax)} \Delta T_{(ax)} = -\lambda_{ax} \frac{dT}{dz} \quad (3.82)$$



where  $h_{cd(rad)}$  and  $h_{cd(ax)}$  are the conduction heat transfer coefficient in the radial and axial directions,  $\lambda_{ra}$  and  $\lambda_{ax}$  are the effective conductivity in the radial and axial directions respectively. The subscripts 'r' and 'z' indicates the radial and axial coordinates.

The radial effective conductivity as expressed by Yagi and Kunii is given by [39]

$$\frac{\lambda_{ra}}{\lambda_g} = \lambda_{ra} = \frac{Pe}{Kr} + \frac{\lambda_o}{\lambda_g} \quad (3.83)$$

The axial effective conductivity as expressed by Yagi, Kunii and Wakao is given by [39]

$$\frac{\lambda_{ax}}{\lambda_g} = \hat{\Lambda}_{ax} = \frac{Pe}{Kz} + \frac{\lambda_o}{\lambda_g} \quad (3.84)$$

where  $\lambda_g$  is conductivity of the gas, Pe is Peclet number,  $\lambda_o$  is stagnant gas conductivity, Kr and Kz are constants as expressed in equation (3.85) and (3.86) respectively.

$Kr$  was described by Schluender as a constant depending on the ratio of sphere diameter to core diameter ( $d/D$ ) given by [39]

$$Kr = 8 \left[ 2 - \left( 1 - 2 \frac{d}{D} \right)^2 \right] \quad (3.85)$$

The constant  $Kz$  was determined by Yagi et al to be equal to 1.3 for Peclet number (Pe) equal to 30 [39].

i.e.  $Kz = 1.3$  for  $Pe = 30$ . (3.86)

Considering equations (3.83) and (3.84), the first terms describe the contribution of convection on conduction mode, which is different for the radial and axial coordinates. The second terms of the same equations account for heat conduction through the solid and fluid phase and additionally for temperature radiation.

Using the relationship established by Schlunder, equation (3.85) and Yagi et al, equation (3.86), equations (3.83) and (3.84) can be expressed as

$$\frac{\lambda_{ra}}{\lambda_g} = \Lambda_{ra} = \frac{30}{8 \left[ 2 - \left( 1 - 2 \frac{d}{D} \right)^2 \right]} + \frac{\lambda_o}{\lambda_g} \quad (3.87)$$

and

$$\frac{\lambda_{ax}}{\lambda_g} = \Lambda_{ax} = \frac{30}{1.3} + \frac{\lambda_o}{\lambda_g} \quad (3.88)$$

Several heat transfer mechanisms influences the stagnant gas conductivity,  $\lambda_o$ .

These include:

1. conduction through the gaseous phase,
2. conduction through the solid phase,
3. heat radiation solid-solid and through the void pore area to the next layer,
4. conduction through the contact area, and
5. pressure dependent conductivity.

A comprehensive review has been carried out on numerous models for the determination of the effective thermal conductivity [42], and the Zehner-Schlunder model is able to account for all the effects mentioned above.

Zehner and Schlunder, determined the quantity  $\frac{\lambda_o}{\lambda_g}$  and came out with the expression [39,42]

$$\frac{\lambda_o}{\lambda_g} = (1 - \sqrt{1 - \varepsilon}) \frac{\lambda_{gap}}{\lambda_g} + \sqrt{1 - \varepsilon} \frac{\lambda_{fs}}{\lambda_g} \quad (3.89)$$

where  $\lambda_{gap}$  is the effective thermal conductivity across the gap between pebbles and  $\lambda_{fs}$  is the effective thermal conductivity through the fluid and solid phase.

From equation (3.89), the first term describes the heat flux through the gap between neighbouring spheres due to heat conduction and radiation, with  $(1 - \sqrt{1 - \varepsilon})$  being the area contribution of the gap to the total area normal to the flux. The second term of equation (3.89) on the other hand describes the heat conducted and radiated through the fluid and solid phases from layer to layer.

Using Zehner-Schlunder expression, i.e. equation (3.89), equations (3.87) and (3.88) are respectively further expressed as

$$\frac{\lambda_{ra}}{\lambda_g} = \Lambda_{ra} = \frac{30}{8 \left[ 2 - \left( 1 - 2 \frac{d}{D} \right)^2 \right]} + (1 - \sqrt{1 - \varepsilon}) \frac{\lambda_{gap}}{\lambda_g} + \sqrt{1 - \varepsilon} \frac{\lambda_{fs}}{\lambda_g} \quad (3.90)$$

and

$$\frac{\lambda_{ac}}{\lambda_g} = \Lambda_{ac} = \frac{30}{1.3} + (1 - \sqrt{1 - \varepsilon}) \frac{\lambda_{gap}}{\lambda_g} + \sqrt{1 - \varepsilon} \frac{\lambda_{fs}}{\lambda_g} \quad (3.91)$$

where

$$\frac{\lambda_{gap}}{\lambda_g} = 1 + \varepsilon Nur \quad (3.92)$$

The parameter Nur is expressed as [39];

$$Nur = \frac{4\sigma T^3}{\varepsilon_r} \frac{d}{\lambda_g} \quad (3.93)$$

Substituting equation (3.93) into equation (3.92) gives

$$\frac{\lambda_{gap}}{\lambda_g} = 1 + \frac{4\varepsilon\sigma T^3}{\varepsilon_r} \frac{d}{\lambda_g} \quad (3.94)$$

where;

$\sigma$  is Stefan – Boltzmann constant [ $\sigma = 5.775 \times 10^{-8} \text{ W/m}^2\text{T}^4$ ]

T is absolute temperature [K]

$\varepsilon_r$  is emissivity of the solid particles

The expression for the quantity  $\frac{\lambda_{fs}}{\lambda_g}$  is given by [39];

$$\frac{\lambda_{fs}}{\lambda_g} = \frac{2}{N-M} \left[ \frac{BN-M}{(N-M)^2} \ln \frac{N}{M} - \frac{B-1}{N-M} + \frac{B+1}{2M} (N-M-1) \right] \text{ for } M \neq N \quad (3.95)$$

and

$$\frac{\lambda_{fs}}{\lambda_g} = \frac{1}{(B-1)M} \left[ \frac{2}{3M} \frac{B^3-1}{B-1} - (B+1)(1-Nur) \right] \text{ for } M = N, \quad (3.96)$$

where

$$M = B \frac{\lambda_g}{\lambda_s} \text{ and } N = 1 + Nur \frac{\lambda_g}{\lambda_s} \quad (3.97)$$

$\lambda_s$  is conductivity of the solid particles.

$$\text{Also } B = 1.25 \left( \frac{1-\varepsilon}{\varepsilon} \right)^{1.1} \quad (3.98)$$

### 3.3. MATERIAL PROPERTIES OF HELIUM

The fluid material properties were all expressed in terms the the fluid temperature and pressure.

#### 3.3.1. MASS DENSITY OF HELIUM

The mass density of helium ( $\text{kg/m}^3$ ) was calculated using the equation [40]

$$\rho = 48.14 \frac{P}{T} \left( 1 + 0.446 \times \frac{P}{T^{1.2}} \right)^{-1} \quad (3.99)$$

#### 3.3.2. DYNAMIC VISCOSITY

The dynamic viscosity (Pa.s) was calculated using the equation [40]

$$\eta = 3.674 \times 10^{-7} T^{0.7} \quad (3.100)$$

#### 3.3.3. THERMAL CONDUCTIVITY

The thermal conductivity (W/m.K) was calculated using the equation [40]

$$\lambda = 2.682 \times 10^{-3} \left( 1 + 1.123 \times 10^{-3} \times P \right) \times T^{0.71} \left( 1 - 2 \times 10^{-4} \times P \right) \quad (3.101)$$

where P is the pressure (bar) and T is the gas temperature (K)

$$1.2 \leq D/d \leq 58 \text{ and } H \geq 4d [3, 25, 40, 44]$$

### 3.4 DEVELOPMENT OF THE CODE FOR THERMAL ANALYSIS

For the thermal analyses, the thermal-hydraulic code PEBTAN was applied. The code was developed to solve for the heat transfer and fluid flow, as well as the pressure drop over the core of the pebble bed high temperature reactor.

The code was written in FORTRAN 95 and enabled the simulation of various conditions and scenarios. The mass density, the dynamic viscosity and thermal conductivity of the gas and the fuel were calculated at the gas temperature and pressure. The code correctly calculated the convective heat transfer coefficient, the convective heat transfer, the temperature distribution in the fuel pebble, the effective radial heat conductivity, the pressure drop, the pressure drop coefficient and the effects of porosity on heat transfer and pressure drop using the reactor thermal power, the system pressure, inlet and outlet temperatures, core height, core diameter, coolant mass flow rate and the fuel size as the input data. With the input parameters specified, the code simulate either by varying the mass flow rate or the gas temperature or by varying the porosity of the bed depending on the particular analysis.

The code structure consisted of six (6) subroutines comprising; (a) convection heat transfer, (b) conduction/radiation heat transfer, (c) temperature profile in the fuel pebble, (d) effects of porosity on heat transfer and pressure drop, (e) effects of core to fuel element diameter ratio on pressure drop, (f) pressure drop through friction across the pebble bed. The PEBTAN code is shown in appendix A

The code could perform the analyses of each of the six subroutines separately by selecting the subroutine of interest. The code could also perform the analyses of the six subroutines as a single integrated unit.

Figure 3.2 shows the main computational flow chart with subroutines of the single integrated unit. The code calls in six (6) subroutines (i.e. the six modules) to calculate different sets of data. Figure 3.3-3.8 shows the flow chart for each of the separate modules as contained in the single integrated unit.

The execution of the code could be terminated by the user after performing analyses of any of the subroutines of interest or a combination of subroutines. Output files were created to record different sets of tabulated data each containing completely explicit headings.

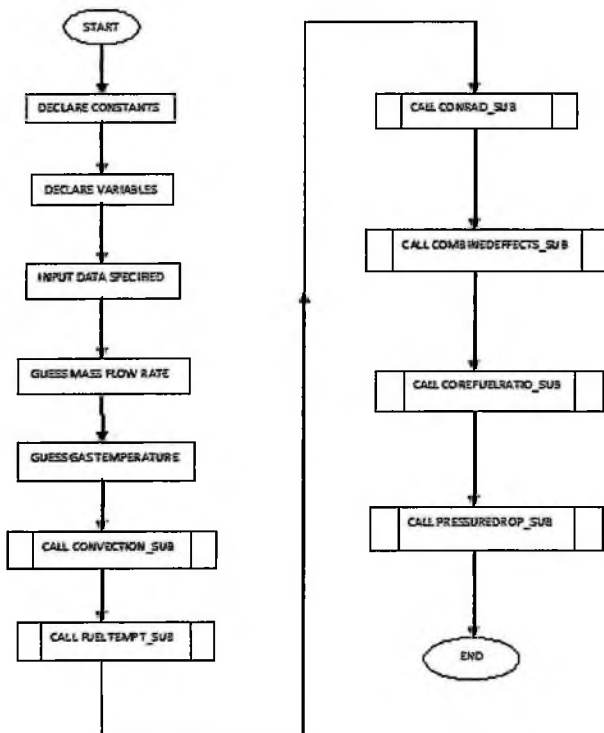
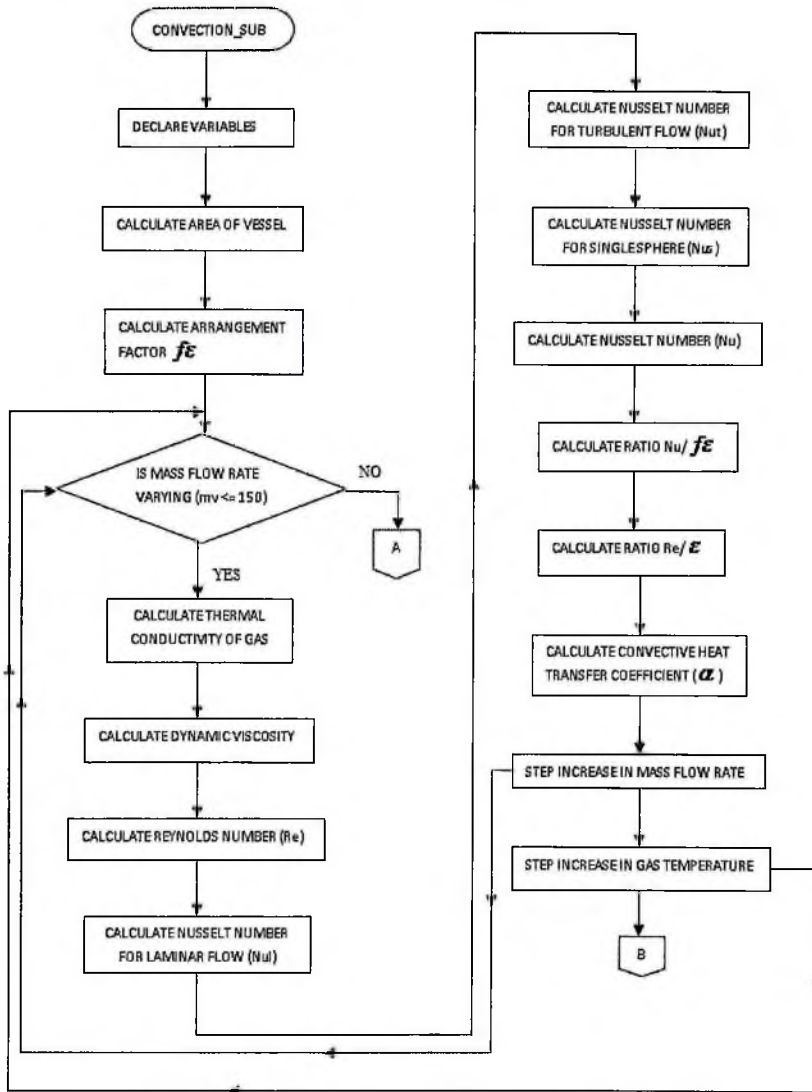


Fig. 3.2: Main Computational Flow Chart



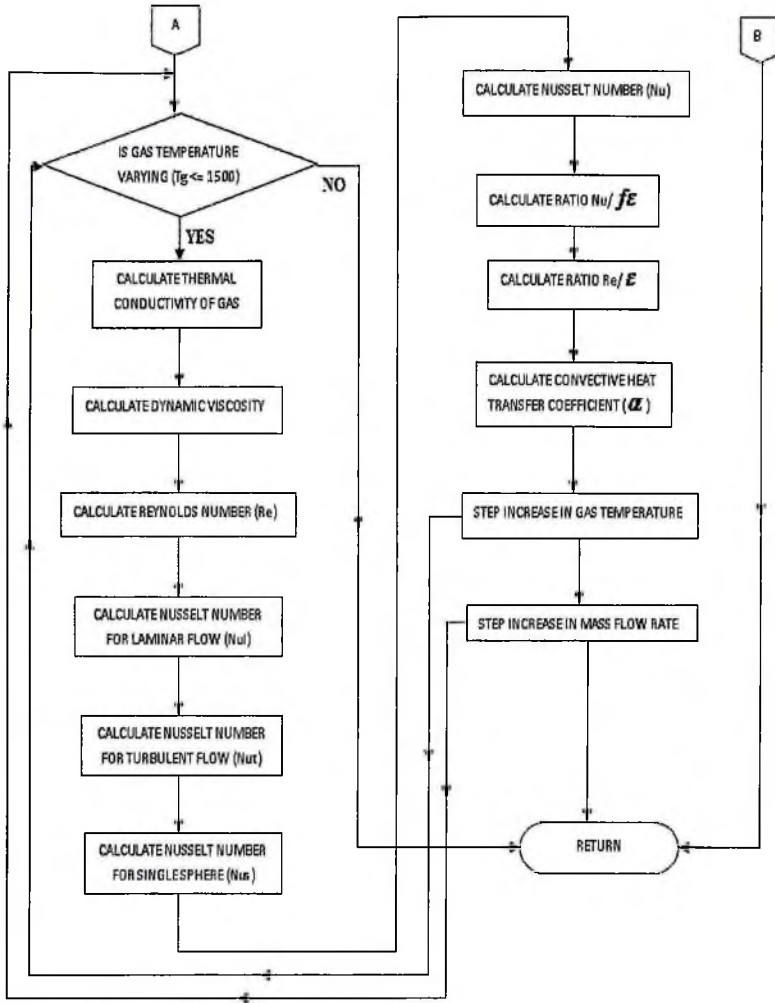


Fig. 3.3: Computational Flow Chart for CONVECTION\_SUB

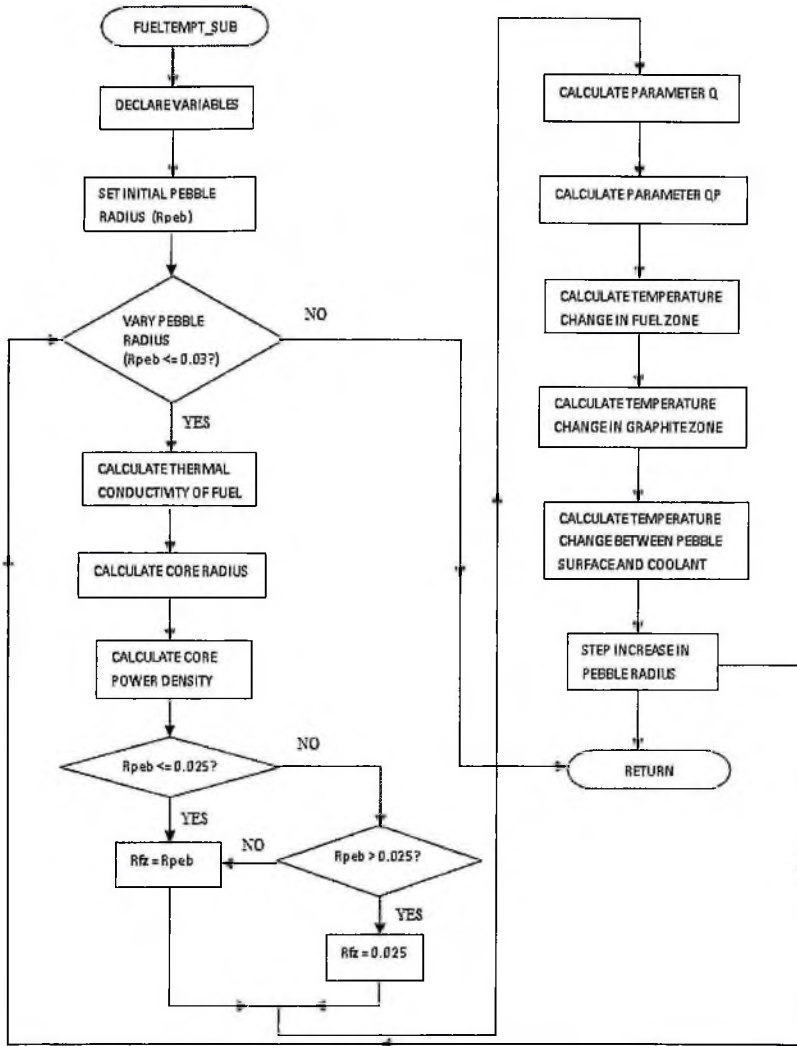


Fig. 3.4: Computational Flow Chart for FUELTEMPT\_SUB

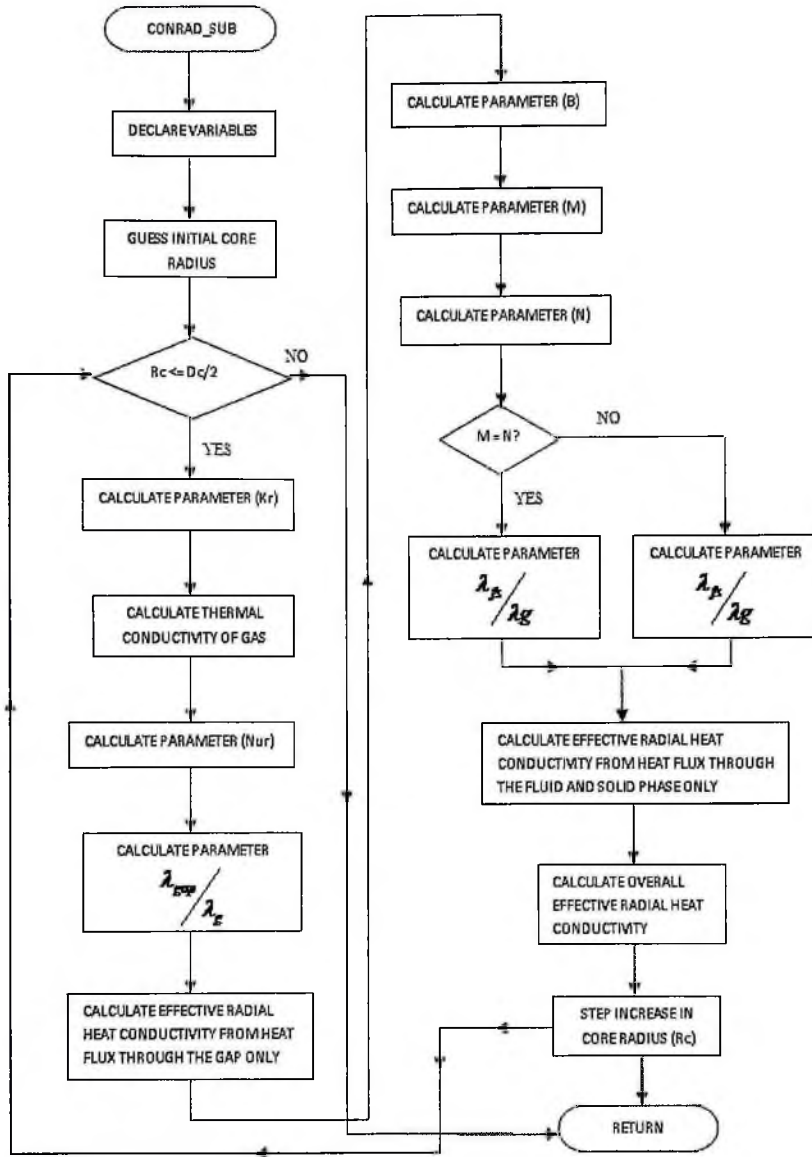


Fig. 3.5: Computational Flow Chart for CONRAD\_SUB

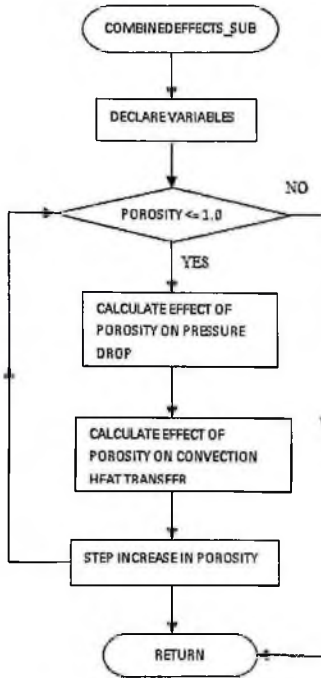


Fig. 3.6: Computational Flow Chart for COMBINEEFFECTS\_SUB

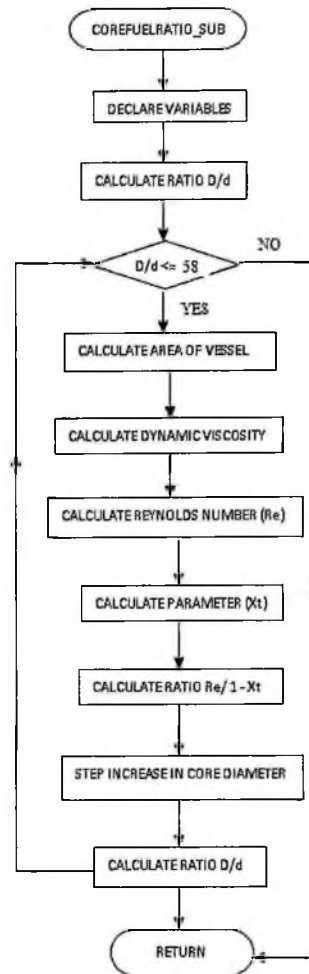


Fig. 3.7: Computational Flow Chart for COREFUELRTIO\_SUB

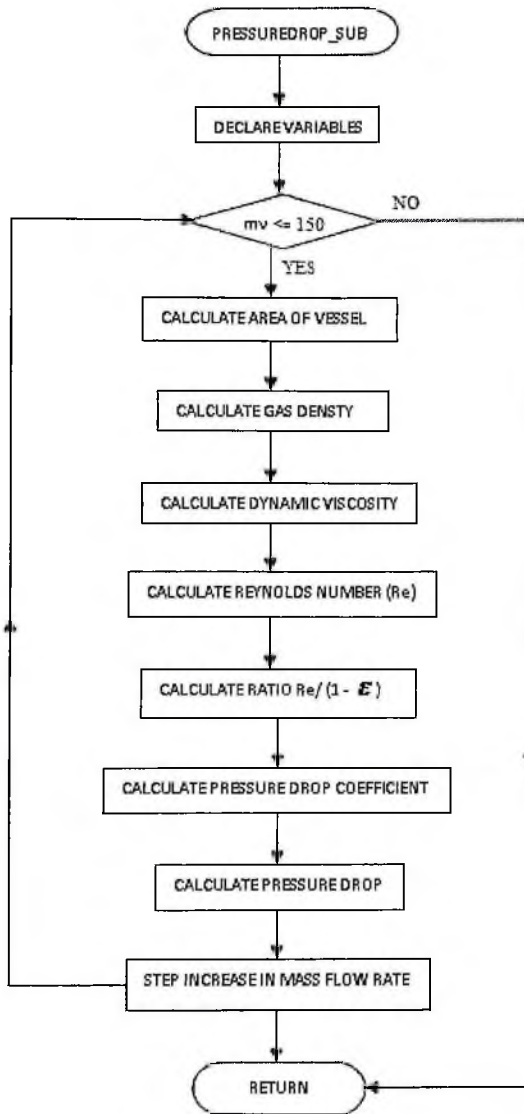


Fig. 3.8: Computational Flow Chart for PRESSUREDROP\_SUB

### 3.4.1. INPUT DATA

The input data to the code is given in the Table 3.1 [4]

Table 3.1: Parameters used in the analyses.

<b>PARAMETER</b>	<b>VALUE</b>
Thermal Power ( $MW_{th}/MW_e$ )	250/120
Coolant	Helium
Helium inlet/outlet temperature (K)	793/1173
Helium pressure (MPa)	8.0
Helium mass flow rate (kg/s)	120 (100% full power)
Core diameter (m)	3.5
Core height (m)	10.0
Fuel pebble diameter (m)	0.06
Porosity of the bed	0.39

### 3.4.2 PROGRAM SOLUTION AND IMPLEMENTATION ALGORITHM

This subsection describes the sequence of simulations performed and how the code solved the set of analytical equations developed for the thermal analysis of the pebble bed nuclear reactor.

#### 3.4.2.1 SIMULATION OF PRESSURE DROP ACROSS THE PEBBLE BED

The pressure drop through friction across the pebble bed is an important phenomena that ultimately affects the heat transfer effectiveness. For different coolant mass flow rates, equation (3.12) and (3.17) were solved to determine the pressure drop and the pressure drop coefficient across the bed.

The influence of porosity on pressure drop was determined using equation (3.26) by varying the porosity between 0.0 and 1.0. The analysis was done for both laminar flow and turbulent flow.

For the pebble bed nuclear reactor, the ratio of core diameter to fuel element diameter is very large. Thus, taken into account the dependence of porosity on core to fuel element diameter ( $D/d$ ), simulation was performed to determine the effect of the diameter ratio on pressure drop. Equation (3.27) was solved and the corresponding Reynolds number determined by varying the core diameter.

#### 3.4.2.2 SIMULATION OF CONVECTIVE HEAT TRANSFER

The temperature dependence of the convective heat transfer coefficient that follows from equation (3.35b) was simulated for different mass flow rates of the coolant. The code solved equation (3.47) and (3.48) and input the values into equation (3.44) and together with equation (3.43), the code solves equation (3.42). Finally, the convective heat transfer coefficient was evaluated from equation (3.35b). The calculations were done by varying the mass flow rate of the coolant at specified temperature(s) and secondly by varying the coolant temperature at specified coolant mass flow rate. To investigate the influence of porosity on convective heat transfer, equation (3.41) was solved by varying the porosity between 0.0 and 1.0

#### 3.4.2.3 SIMULATION OF TEMPERATURE PROFILE IN THE FUEL PEBBLE

The simulation of the distribution of temperature in the fuel pebble was done with the assumption that (a) the coolant temperature surrounding the pebble was uniform and (b) the thermal power was generated within the fuelled region of the pebble. The maximum temperature within the pebble was at the centre of the pebble. Thus, by varying the pebble radius, the temperature distribution in the fuel pebble was obtained from equations (3.61, 3.77).

#### 3.4.2.4 SIMULATION OF EFFECTIVE THERMAL CONDUCTIVITY ACROSS THE PEBBLE BED CORE

The effective radial heat conductivity of a core under normal operation conditions is necessary for the calculation of the mixing effect of hot gas streaks. For a specified gas temperature, pressure and coolant mass flow rate, equations (3.85, 3.89, 3.92, 3.93 and 3.95 to 3.98) were solved by varying the core radius or the gas temperature. The simulation was performed by first assuming that the contribution to the effective radial heat conductivity was only from the heat flux through the gap between neighbouring spheres due to heat conduction and radiation. The next assumption was that the contribution to the effective radial heat conductivity was only from the heat conducted and radiated through the fluid and solid phase from layer to layer. The overall effective radial heat conductivity was analysed by taken into account the effects of the two assumptions above.

### 3.5 SUMMARY

The mathematical formulation of the model and the set of equations for the prediction of the related phenomena have been presented. In formulating the model, the effect of porosity on heat transfer as well as pressure drop was considered and accounted for.

A simulation code called PEBTAN written in FORTRAN 95 has been developed to analyse, predict and evaluate the thermal response of the pebble bed nuclear reactor. The code was carefully developed to simulate and analyse various conditions and scenarios including the convection heat transfer, distribution of temperature in a fuel pebble, effective radial heat conductivity distribution across the pebble bed core and the pressure drop through friction in the pebble bed.

In the next chapter results obtained from the simulation experiments have been presented and discussed. Results are presented in the form of graphs.

## CHAPTER FOUR

### RESULTS AND DISCUSSION

The chapter discusses the results obtained from the simulation experiments. The results are presented graphically.

#### 4.1 PRESSURE DROP

The pressure drop profile across the pebble bed is shown in Figs 4.1, 4.2, and 4.3. Increase in coolant flow rate reduces the fluid friction between the pebble surface and the fluid, induced as a result of the fluid viscosity. The pressure drop coefficient consequently reduces with increased coolant flow rate as can be seen in Fig 4.1. by solving equation (3.17).

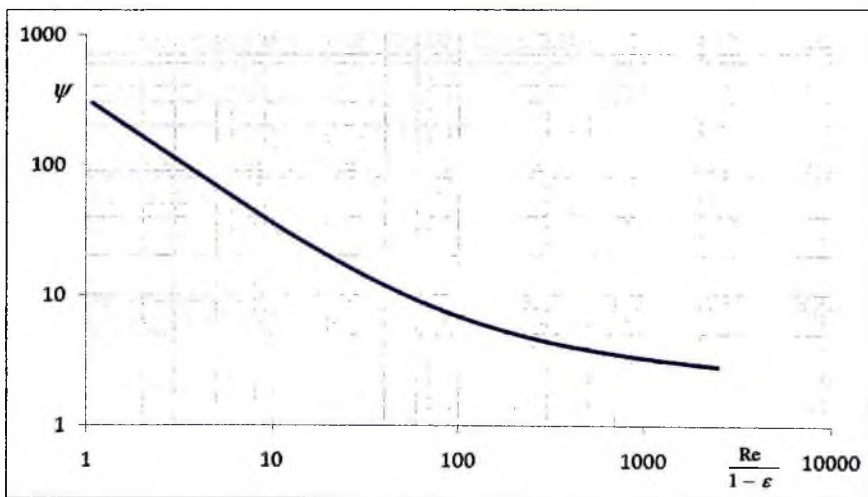


Fig. 4.1: Pressure drop coefficient against modified Reynolds number. Equation (3.17)

The pressure drop created by the resistance to flow in the pebble bed can be varied by varying the coolant mass flow rate as all other parameters are fixed either by the reactor geometry or coolant choice. Fig. 4.2 shows the pressure drop model (eqn. 3.12) across the bed which increases with increasing Reynolds number (which is a direct function of coolant mass flow rate).

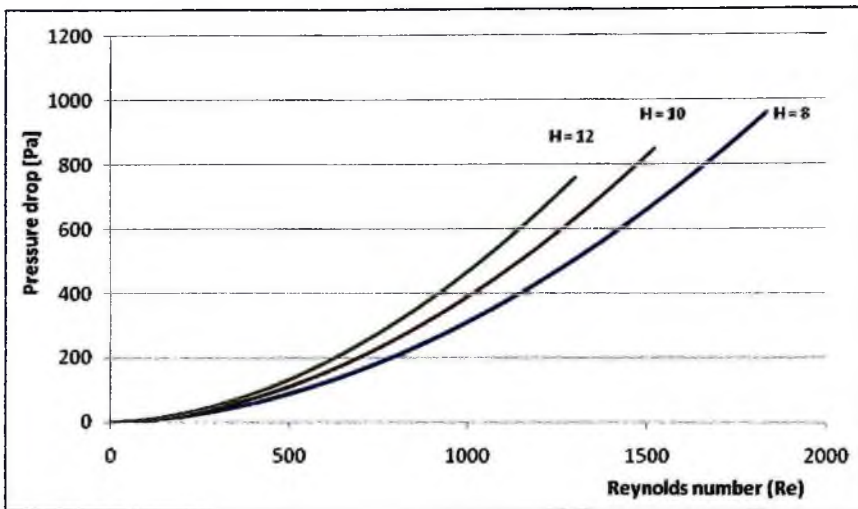


Fig. 4.2: Pressure drop profile for different core height. Equation (3.12)

The flow of coolant causes pressure drop which should not be too high (not exceeding 2% of the system pressure) since high pressure drop across the bed requires high pumping power to pump the coolant. The coolant mass flow rate is however limited by both the minimum and maximum allowable temperatures in the core. The results indicate a very low pressure drop which means that there is considerable reduction of leakage or bypass flow and that the bulk of the helium coolant flows through the voids between the fuel pebbles in the core and extract

the heat from the fuel. Further observation from the graph shows that the pressure drop increases with increasing core height.

The effect of core diameter to fuel element diameter on pressure drop was simulated based on equations (3.27 to 3.29) and the result is plotted in Fig. 4.3.

From the plot it can be observed that smaller  $D/d$  ratio result in higher  $\frac{Re}{1-\epsilon_f}$  and larger  $D/d$  ratio result in lower  $\frac{Re}{1-\epsilon_f}$ .

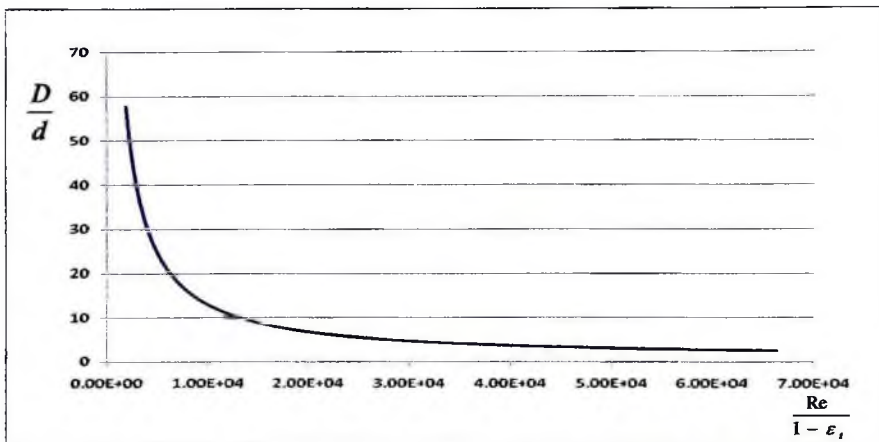


Fig. 4.3: Limiting curve of the diameter ratio as a function of modified Reynolds number.

Furthermore from equations 3.28 and 3.29, for larger  $D/d$  ratio, the pressure drop coefficient  $\psi_f$  increases thus increasing the pressure drop. On the other hand, for smaller  $D/d$  ratio, the pressure drop coefficient  $\psi_f$  decreases thus decreasing the pressure drop. The effect is that with larger  $D/d$  ratio and the corresponding higher pressure drop over the core, higher coolant mass flow rate has to be transferred to the core and this requires more pumping power per coolant flow.

## 4.2 CONVECTIVE HEAT TRANSFER

The heat transfer profile is shown in Fig. 4.4 by solving the system of equations 3.45, 3.47 and 3.48. Referring to equation (3.30), it is observed that to influence the heat transfer, either the convective heat transfer coefficient is increased or the heated surface area is increased or the temperature difference between the pebble surface and the bulk coolant is increased.

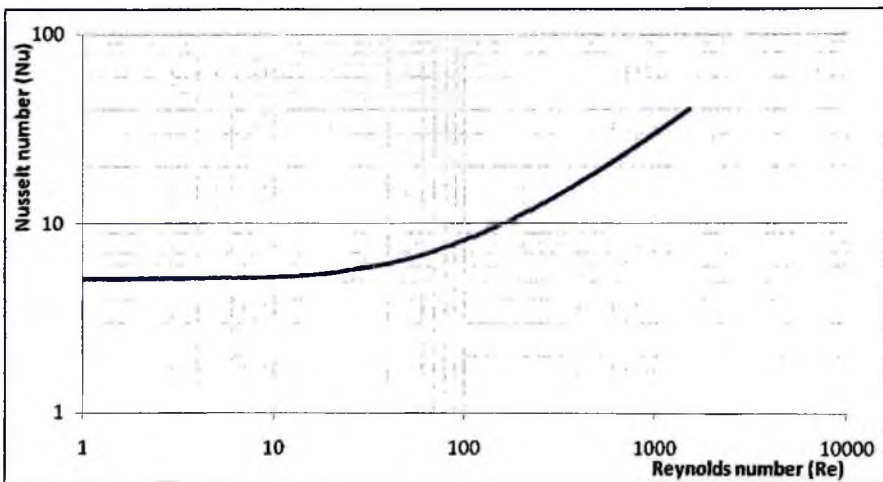


Fig. 4.4: Convective heat transfer for pebble bed at  $Pr = 0.7$  and  $\varepsilon = 0.39$

From the graph, the heat transfer increases with increasing Reynolds number which is a function of mass rate of flow, meaning, an increase in the mass rate of flow enables the coolant to transfer more heat from the core. For low Reynolds number (i.e.  $Re < 100$ ), the heat transfer rate seems to be independent of Reynolds number. The quantity of heat that the coolant can transfer from the core depends on the coolant inlet temperature and pressure. The magnitude of the heat

transfer coefficient affect the heat transfer process and is influenced by a number of parameters such as the geometry, the coolant flow rate and temperature, the flow condition and the fluid type.

Figures 4.5 and 4.6 show the temperature dependence of the convective heat transfer coefficient for different mass flow rates that follows from the solution to the set of equations 3.35b, 3.45, 3.47 and 3.48.

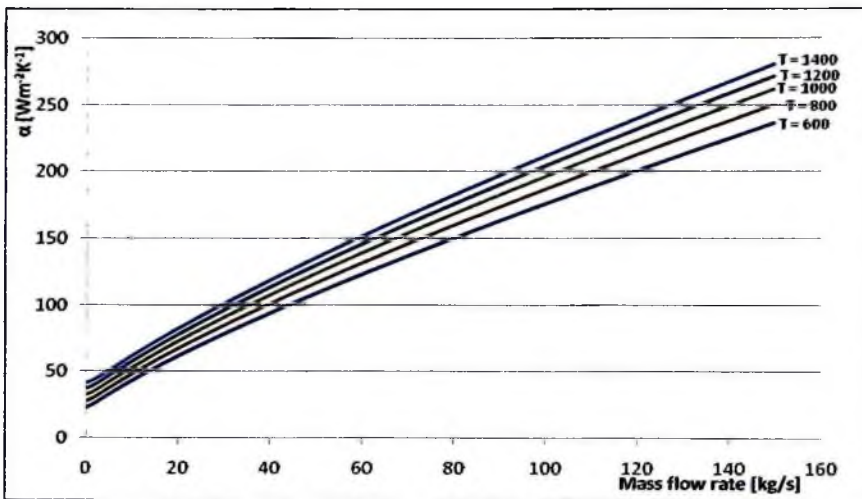


Fig. 4.5: Mass flow rate dependence of heat transfer coefficient.

From the graphs, the heat transfer coefficient increases with increasing temperature and coolant mass rate of flow. From the expression,

$$T_{surf} = T_g + \frac{Q}{\alpha A_p},$$

increasing the convective heat transfer coefficient brings the fluid and the pebble surface temperature closer to each other which may frustrate the heat transfer.

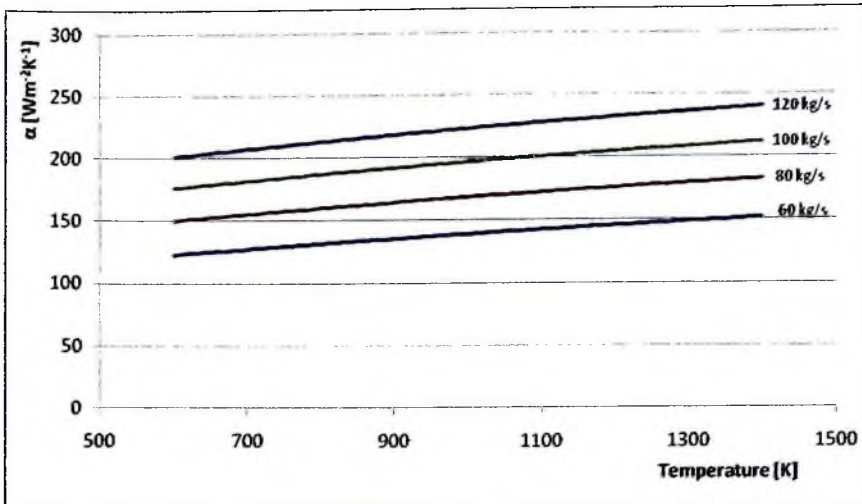


Fig. 4.6: Temperature dependence of heat transfer coefficient.

Again from the graphs of Figs. 4.5 and 4.6, the convective heat transfer coefficient increases uniformly with increasing coolant temperature and mass rate of flow which means that there is appreciable temperature difference between the fluid temperature and the pebble surface temperature. The heat transfer process is therefore improved.

### 4.3 TEMPERATURE PROFILE IN THE FUEL PEBBLE

The distribution of temperature in a fuel pebble, Fig. 4.7, was obtained by solving equations (3.61 and 3.77). From the plot, it is observed that the temperature difference increases from the centre to the surface of the fuel pebble. The larger temperature change in the fuel zone of the pebble as compared with a smaller temperature change in the graphite zone is due to the coolant temperature surrounding the fuel pebble.

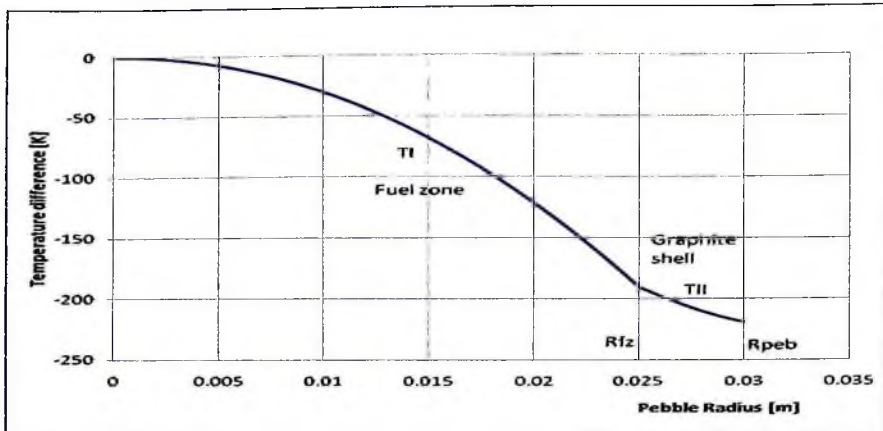


Fig. 4.7: Temperature profile in a fuel pebble

The conditions that determine the fuel temperature in the pebble are the surface temperature of the pebble and the power generated by a pebble. For all transients with a sustained helium flow, the hottest surface temperatures are found at the bottom of the core since coolant flow from the top of the core to the bottom.

#### 4.4 EFFECTIVE RADIAL THERMAL CONDUCTIVITY

The result of the effective radial thermal conductivity distribution across the pebble bed core based on equation (3.90, and 3.92 to 3.98) is plotted in Fig. 4.8. The plot shows almost constant effective heat conductivity for all the three scenarios simulated.

Observation from the graph indicates that the contribution to the overall effective thermal conductivity is largely as a result of the heat conducted and radiated through the fluid and solid phase from layer to layer with the heat flux through the

gap between neighbouring spheres due to heat conduction and radiation contributing less. This observation is as a result of large contact surfaces between the pebbles as compared with the gaps between pebbles.

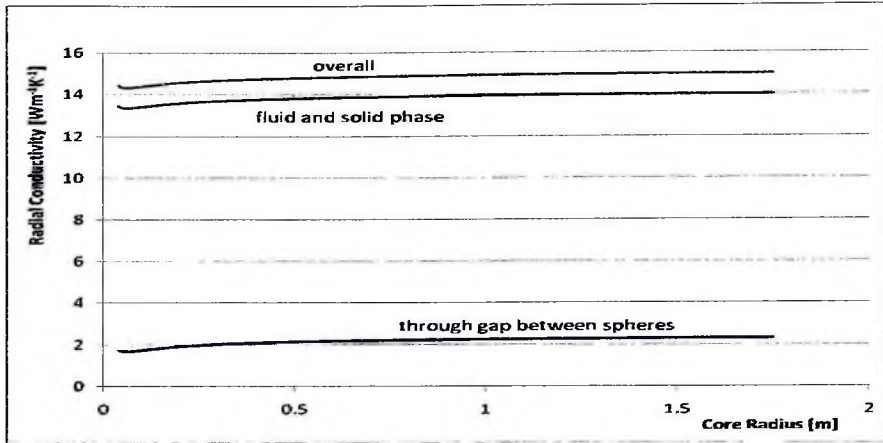


Fig. 4.8: Effective radial conductivity distribution across the pebble bed.

The strong temperature dependence of the effective thermal conductivity of the pebble bed (eqn. 3.90, and 3.92 to 3.98) was observed as shown in Fig. 4.9.

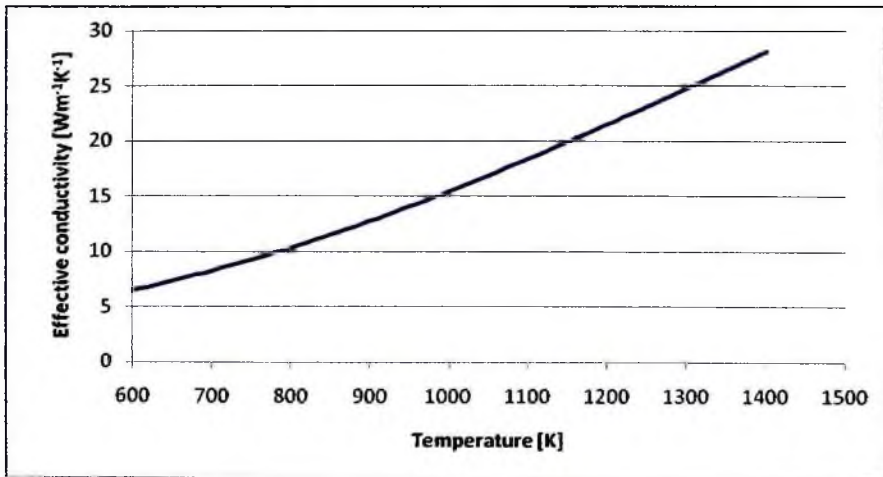


Fig. 4.9: Effective thermal conductivity of the pebble bed in helium.

The effective thermal conductivity of pebble bed is influenced by many parameters with varying degrees. Parameters such as the thermal conductivity of the fuelled pebbles and the gas (helium), the gas pressure and the bed packing fraction have significant impact on the thermal conductivity of the pebble bed. To adequately account for the gas conductivity and pressure effect on the effective thermal conductivity, the thermal conductivity of the gas was modeled by expressing the gas conductivity in terms of the gas pressure and temperature. Other parameters such as the pebble size and surface roughness have less impact on the thermal conductivity of the pebble bed.

#### **4.5 EFFECTS OF POROSITY ON HEAT TRANSFER AND PRESSURE DROP**

The porosity of the pebble bed is very important to the mechanisms of heat and mass transfer as well as flow and pressure drop of the coolant throughout the pebble bed. Figs. 4.10 and 4.11 show the effect of porosity on convective heat transfer (for  $n^* = 0.6$ , i.e.  $5 \times 10^2 < Re < 10^4$  and  $n^* = 0$ , i.e. very low Reynolds number) and pressure drop ( $n = 1$  for laminar flow and  $n = 0.1$  for turbulent flow) that follows from equations (3.41 and 3.26) respectively.

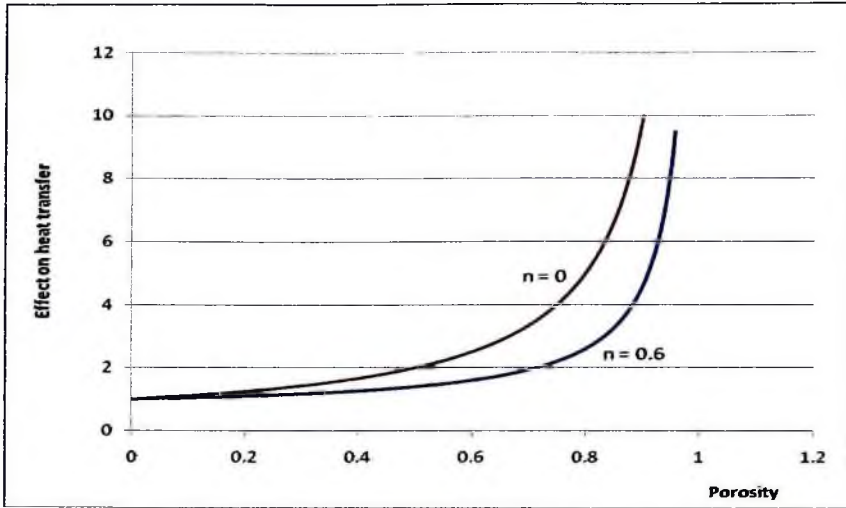


Fig. 4.10: Effect of porosity on heat transfer. Equation (3.41)

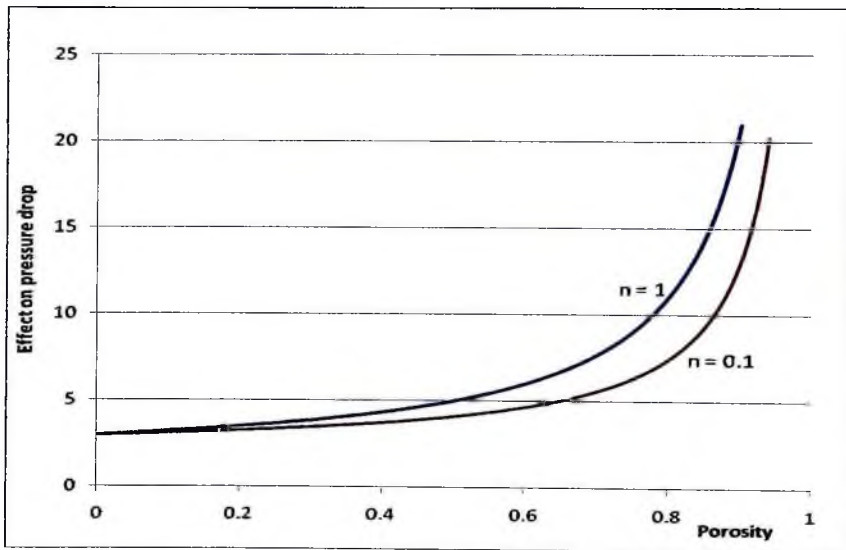


Fig. 4.11: Effect of porosity on pressure drop. Equation (3.26)

From the graphs, the magnitude of the effect of porosity on both convective heat transfer and pressure drop increases with increasing porosity.

From Fig. 4.10, the effect of porosity on heat transfer is more pronounced for low Reynolds number where the flow rate is also low. The magnitude of the effect is such that a positive variation of porosity results in a negative variation of heat transfer by a factor of  $\frac{1-n\varepsilon}{1-\varepsilon}$  for  $n' = 0.6$  and  $n' = 0$ .

The effect of porosity on pressure drop as shown in Fig. 4.11 is high for laminar flow than that of turbulent flow. In both flow regimes, a positive variation of porosity causes a negative relative variation of pressure drop by a factor  $\frac{3-\varepsilon(2-n)}{1-\varepsilon}$  for  $n = 1$  and  $n = 0.1$ .

The essential effects the porosity has on heat transfer and pressure drop can be observed from Figs. 4.10 and 4.11. For instance at  $\varepsilon = 0.39$ , an error of 1% in  $\varepsilon$  causes an error of 1.64% and 1.26% for heat transfer (for  $n = 0$  and  $n = 0.6$  respectively) and an error of 4.28% and 3.70% for pressure drop (for  $n = 1.0$  and  $n = 0.1$  respectively). From these results, one can conclude that the magnitude of the effect of porosity on pressure drop is more pronounced than the effect on heat transfer.

## CHAPTER FIVE

### CONCLUSION AND RECOMMENDATIONS

#### 5.1 CONCLUSIONS

A simplified analytical model of the pebble bed nuclear reactor heat transfer and loss of pressure through friction have been developed to analyse the convective heat transfer, the temperature distribution in the fuel pebble, the conduction and radiation heat transfer, loss of pressure through friction in the pebble bed and the effect of porosity on heat transfer as well as pressure drop. The set of equations for the prediction of the related phenomena have been presented. The developed model has been implemented on a personal computer using FORTRAN 95 programming language. The code, PEBTAN, correctly calculates the convective heat transfer coefficient, the convective heat transfer, the temperature distribution in the fuel pebble, effective radial thermal conductivity, pressure drop, pressure drop coefficient and the effect of porosity on heat transfer as well as pressure drop.

Results obtained from simulation experiments are well represented by experimental results as reported in [39, 40, 42]. Various experimental and theoretical models have been performed with good correlation between experimental results and that predicted by the Zehner-Schluender correlation [39, 42]. Thus, the effective thermal conductivity of the pebble bed nuclear reactor is most reliably predicted by the models of [39, 42]. The pressure drop coefficient

and hence the pressure drop can be correlated according to [39, 40, 42] over the entire Reynolds number range of interest. The influence of porosity and its distribution across the bed has been pointed out. In particular the influence of porosity on heat transfer and pressure drop is addressed.

The study provides understanding of the thermal-hydraulic analysis of the pebble bed high temperature gas cooled nuclear reactor. The model can serve as the basis for a more detailed three dimensional computational fluid dynamics analysis techniques. In particular the outcomes of the present study are;

1. The increase in the convective heat transfer coefficient is uniform indicating that there is appreciable temperature difference between the fluid temperature and the pebble surface temperature thus making it possible to achieve high thermal efficiency (i.e. high heat transfer rate)
2. Effective radial heat conductivity is largely as a result of heat conducted and radiated through the fluid and solid phase from layer to layer with the heat flux through the gap between neighbouring spheres due to heat conduction and radiation contributing less
3. The pressure drop is small which means that less pumping power is required and hence higher efficiency. The pressure drop should not be too high (not exceeding 2% of the system pressure). The smaller pressure drop indicates that leakage or bypass flow is less and therefore high proportion of the helium coolant flows through the paths defined by the voids between the heated fuel pebbles in the core to extract the heat from the

pebbles during normal operation. The temperature of the pebbles during normal operation is consequently reduced which will also lead to lower temperatures during loss of forced cooling events.

4. The magnitude of the effect of porosity on pressure drop is higher than the effect of porosity on heat transfer.
5. The model can adequately account for the heat transfer phenomena as well as loss of pressure through friction in the pebble bed type high temperature nuclear reactor. In other words, the model can reliably predict the thermal response of the pebble bed nuclear reactor.

## 5.2 RECOMMENDATIONS

A more detailed study of the thermal-hydraulic behaviour of the pebble bed nuclear reactor is proposed using thermo-hydraulic models such as computational fluid dynamics (CFD) technique.

CFD is an excellent tool to solve heat transfer problems, as in pebble bed modular reactor, because it can solve the convection, conduction and thermal radiation heat transfer mechanisms in arbitrary geometries in as much detail as possible to see the effect of detail features on the expected temperatures and pressures.

The CFD model is therefore strongly recommended due to the ability of the model to assess detailed thermodynamic behaviour of the reactor both in steady state and transients. This can be achieved by developing the governing equations

for the conservation of mass, momentum and energy for the fluid which can be solved either in 1-dimensional, 2-dimensional or 3-dimensional using finite difference, finite element or finite volume method.

A detailed study of the core neutronic model for the pebble bed modular reactor is also recommended. Neutronic codes such as VSOP, TINTE and MCNP are used for different types of analysis and for cross checking between codes. Also interfacing of core neutronic models with other systems (for example the reactor core thermal-hydraulic model, the power conversion unit model) is recommended for future study.

## REFERENCES

- [1] Kyu-Hyun Han, Kyong-Won Seo, Dae-Hyun Hwang and Soon Heung Chang, Development of a thermal analysis code for gas cooled reactors with annular fuels., Nuclear Eng. Des., Vol. 236, 2006, pp. 164-178.
- [2] Driscoll M. J. and Hejzlar P., Reactor physics challenges in GEN-IV reactor design. Nuclear Eng. Tech., Vol. 37, 2005, pp. 1-10
- [3] Huda M. Q. and Obara T., Development and testing of analytical models for the pebble type HTRs., Annals of Nuclear Energy, Vol. 35, 2008, pp. 1994-2005
- [4] Kadak A. C., A future for nuclear energy, pebble bed reactors, MIT, 2004, Massachusetts Institute of Technology, U.S.A
- [5] Kadak A. C., High temperature gas cooled reactors, MIT, 2000, Massachusetts Institute of Technology, U.S.A
- [6] Casper-Petten V. E., Dynamics of the pebble bed nuclear reactor in the direct brayton cycle., PhD. Thesis, Delft University of Technology, 2000
- [7] Hans D. Gougar, Abderrafi M. Ougouag and William K. Terry., Advanced core design and fuel management for pebble bed reactors., INEEL/EXT-04- 02245 2004
- [8] Pieter J. Venter and Mark N. Mitchell., Integrated design approach of the pebble bed modular reactor using models., Nuclear Eng. Des. Vol. 237, 2007, pp. 1341-1353.

- [9] Christian Charlier, Robert Fagerholm, John Slabber, and Joseph L. Shayi., Safeguarding the pebble bed modular reactor-A new challenge for the IAEA, 2007.
- [10] Richard R. Schultz et al., Next generation nuclear plant, Idaho National Laboratory, 2008, U.S.A
- [11] Lohnert G. and Reutler H., The modular HTR-a new design of high temperature pebble bed reactor., J. Br. Nucl. Energy Soc., Vol. 22, 1983, pp. 197
- [12] Zuying Gao, and Lei Shi., Thermal hydraulic calculation of HTR-10 for initial and equilibrium core., Nuclear Eng. Des., Vol. 218, 2002, pp.51-64.
- [13] John Slabber., PBMR safety design approach., A technology roadmap for generation IV nuclear energy systems, DOE, U.S.A, 2002
- [14] Scherer W., Gerwin H., Kindt T.and Patscher W., Analysis of reactivity and temperature transient experiments at the AVR high temperature reactor., Nuclear Science and Engineering., Vol. 97, 1987, pp. 58-63.
- [15] Nickel H., HTR coated particles and fuel elements., Presentation at the HTR/RCS 2002 high temperature reactor school, Cadarache, France, 2002
- [16] Marina D. Savkina., Probabilistic accident analysis of the pebble bed modular reactor for use with risk informed regulations. M.Sc. Thesis, Massachusetts Institute of Technology (MIT), 2004, pp. 16-26.
- [17] <http://en.wikipedia.org/wiki/pebble-bed/reactor> (August 5, 2008)

- [18] Kadak A. C., MIT pebble bed reactor project., Nuclear Science and Engineering Department, Massachusetts Institute of Technology, U.S.A, 2007
- [19] Du Toit C. G., Rousseau P. G, Greyvenstein G. P. and Landman W. A., A systems CFD model of a packed bed high temperature gas cooled nuclear reactor. International Journal of thermal sciences, Vol. 45, 2006, pp.70-85.
- [20] Greyvenstein G. P. and Van Antwerpen H. J., A finite volume based network method for the prediction of heat, mass and momentum transfer in a pebble bed reactor., 2<sup>nd</sup> International Topical Meeting on HTR technology, Beijin, China., Sept. 22-24, 2004.
- [21] Dudley T., Bouwer W., De Villiers P., Wang Z., The thermal-hydraulic model for the pebble bed modular reactor (PBMR) plant operator training simulator system., Nuclear Eng. Des, 2008
- [22] Hossain K., Buck M., Bensaid N., Bernnat W., Lohnert G., Development of a fast 3D thermal-hydraulic tool for the design and safety studies for the HTRs., Nuclear Eng. Des., 2008.
- [23] Becker S. and Laurien E., Three-dimensional numerical simulation of flow and heat transport in high temperature nuclear reactors. Nuclear Eng. Des., Vol. 222, 2003, pp. 189-201.
- [24] Jan-Patrice S, Julien C, Brian M and Lewis L., 3-D simulation of the coupled convective, conductive and radiative heat transfer during decay heat removal in an HTR., Nuclear Eng. Des., Vol. 237, 2007, pp. 1923-1937.

- [25] Van der Merwe J., Van Antwerpen H. J. and Mulder E. J., Heat transfer correlation limitations at the pebble bed reflector interface., Proceedings HTR2006: 3<sup>rd</sup> International Topical Meeting on HTR technology, Johannesburg, South Africa, Oct. 1-4, 2006
- [26] Greyvenstein G. P., Van Antwerpen H. J. and Rousseau P. G., The systems CFD approach applied to a pebble bed reactor core., International journal of nuclear energy science and technology, inaugural issue, 2004
- [27] Martin P. Van Stadan., Analysis of the effectiveness of cavity cooling system., 2<sup>nd</sup> International Topical Meeting on HTR technology, Beijing, China, Sept. 22 – 24, 2004
- [28] Ayelet Walter, Alexander Schulz and Guenter Lohnert., Comparison of two models for a pebble bed modular reactor core coupled to a Brayton cycle., Nuclear Eng. Des. Vol. 236, 2006, pp. 603-614.
- [29] Petersen K., The safety concepts of the HTRs with natural heat removal for the core in accidents., Juel-1872, 1983.
- [30] Breitbach G. and Barthels H., The radiant heat transfer in the high temperature reactor core after failure of the afterheat removal systems., Nuclear technology, Vol. 49, 1980, pp. 392-399.
- [31] Arcot R. B., David C. T. Pel., Heat transfer in gas-solid packed bed system-3. Overall heat transfer rates in adiabatic beds., Ind. Eng. Chem. Process Des. Dev., Vol. 18, 1979, pp. 47



- [32] Du Toit C. G., The numerical determination of the variation in the porosity of the pebble bed core., School for Mechanical and Materials Engineering, Potchefstroom University for CHE, South Africa.
- [33] Du Toit C. G., Analysis of the radial variation in the porosity of annular packed beds., Proceedings HTR2006: 3<sup>rd</sup> International Topical Meeting on HTR technology, Johannesburg, South Africa, Oct 1-4, 2006.
- [34] Du Toit C. G., Radial variation in porosity in annular packed beds., Nuclear Eng. Des., Vol. 238, 2008, pp. 3073-3079.
- [35] Motoo Fumizawa, Yoshihi Kaneto and Masanori Izumi., Porosity effect in the core thermal hydraulics for ultra high temperature gas cooled reactor.
- [36] Vortmeter D. and Schuster J., Evaluation of steady flow profiles in the rectangular and circular packed beds by a variational method., Chemical Eng. Sci., Vol. 38, pp. 1691-1699.
- [37] Goodling J. S., Vachon R. I., Stelpflug W. S. and Ying S. J., Radial porosity distribution in cylindrical beds packed with spheres., Power technology, Vol. 35, 1983, pp. 23-29.
- [38] Sederman A. J., Alexander P. and Gladden L. F., Structure of packed bed probed by magnetic resonance imaging., Power technology, Vol. 117, 2001, pp. 255-269.
- [39] Achenbach E. Helium cooled systems, HTR-pebble bed design, in Heat transfer and fluid flow in nuclear systems, edited by Henri Fenech, pp. 381-405, Pergamon Press Inc., New York, 1981

- [40] KTA standards, Reactor core design of High Temperature Gas-Cooled Reactors, Nuclear safety standards commission, KTA standards 3102.1 (1978), 3102.2 (1983), 3102.3 (1981).
- [41] Haipeng Li, Xiaojin Huang, Liangju Zhang., A simplified mathematical dynamic model of the HTR-10 high temperature gas-cooled reactor with control system design purpose., *Annals of nuclear energy*, Vol.35, 2008, pp. 1642-1651.
- [42] Achenbach E., Heat and fluid flow characteristics of packed beds., *Experimental thermal and fluid science.*, Vol. 10, 1995, pp. 17-27
- [43] William Frederik Geert Van Rooijen., Improving fuel cycle design and safety characteristics of a gas cooled fast reactor., IOS press, 2006, pp. 49-52.
- [44] Rousseau P. G. and Greyvenstein G. P., One dimensional reactor model for the integrated simulation of the PBMR power plant.

## APPENDIX A

---

### THE PEBTAN CODE FOR THERMAL ANALYSIS OF THE PEBBLE BED HIGH TEMPERATURE GAS COOLED REACTOR.

---

PROGRAM MAINFINAL

IMPLICIT NONE

REAL, PARAMETER :: PI = 3.142857, d = 0.06, Pr = 0.7, Pe = 30

REAL, PARAMETER :: q = 5.77E-8, Er = 0.88, Ys = 50, HTC = 230

REAL (KIND=3) :: Tg, Re, e, mv, A, H, Dc, DNV, PRS

REAL (KIND=3) :: TCOG, Nur, B, M1, N1, Ygap, Yfs, Kr, rHgap, rHfs, rHOV,  
Rc, Nul

REAL (KIND=3) :: Nut, Nus, Nu, Fe, HTCEFF, mu, mve, nt, kl, dPt, dNul

REAL (KIND=3):: dP, n, ev, MDRe, PDCEFF, PDRDP, DENSTY, m, Xt, Dv,  
CTFED, MDREt, k, dNu

REAL (KIND=3) :: DTI, DTII, QP, TCD, QC, CPD, DTc, Rfz, Rpeb, Tgv, PW,  
Tin, Tout, Tgcd, Reff

INTEGER :: Tgc, mvc, SWITCH

CHARACTER(LEN=\*),PARAMETER::SYHEAD='(9(2X,A30,4(A8,A30)))'

CHARACTER(LEN=\*),PARAMETER::SYDATA='(9(6X,F30.4,4(A8,F30.4)))'

---

```
OPEN(21,FILE='MNHTCEFFOUT.csv', FORM='FORMATTED', ACCESS='SEQUENTIAL', & ACTION='READWRITE', STATUS='REPLACE')
WRITE(21,SYHEAD)'MASS FLOW RATE',,, 'HEAT TRANSFER COEFFICIENT'
```

```
OPEN(22,FILE='MNHTRATIOOUT.csv', FORM='FORMATTED', ACCESS='SEQUENTIAL', & ACTION='READWRITE', STATUS='REPLACE')
WRITE(22,SYHEAD)'REYNOLDS NO',,, 'NUSELT NO.'
```

```
OPEN(23,FILE='MNTEMPTOUT.csv', FORM='FORMATTED', ACCESS='SEQUENTIAL', & ACTION='READWRITE', STATUS='REPLACE')
WRITE(23,SYHEAD)'GAS TEMPERATURE',,, 'HEAT TRANSFER COEFFICIENT'
```

```
OPEN (24, FILE='MNFUELPROFLOUT.csv', FORM='FORMATTED', ACCESS='SEQUENTIAL', ACTION='READWRITE', STATUS='REPLACE')
WRITE (24,SYHEAD) 'PEBBLE RADIUS',,, 'FUEL TEMPT',,, 'SHELL TEMPT',,, 'COOLANT TEMPT'
```

```
OPEN(25,FILE='MNCONRADOUT.csv', FORM='FORMATTED', ACCESS='SEQUENTIAL', ACTION='READWRITE', STATUS='REPLACE')
WRITE(25,SYHEAD)'CORE RADIUS',,, 'HEAT FLUX-GAP(r)',,, 'HEAT FLUX-SOLID(r)',,, 'HEAT FLUX- OVERALL(r)'
```

```
OPEN (27, FILE='MNCBNEFFOUT.csv', FORM='FORMATTED', ACCESS='SEQUENTIAL', ACTION='READWRITE', STATUS='REPLACE')
WRITE (27,SYHEAD)'POROSITY',,, 'EFFECTS ON PRSS DROP/HEAT TRNF'
```

```
OPEN (28, FILE = 'MNDIAMRATIOOUT.csv', FORM = 'FORMATTED',  
ACCESS = 'SEQUENTIAL', ACTION = 'READWRITE', STATUS =  
'REPLACE')
```

```
WRITE (28,SYHEAD)'MODIFIED REY NO.,',',', 'CORE FUEL DIAM'
```

```
OPEN (29, FILE = 'MNCOEFFOUT.csv', FORM = 'FORMATTED', ACCESS =  
'SEQUENTIAL', ACTION = 'READWRITE', STATUS = 'REPLACE')
```

```
WRITE (29,SYHEAD)'MODIFIED RE NUMBER',',', 'PRESSURE  
COEFFICIENT'
```

```
OPEN (31, FILE = 'MNCOMPAROUT.csv', FORM = 'FORMATTED', ACCESS  
= 'SEQUENTIAL', ACTION = 'READWRITE', STATUS = 'REPLACE')
```

```
WRITE (31,SYHEAD)'REYNOLDS NUMBER',',', 'PRESSURE DROP'
```

```
OPEN (32, FILE = 'MNCNRDRreffOUT.csv', FORM = 'FORMATTED', ACCESS  
= 'SEQUENTIAL', ACTION = 'READWRITE', STATUS = 'REPLACE')
```

```
WRITE(32,SYHEAD)'TEMPERATURE',',', 'EFFECTIVE CONDUCTIVITY'
```

```
OPEN (51, FILE = 'SPHTCEFFOUT.csv', FORM = 'FORMATTED', ACCESS =  
'SEQUENTIAL', & ACTION = 'READWRITE', STATUS = 'REPLACE')
```

```
WRITE (51,SYHEAD)'MASS FLOW RATE',',', 'HEAT TRANSFER  
COEFFICIENT'
```

```
OPEN (52, FILE = 'SPHTRATIOOUT.csv', FORM = 'FORMATTED', ACCESS  
= 'SEQUENTIAL', ACTION = 'READWRITE', STATUS = 'REPLACE')
```

```
WRITE (52,SYHEAD)'REYNOLDS NO.,',', 'NUSELT NO.'
```

```
OPEN (53, FILE = 'SPTEMPTOUT.csv', FORM = 'FORMATTED', ACCESS =  
'SEQUENTIAL', & ACTION = 'READWRITE', STATUS = 'REPLACE')
```

```
WRITE(53,SYHEAD)'GAS TEMPERATURE',',', 'HEAT TRANSFER  
COEFFICIENT'
```

```
OPEN (54, FILE = 'SPFUELPROFLOUT.csv', FORM = 'FORMATTED',  
ACCESS = 'SEQUENTIAL', ACTION = 'READWRITE', STATUS =  
'REPLACE')
```

```
WRITE (54,SYHEAD) 'PEBBLE RADIUS',,, 'FUEL TEMPT',,, 'SHELL  
TEMPT',,, 'COOLANT TEMPT'
```

```
OPEN (55, FILE = 'SPCONRADOUT.csv', FORM = 'FORMATTED', ACCESS  
= 'SEQUENTIAL', ACTION = 'READWRITE', STATUS = 'REPLACE')
```

```
WRITE(55,SYHEAD)'CORE RADIUS',,, 'HEAT FLUX-GAP(r)',,, 'HEAT  
FLUX-SOLID(r)',,, 'HEAT FLUX-OVERALL(r)'
```

```
OPEN (57, FILE = 'SPCBNEFFOUT.csv', FORM = 'FORMATTED', ACCESS =  
'SEQUENTIAL', ACTION = 'READWRITE', STATUS = 'REPLACE')
```

```
WRITE (57,SYHEAD)'POROSITY',,, 'EFFECTS ON PRSS DROP/HEAT  
TRNF'
```

```
OPEN (58, FILE = 'SPDIAMRATIOOUT.csv', FORM = 'FORMATTED',  
ACCESS = 'SEQUENTIAL', ACTION = 'READWRITE', STATUS =  
'REPLACE')
```

```
WRITE (58,SYHEAD)'MODIFIED REY NO.',,, 'CORE FUEL DIAM'
```

```
OPEN (59, FILE = 'SPCOEFFOUT.csv', FORM = 'FORMATTED', ACCESS =  
'SEQUENTIAL', & ACTION = 'READWRITE', STATUS = 'REPLACE')
```

```
WRITE (59,SYHEAD)'MODIFIED RE NUMBER',,, 'PRESSURE  
COEFFICIENT'
```

```
OPEN (61, FILE = 'SPCOMPAROUT.csv', FORM = 'FORMATTED', ACCESS  
= 'SEQUENTIAL', ACTION = 'READWRITE', STATUS = 'REPLACE')
```

```
WRITE (61,SYHEAD)'REYNOLDS NUMBER',,, 'PRESSURE DROP'
```

```

OPEN (62,FILE = 'SPCNRDR effOUT.csv', FORM = 'FORMATTED', ACCESS
= 'SEQUENTIAL', &ACTION = 'READWRITE', STATUS = 'REPLACE')
WRITE (62,SYHEAD)'TEMPERATURE',',', 'EFFECTIVE CONDUCTIVITY'

```

```

WRITE (*,*)
WRITE (*,*)'READ INSTRUCTIONS CAREFULLY'
WRITE (*,*)

```

```

50 PRINT *, "INPUT: SWITCH (enter 1-MAIN, 2-CONV, 3-FUELTEMP, 4-
CONRAD, 5-POROSITY, 6-RATIO, 7-DROP, 8 TO END PROGRAM)"

```

```

READ *, SWITCH
WRITE (*,*)
WRITE (*,*)
GO TO (10, 20, 30, 40, 60, 70, 80, 100) SWITCH
100 stop

```

```

20 WRITE (*,*)
WRITE (*,*)'THIS SECTION ANALYSE THE CONVECTION HEAT
TRANSFER ONLY'
WRITE (*,*)'.....'
WRITE (*,*)
PRINT*, "INPUT: Dc = CORE DIAMETER"
READ*, Dc
PRINT*, "INPUT: e = POROSITY OF BED"
READ*, e
PRINT*, "INPUT: H = HEIGHT OF BED"
READ*, H
PRINT*, "INPUT: PRS = HELIUM PRESSURE"
READ*, PRS
DO Tgc = 600,1400,200

```

```

PRINT*, "INPUT: mv = HELIUM MASS FLOW RATE"
READ*, mv
DO WHILE (mv <= 150)
A = 2*(PI)*(Dc/2)*((Dc/2) + H)
Fe = 1.0 + 1.5*(1 - e)
TCOG = 2.682E-3*(1+1.123E-3*PRS)*(Tgc**0.71)*(1-2.0E-4*PRS)
DNV = 3.674E-7*(Tgc**0.7)
RE = ((mv/A)*d)/DNV
Nul = 0.664*((RE/e)**(1/2))*(Pr**(1/3))
Nut = (0.037*((RE/e)**0.8)*Pr)/(1+2.443*((RE/e)**0.1)*((Pr**(2/3))-1))
Nus = 2+(sqrt((Nul**2)+(Nut**2)))
Nu = Fe*Nus
HTCEFF = (Nu*TCOG)/d
WRITE(51,SYDATA)mv,',',HTCEFF
WRITE(52,SYDATA)RE,',',NU
mv = mv + 0.5
END DO
END DO
DO mvc = 60,120,20
PRINT*, "INPUT: Tgv = GAS TEMPERATURE (VARYING FROM 600 - 1400
IN STEPS OF 10)"
READ*, Tgv
DO WHILE (Tgv <= 1400)
A = 2*(PI)*(Dc/2)*((Dc/2) + H)
Fe = 1.0 + 1.5*(1 - e)
TCOG = 2.682E-3*(1+1.123E-3*PRS)*(Tgv**0.71)*(1-2.0E-4*PRS)
DNV = 3.674E-7*(Tgv**0.7)
RE = ((mvc/A)*d)/DNV
Nul = 0.664*((RE/e)**(1/2))*(Pr**(1/3))
Nut = (0.037*((RE/e)**0.8)*Pr)/(1+2.443*((RE/e)**0.1)*((Pr**(2/3))-1))
Nus = 2+(sqrt((Nul**2)+(Nut**2)))

```

```

Nu = Fe*Nus
HTCEFF = (Nu*TCOG)/d
WRITE(53,SYDATA)Tgv,',',HTCEFF
Tgv = Tgv + 10
END DO
END DO
CLOSE(51, STATUS = 'KEEP')
CLOSE(52, STATUS = 'KEEP')
CLOSE(53, STATUS = 'KEEP')
WRITE (*,*)
WRITE (*,*)'END OF THIS SECTION. CHOOSE ANOTHER SECTION OR
END PROGRAM. READ INSTRUCTION'
WRITE (*,*)
WRITE (*,*)
GO TO 50

30 WRITE (*,*)
WRITE (*,*) 'THIS SECTION ANALYSE THE TEMPERATURE PROFILE IN
A FUEL PEBBLE ONLY'
WRITE (*,*)'.....'
WRITE (*,*)
PRINT*, 'INPUT: PW = THERMAL POWER OF THE REACTOR ("250MW
FULL POWER", "125MW HALF POWER", "62.5MW QUATER POWER")'
READ*, PW
PRINT*, 'INPUT: Tin = INLET GAS TEMPERATURE'
READ*, Tin
PRINT*, 'INPUT: Tout = OUTLET GAS TEMPERATURE'
READ*, Tout
PRINT*, 'INPUT: H = CORE HEIGHT'
READ*, H
PRINT*, 'INPUT: Dc = CORE DIAMETER'

```

```

READ*, Dc
PRINT*, 'INPUT: e = POROSITY OF THE BED (0.36,< e <0.42)'
READ*, e
Rpeb = 0.0001
DO WHILE (Rpeb <= 0.03)
Tg = (Tin + Tout)/2.0
TCD = (((2.549E-4*Tg)+1.5)/1.163)*(4.1868E3/3600)
Rc = Dc/2.0
CPD = PW/(PI*(Rc**2.0)*H)
IF (Rpeb <= 0.025)THEN
Rfz = Rpeb
ELSE IF (Rpeb > 0.025) THEN
Rfz = 0.025
END IF
QC = (CPD/(1-e))*((Rpeb/Rfz)**3)
Qp = (4/3)*Qc*PI*(Rfz**3)
DTI = -(Qp/(8*TCD*PI*Rfz))
DTII = -((Qp/(4*PI*TCD))*((1/Rfz) - (1/Rpeb)))
DTc = Qp/(4*PI*HTC*(Rpeb**2))
WRITE(54,SYDATA)Rpeb,',',DTI,',',DTII,',',DTc
Rpeb = Rpeb + 0.0001
END DO
CLOSE(54,STATUS = 'KEEP')
WRITE (*,*)
WRITE (*,*)'END OF THIS SECTION. CHOOSE ANOTHER SECTION OR
END PROGRAM. READ INSTRUCTION'
WRITE (*,*)
WRITE (*,*)
GO TO 50

```

```

40 WRITE (*,*)
WRITE (*,*) 'THIS SECTION ANALYSE THE CONDUCTION/RADIATION
HEAT TRANSFER ONLY'
WRITE (*,*)'.....!'
WRITE (*,*)
PRINT *, "INPUT: Dc  = CORE RADIUS"
READ *, Dc
PRINT *, "INPUT: PRS  = HELIUM PRESSURE"
READ *, PRS
PRINT *, "INPUT: Tin  = INLET GAS TEMPERATURE"
READ *, Tin
PRINT *, "INPUT: Tout  = OUTLET GAS TEMPERATURE"
READ *, Tout
PRINT *, "INPUT: e  = POROSITY OF BED"
READ *, e
PRINT *, "INPUT: Tgcd  = VARIABLE GAS TEMPERATURE"
READ *, Tgcd
Rc = 0.04
DO WHILE (Rc <= (Dc/2))
Tg = (Tin + Tout)/2.0
Kr = 8*(2-(1-(2*(d/(2*Rc))))**2)
TCOG = 2.682E-3*(1.0 + 1.123E-3*PRS)*(Tg**0.71)*(1.0 - (2.0E-4*PRS))
Nur = ((4*q*(Tg**3))/((2/Er) - 1))*(d/TCOG)
Ygap = 1 + e*Nur
rHgap = ((Pe/Kr) + ((1 - SQRT(1 - e))*Ygap))*TCOG
B = 1.25*((1 - e)/e)**1.1
M1 = B*(TCOG/Ys)
N1 = 1 + (Nur*(TCOG/Ys))
IF (M1 == N1) THEN
Yfs = (1/((B-1)*M1))*(((2/3*M1)*((B**3)-1)/(B-1))-((B+1)*(1-Nur)))
ELSE IF (M1.NE.N1)THEN

```

```

Yfs=(2/(N1-M1))*(((B*N1-M1)/((N1-M1)**2))*LOG(N1/M1))-((B-1)/(N1-
M1))+(((B+1)/(2*M1))*(N1-M1-1)))
rHfs = ((Pe/Kr) + ((SQRT(1-e))*Yfs))*TCOG
rHOV = (((Pe/Kr) + ((1 - SQRT(1 - e))*Ygap)) + ((SQRT(1 - e))*Yfs))*TCOG
WRITE(55,SYDATA)Rc,',',rHgap,',',rHfs,',',rHOV
Rc = Rc + 0.001
END IF
END DO
DO WHILE (Tgcd <= 1400)
Kr = 8*(2-(1-(2*(d/(Dc))))**2)
TCOG = 2.682E-3*(1.0 + 1.123E-3*PRS)*(Tgcd**0.71)*(1.0 - (2.0E-4*PRS))
Nur = ((4*q*(Tgcd**3))/((2/Er) - 1))*(d/TCOG)
Ygap = 1 + e*Nur
B = 1.25*((1 - e)/e)**1.1
M = B*(TCOG/Ys)
N = 1 + (Nur*(TCOG/Ys))
IF (M == N) THEN
Yfs = (1/((B-1)*M))*(((2/3*M)*((B**3)-1)/(B-1))-((B+1)*(1-Nur)))
ELSE IF (M.NE.N)THEN
Yfs      =      (2/(N-M))*(((B*N-M)/((N-M)**2))*LOG(N/M))-((B-1)/(N-
M))+(((B+1)/(2*M))*(N-M-1)))
Reff = (((Pe/Kr) + ((1 - SQRT(1 - e))*Ygap)) + ((SQRT(1 - e))*Yfs))*TCOG
WRITE(62,SYDATA)Tgcd,',',Reff
Tgcd = Tgcd + 10.0
END IF
END DO
CLOSE(55, STATUS = 'KEEP')
CLOSE(62, STATUS = 'KEEP')
WRITE (*,*)
WRITE (*,*)'END OF THIS SECTION. CHOOSE ANOTHER SECTION OR
END PROGRAM. READ INSTRUCTION'

```

```

WRITE (*,*)
WRITE (*,*)
GO TO 50

60 WRITE (*,*)
WRITE (*,*)'THIS SECTION ANALYSE THE INFLUENCE OF POROSITY
ON HEAT TRANSFER & PRESSURE DROP ONLY'
WRITE (*,*)'.....!'
WRITE (*,*)
PRINT *, "INPUT: ev = THE VARIATION OF POROSITY OF THE BED"
READ *, ev
PRINT *, "INPUT: n = FOR LAMINAR FLOW (n=1)"
READ *, n
PRINT *, "INPUT: k = FOR HIGH HIGH REYNOLDS NUMBER (k=0.6)"
READ *, k
PRINT *, "INPUT: nt = FOR TURBULENT FLOW (n=0.1)"
READ *, nt
PRINT *, "INPUT: kl = FOR LOW REYNOLDS NUMBER (k=0) "
READ *, kl
DO WHILE (ev <= 1.0)
dP = (3-ev*(2-n))/(1-ev)
dPt = (3-ev*(2-nt))/(1-ev)
IF (ev >= 1)THEN
WRITE (*,*)
END IF
dNu = (1 - k*ev)/(1 - ev)
dNul = (1-kl*ev)/(1-ev)
IF (ev >= 1)THEN
WRITE (*,*)
END IF
WRITE(57,SYDATA) ev,',',dP,',',dPt,',',dNu,',',dNul

```

```

ev = ev + 0.005
END DO
CLOSE(57, STATUS = 'KEEP')
WRITE (*,*)
WRITE (*,*)'END OF THIS SECTION. CHOOSE ANOTHER SECTION OR
END PROGRAM. READ INSTRUCTION'
WRITE (*,*)
WRITE (*,*)
GO TO 50

```



```

70 WRITE (*,*)
WRITE (*,*)'THIS SECTION ANALYSE THE CORE TO FUEL ELEMENT
DIAMETER RATIO ONLY'
WRITE (*,*)'.....!'
WRITE (*,*)
PRINT *, "INPUT: Tin = INLET GAS TEMPERATURE"
READ *, Tin
PRINT *, "INPUT: Tout = OUTLET GAS TEMPERATURE"
READ *, Tout
PRINT *, "INPUT: H = THE CORE HEIGHT"
READ *, H
PRINT *, "INPUT: m = THE HELIUM MASS FLOW RATE"
READ *, m
PRINT *, "INPUT: Dv = VARIABLE CORE DIAMETER (>=0.15)"
READ *, Dv
CTFED = Dv/d
DO WHILE (CTFED <= 58)
Tg = (Tin + Tout)/2.0
A = 2*(Pi)*(Dv/2)*((Dv/2) + H)
DNV = (3.674E-7*(Tg**0.7))
Re = ((m/A)*d)/DNV

```

```

Xt = (0.78/(CTFED**2)) + 0.375
MDREt = Re/(1-Xt)
WRITE(58,SYDATA) MDREt ,',', CTFED
Dv = Dv + 0.02
CTFED = Dv/d
ND DO
CLOSE(58,STATUS = 'KEEP')
WRITE (*,*)
WRITE (*,*)'END OF THIS SECTION. CHOOSE ANOTHER SECTION OR
END PROGRAM. READ INSTRUCTION'
WRITE (*,*)
WRITE (*,*)
GO TO 50

80 WRITE(*,*)
WRITE (*,*)'THIS SECTION ANALYSE THE PRESSURE DROP THROUGH
THE CORE ONLY'
WRITE (*,*)'.....'
WRITE (*,*)
PRINT *, "INPUT: Dc = CORE DIAMETER"
READ *, Dc
PRINT *, "INPUT: PRS = HELIUM PRESSURE"
READ *, PRS
PRINT *, "INPUT Tin = INLET TEMPERATURE OF GAS"
READ *, Tin
PRINT *, "INPUT Tout = OUTLET TEMPERATURE OF GAS"
READ *, Tout
PRINT *, "INPUT e = POROSITY OF THE BED"
READ *, e
PRINT *, "INPUT: mve = HELIUM MASS FLOW RATE"
READ *, mve

```

```

PRINT *, "INPUT: H = CORE HEIGHT"
READ *, H
DO WHILE (mve <= 150)
  Tg = (Tin + Tout)/2.0
  A = 2*(Pi)*(Dc/2)*((Dc/2) + H)
  DENSTY = 48.14*(PRS/Tg)*((1+(0.446*(PRS/(Tg**1.2))))**(-1.0))
  DNV= (3.674E-7*(Tg**0.7))
  Re = ((mve/A)*d)/DNV
  MDRRe = Re/(1-e)
  PDCEFF = (320/MDRe) + (6/(MDRe**0.1))
  WRITE(59,SYDATA)MDRe,',',PDCEFF
  PDROP = PDCEFF*(H/d)*((1-e)/(e**3.0))*(1/(2*DENSTY))*((mve/A)**2)
  WRITE(61,SYDATA)Re,',',PDROP
  mve = mve + 0.5
END DO
CLOSE(59, STATUS = 'KEEP')
CLOSE(61, STATUS = 'KEEP')
WRITE (*,*)
WRITE (*,*)'END OF THIS SECTION. CHOOSE ANOTHER SECTION OR
END PROGRAM. READ INSTRUCTION'
WRITE (*,*)
WRITE (*,*)
GO TO 50

10 WRITE (*,*)
WRITE (*,*) 'THIS SECTION COMBINES ALL THE SEPERATE MODULES'
WRITE (*,*)'.....!'
WRITE (*,*)
PRINT*, "INPUT: Tin = INLET GAS TEMPERATURE"
READ*, Tin
PRINT*, "INPUT: Tout = OUTLET GAS TEMPERATURE"

```

```
READ*, Tout
PRINT*, "INPUT: PRS = HELIUM PRESSURE"
READ*, PRS
PRINT*, "INPUT: PW = THERMAL POWER OF THE REACTOR ('250MW
FULL POWER', '125MW HALF POWER', '62.5MW QUATER POWER')"
READ*, PW
PRINT*, "INPUT: e = POROSITY OF THE BED (0.36<e<0.42)"
READ*, e
PRINT*, "INPUT: H = HEIGHT OF BED (FIXED)"
READ*, H
PRINT*, "INPUT: Dc = CORE DIAMETER"
READ*, Dc
PRINT *, "INPUT: n = FOR LAMINAR OR TURBULENT (n=1 )"
READ*, n
PRINT *, "INPUT: k = FOR HIGH HIGH REYNOLDS NUMBER(k = 0.6)"
READ *, k
PRINT *, "INPUT: nt = FOR TURBULENT FLOW (n=0.1)"
READ *, nt
PRINT *, "INPUT: kl = FOR LOW REYNOLDS NUMBER (k=0) "
READ *, kl
PRINT *, "INPUT: ev = THE VARIATION OF POROSITY OF THE BED"
READ *, ev
PRINT *, "INPUT: m = HELIUM MASS FLOW RATE (FIXED)"
READ *, m
PRINT *, "INPUT: Dv = VARIATION OF CORE DIAMETER"
READ *, Dv
PRINT *, "INPUT: mu = mve VARIATION OF MASS FLOW RATE"
READ *, mu
PRINT *, "INPUT: Tgcd = VARIABLE GAS TEMPERATURE"
READ *, Tgcd
```

CALLCONVECTION\_SUB

(Re,Nul,Nut,Nus,Fe,Nu,TCOG,DNV,A,H,e,PRS,mv,Dc,HTCEFF,Tgv,Tgc,mvc)

CALLFUELTEMP\_TSUB

(e,Dc,H,Tg,DTI,DTII,QP,TCQ,QC,CPD,Rc,DTc,Rfz,Rpeb,Tin,Tout)

CALLCONRAD\_SUB

(Tg,TCOG,Nur,B,M1,N1,e,Ygap,Yfs,Kr,rHgap,rHfs,rHOV,Dc,Rc,PRS,Tin,Tout,  
Tgcd, Reff)

CALL COMBINEDEFFECTS\_SUB (dP, n, ev, dNu, k, nt, kl, dPt, dNul)

CALL COREFUEL\_RATIOSUB (Tg, A, DNV, Xt, Dv, CTFED, MDREt, Re, m,  
H,Tin,Tout)

CALL PRESSURE\_DROP\_SUB (PDROP, PDCEFF, Re, DENSTY, DNV, A, e,  
Tg, MDRe, PRS, mu, Dc, H,Tin,Tout)

WRITE(21,SYDATA)mv,',',HTCEFF

WRITE(22,SYDATA)RE,',',NU

WRITE(23,SYDATA)Tgv,',',HTCEFF

WRITE(24,SYDATA)Rpeb,',',DTI,',',DTII,',',DTc

WRITE(25,SYDATA)Rc,',',rHgap,',',rHfs,',',rHOV

WRITE(27,SYDATA)ev,',',dP,',',dPt,',',dNu,',',dNul

WRITE(28,SYDATA)MDREt,',',CTFED

WRITE(29,SYDATA)MDRe, PDCEFF

WRITE(31,SYDATA)Re,',',PDROP

WRITE(32,SYDATA)Tgcd,',',Reff

CLOSE(21, STATUS = 'KEEP')

CLOSE(22, STATUS = 'KEEP')

CLOSE(23, STATUS = 'KEEP')

```

CLOSE(24, STATUS = 'KEEP')
CLOSE(25, STATUS = 'KEEP')
CLOSE(27, STATUS = 'KEEP')
CLOSE(28, STATUS = 'KEEP')
CLOSE(29, STATUS = 'KEEP')
CLOSE(31, STATUS = 'KEEP')
CLOSE(32, STATUS = 'KEEP')

```

```

WRITE (*,*)
WRITE (*,*) 'END OF THIS SECTION. CHOOSE ANOTHER SECTION OR
END PROGRAM. READ INSTRUCTION'
WRITE (*,*)
WRITE (*,*)
GO TO 50

```

```

CONTAINS
!! SUBROUTINES

```

```

SUBROUTINE
CONVECTION_SUB(Re,Nul,Nut,Nus,Fe,Nu,TCOG,DNV,A,H,e,PRS,mv,Dc,H
TCEFF,Tgv, Tgc,mvc)

```

```

IMPLICIT NONE
REAL(KIND=3) ::
Tgv,Re,Nul,Nut,Nus,Fe,Nu,TCOG,DNV,A,H,e,PRS,mv,Dc,HTCEFF
INTEGER :: Tgc, mvc
DO Tgc = 600,1400,200
PRINT*, "INPUT: mv = HELIUM MASS FLOW RATE"
READ*, mv
DO WHILE (mv <= 150)
A = 2*(PI)*(Dc/2)*((Dc/2) + H)

```

```

Fe = 1.0 + 1.5*(1 - e)
TCOG = 2.682E-3*(1+1.123E-3*PRS)*(Tgc**0.71)*(1-2.0E-4*PRS)
DnV = 3.674E-7*(Tgc**0.7)
Re = ((mv/A)*d)/DnV
Nul = 0.664*((Re/e)**(1/2))*(Pr**(1/3))
Nut = (0.037*((Re/e)**0.8)*Pr)/(1+2.443*((Re/e)**0.1)*((Pr**(2/3))-1))
Nus = 2+(sqrt((Nul**2)+(Nut**2)))
Nu = Fe*Nus
HTCEFF = (Nu*TCOG)/d
WRITE(21,SYDATA)mv,',',HTCEFF
WRITE(22,SYDATA)RE,',',NU
mv = mv + 0.5
END DO
END DO
DO mvc = 60,120,20
PRINT*, "INPUT: Tgv = GAS TEMPERATURE (VARYING FROM 600
1400 IN STEPS OF 10)"
READ*, Tgv
DO WHILE (Tgv <= 1400)
A = 2*(PI)*(Dc/2)*((Dc/2) + H)
Fe = 1.0 + 1.5*(1 - e)
TCOG = 2.682E-3*(1+1.123E-3*PRS)*(Tgv**0.71)*(1-2.0E-4*PRS)
DnV = 3.674E-7*(Tgv**0.7)
Re = ((mvc/A)*d)/DnV
Nul = 0.664*((Re/e)**(1/2))*(Pr**(1/3))
Nut = (0.037*((Re/e)**0.8)*Pr)/(1+2.443*((Re/e)**0.1)*((Pr**(2/3))-1))
Nus = 2+(sqrt((Nul**2)+(Nut**2)))
Nu = Fe*Nus
HTCEFF = (Nu*TCOG)/d
WRITE(23,SYDATA)Tgv,',',HTCEFF
Tgv = Tgv + 10

```

```

END DO
END DO
RETURN
END SUBROUTINE CONVECTION_SUB

```

```

SUBROUTINE
FUELTEMP_TSUB(e,Dc,H,Tg,DTI,DTII,QP,TCD,QC,CPD,Rc,DTc,Rfz,Rpeb,T
in,Tout)

```

```

IMPLICIT NONE

```

```

REAL(KIND=3) :: DTI, Qp, TCD, QC, CPD, Rc, DTII, DTc,Rfz, Rpeb, e, Dc, H,
Tg, Tin, Tout

```

```

Rpeb = 0.0001

```

```

DO WHILE (Rpeb <= 0.03)

```

```

Tg = (Tin + Tout)/2

```

```

TCD = (((2.549E-4*Tg)+1.5)/1.163)*(4.1868E3/3600)

```

```

Rc = Dc/2

```

```

CPD = PW/(PI*(Rc**2)*H)

```

```

IF (Rpeb <= 0.025)THEN

```

```

Rfz = Rpeb

```

```

ELSE IF (Rpeb > 0.025) THEN

```

```

Rfz = 0.025

```

```

END IF

```

```

QC = (CPD/(1-e))*((Rpeb/Rfz)**3)

```

```

Qp = (4/3)*QC*PI*(Rfz**3)

```

```

DTI = -(Qp/(8*TCD*PI*Rfz))

```

```

DTII = -((Qp/(4*PI*TCD))*((1/Rfz) - (1/Rpeb)))

```

```

DTc = Qp/(4*PI*HTC*(Rpeb**2))

```

```

WRITE(24,SYDATA)Rpeb,',',DTI,',',DTII,',',DTc

```

```

Rpeb = Rpeb + 0.0001

```

```

END DO
RETURN
END SUBROUTINE FUELTEMP_T_SUB

```

```

SUBROUTINE

```

```

CONRAD_SUB(Tg,TCOG,Nur,B,M1,N1,e,Ygap,Yfs,Kr,rHgap,rHfs,rHOV,Dc,
Rc,PRS,Tin,Tout,Tgcd,Reff)

```

```

IMPLICIT NONE

```

```

REAL(KIND=3) ::Tg,TCOG,Nur,B,M1,N1,e,Ygap,Yfs,Kr,rHgap,rHfs,rHOV,Dc,
Rc,PRS,Tin,

```

```

Tout,Tgcd,Reff

```

```

Rc = 0.04

```

```

DO WHILE (Rc <= (Dc/2))

```

```

Tg = (Tin + Tout)/2.0

```

```

Kr = 8*(2 - (1 - 2*(d/(2*Rc)))**2)

```

```

TCOG = 2.682E-3*(1.0 + 1.123E-3*PRS)*(Tg**0.71)*(1.0 - (2.0E-4*PRS))

```

```

Nur = ((4*q*(Tg**3))/((2/Er) - 1))*(d/TCOG)

```

```

Ygap = 1 + e*Nur

```

```

rHgap = ((Pe/Kr) + ((1 - SQRT(1 - e))*Ygap))*TCOG

```

```

B = 1.25*((1 - e)/e)**1.1

```

```

M1 = B*(TCOG/Ys)

```

```

N1 = 1 + (Nur*(TCOG/Ys))

```

```

IF (M1 == N1) THEN

```

```

Yfs = (1/((B-1)*M1))*(((2/3*M1)*((B**3)-1)/(B-1))-((B+1)*(1-Nur)))

```

```

ELSE IF (M1.NE.N1)THEN

```

```

Yfs=(2/(N1-M1))*(((B*N1-M1)/((N1-M1)**2))*LOG(N1/M1))-((B-1)/(N1-
M1))+((B+1)/(2*M1))*(N1-M1-1))

```

```

rHfs = ((Pe/Kr) + ((SQRT(1-e))*Yfs))*TCOG

```

```

rHOV = (((Pe/Kr) + ((1 - SQRT(1 - e))*Ygap)) + ((SQRT(1 - e))*Yfs))*TCOG

```

```

WRITE(25,SYDATA)Rc,',',rHgap,',',rHfs,',',rHOV
Rc = Rc + 0.001
END IF
END DO
DO WHILE (Tgcd <= 1400)
Kr = 8*(2-(1-(2*(d/(Dc))))**2)
TCOG = 2.682E-3*(1.0 + 1.123E-3*PRS)*(Tgcd**0.71)*(1.0 - (2.0E-4*PRS))
Nur = ((4*q*(Tgcd**3))/((2/Er) - 1))*(d/TCOG)
Ygap = 1 + e*Nur
B = 1.25*((1 - e)/e)**1.1
M = B*(TCOG/Ys)
N = 1 + (Nur*(TCOG/Ys))
IF (M == N) THEN
Yfs = (1/((B-1)*M))*(((2/3*M)*((B**3)-1)/(B-1))-((B+1)*(1-Nur)))
ELSE IF (M.NE.N)THEN
Yfs=(2/(N-M))*(((B*N-M)/((N-M)**2))*LOG(N/M))-((B-1)/(N-
M))+(((B+1)/(2*M))*(N-M-1)))
Reff = (((Pe/Kr) + ((1 - SQRT(1 - e))*Ygap)) + ((SQRT(1 - e))*Yfs))*TCOG
WRITE(32,SYDATA)Tgcd,',',Reff
Tgcd = Tgcd + 10.0
END IF
END DO
RETURN
END SUBROUTINE CONRAD_SUB

```

```

SUBROUTINE COMBINEDEFFECTS_SUB(dP, n, ev, dNu, k, nt, kl, dPt, dNul)

```

```

IMPLICIT NONE

```

```

REAL(KIND=3) :: dP, n, ev, dNu, k,nt, kl, dPt, dNul

```

```

DO WHILE (ev <= 1.0)

```

```

dP = (3-ev*(2-n))/(1-ev)
dPt = (3-ev*(2-nt))/(1-ev)
IF (ev >= 1)THEN
WRITE (*,*)
END IF
dNu = (1 - k*ev)/(1 - ev)
dNul = (1-kl*ev)/(1-ev)
IF (ev >= 1)THEN
WRITE (*,*)
END IF
WRITE(27,SYDATA)ev,',',dP,',',dPt,',',dNu,',',dNul
ev = ev + 0.005
END DO
RETURN
END SUBROUTINE COMBINEDEFFECTS_SUB

```

```

SUBROUTINE COREFUELRATIO_SUB (Tg, A, DNV, Xt, Dv, CTFED,
MDREt, Re, m, H, Tin, Tout)

```

```

IMPLICIT NONE
REAL(KIND=3):: Tg, A, DNV, Xt, Dv, CTFED, MDREt, Re, m, H, Tin, Tout
CTFED = Dv/d
DO WHILE (CTFED <= 58)
Tg = (Tin + Tout)/2.0
A = 2*(Pi)*(Dv/2)*((Dv/2) + H)
DNV = (3.674E-7*(Tg**0.7))
Re = ((m/A)*d)/DNV
Xt = (0.78/(CTFED**2)) + 0.375
MDREt = Re/(1-Xt)
WRITE(28,SYDATA)MDREt,',',CTFED

```

```

Dv = Dv + 0.02
CTFED = Dv/d
END DO
RETURN
END SUBROUTINE COREFUELRATIO_SUB

```

```

SUBROUTINE PRESSUREDROP_SUB (PDROP, PDCEFF, Re, DENSTY,
DNV, A, e, Tg, MDRe, PRS, mu, Dc, H, Tin, Tout)

```

```

IMPLICIT NONE

```

```

REAL(KIND=3):: PDROP, PDCEFF, Re, DENSTY, DNV, A, e, Tg, MDRe,
PRS, mu, Dc, H, Tin, Tout

```

```

DO WHILE (mu <= 150.0)

```

```

Tg = (Tin + Tout)/2.0

```

```

A = 2*(PI)*(Dc/2)*((Dc/2) + H)

```

```

DENSTY = 48.14*(PRS/Tg)*((1+(0.446*(PRS/(Tg**1.2))))**(-1.0))

```

```

DNV = (3.674E-7*(Tg**0.7))

```

```

Re = ((mu/A)*d)/DNV

```

```

MDRe = Re/(1-e)

```

```

PDCEFF = (320/MDRe) + (6/(MDRe**0.1))

```

```

WRITE(29,SYDATA)MDRe,',',PDCEFF

```

```

PDROP = PDCEFF*(H/d)*((1-e)/(e**3.0))*(1/(2*DENSTY))*((mu/A)**2)

```

```

WRITE(31,SYDATA)Re,',',PDROP

```

```

mu = mu + 0.5

```

```

END DO

```

```

RETURN

```

```

END SUBROUTINE PRESSUREDROP_SUB

```

```

END PROGRAM MAINFINAL

```

